AN APPROXIMATE SOLUTION FOR A CONE-CYLINDER IN AXIALLY SYMMETRIC TRANSONIC FLOW

by

James B. Eades, Jr.

B. S. in Aeronautical Engineering

M. S. in Applied Mechanics

Thesis submitted to the Graduate Faculty of the

Virginia Polytechnic Institute

in candidacy for the degree of

DOCTOR OF PHILOSOPHY

in

APPLIED MECHANICS

APPROVED:

Chairman, Advisory Committee

Blacksburg, Virginia

TABLE OF CONTENTS

1. LIST OF SYMBOLS

a, b, $\not{c}$ = constant (Section 7), unless otherwise defined

c = acoustical speed (without subscript infers local value)

C_p = pressure coefficient ($= \frac{p_L - p_\infty}{q_\infty}$)

C_{p_c} = compressible pressure coefficient (Figures 1 and 2)

C_{p_i} = incompressible pressure coefficient (Figure 3)

$E(k)$ = elliptic integral of the first kind (See equations (7.11))

d = slope (Figure 17)

f = symbol for "Function of", body fineness ratio (length/thickness)

F = symbol for "Function of"

G = constant

g = gravitational constant (Section 3)

h = symbol for "Function of"

k = modulus of the elliptic integrals

k' = complimentary modulus of the elliptical integrals ($k'^2 = 1 - k^2$)

K_o = kernel of the integral equation (Section 7)

$K(k)$ = elliptic integral of the first kind (see equations (7.11)).

K_θ = integral value

$\mathfrak{K}_o$ = integral operator (equation (7.20))

M = Mach number

M, m = constant (Section 7), unless otherwise defined

p = pressure (when used with a number subscript, subscript "L" or "stag")

P = scalar pressure potential function

p_μ = weight factor (Section 7)

Q = source strength (volume rate of discharge)

q = free stream dynamic pressure ($\frac{\rho_\infty U^2}{2}$)

R_o = constant radius of the cylindrical portion of the cone-cylinder body

$\overline{r}$ = general position vector measured from a chosen origin

s = arc length

t = time

u_1, u_2, u_3 = general cartesian velocity components

u, v = velocity components parallel to x- and r-axes respectively (Section 8)

u, v, w = perturbational velocity components (Section 3)

U = free stream speed, parallel to x-axis

u^* = $\dfrac{u}{-\dfrac{w(\sigma)\, d\sigma}{2\pi\eta}}$, non-dimensional x-component of the magnitude of the velocity induced by a vortex ring.

v^* = $\dfrac{v}{-\dfrac{w(\sigma)\, d\sigma}{2\pi\eta}}$, non-dimensional r-component of the magnitude of the velocity induced by a vortex ring.

$\overline{V}$ = general velocity vector at position $\overline{r}$.

$w(s)$ = velocity at a point on the body contour

x_1, x_2, x_3 = general cartesian coordinates

x, r = cylindrical coordinates

sgn ( ) = sign of ( )

α = angle of attack

β = Mach factor, $\sqrt{1 - M_\infty^2}$

γ = ratio of specific heats ($\gamma = 1.4$ for air)

$\gamma(x;\xi)$ = vortex ring strength per unit length of axis (x) (Section 7)

Γ = circulation

δ = tn θ_c (for cone)

ζ = transformation coordinate

θ_c = cone semi-apex angle

λ = a parameter (Section 7)

Λ = ratio of nonlinear to linear terms of the perturbational equation of motion (Section 5), unless otherwise noted.

ρ = mass density/unit volume

ϕ = velocity potential function

φ = perturbation velocity potential

τ = perturbation stream function

μ = coefficient of viscosity

σ = variable arc length in a meridian plane, $\sigma = \sigma(\xi,\eta)$

ξ = axial coordinate of the variable pt. π

η = normal coordinate of the variable pt. π

ψ = stream function

$\lambda_{1,2,3}$ = constants

χ = coordinate transformation, (equation (7.41))

$\bar{\nabla}$ = differential operator, $d/d\bar{r}$

Subscripts

μ = index notation

1, 2, 3 = cartesian coordinate indices (as noted); index notation

0 = steady state, reservoir condition or rest condition

L = local

∞ = remote or undisturbed stream condition

$( )_{stag}$ = stagnation condition ($\bar{V} = 0$)

Superscripts

$*$ = (local) sonic conditions, for compressible flow investigation; otherwise as noted

(1) = value at $M_N = 1.0$

$( )'$ = derivative notation

$\overline{( )}$ = a vector quantity

LIST OF FIGURES

2. INTRODUCTION

In the past few years, with the realization of flight at and near the speed of sound, the problem of transonic aerodynamics has become important to the aeronautical engineer. This particular problem has imposed new concepts on known phenomena for compressible flow, and has received attention from many investigators both from the theoretical and experimental point of view.

Though the governing equations for this problem have long been known and formulated, progress in the solution of the problem has been relatively slow compared, say, with the advances made in the study of the subsonic and supersonic flow case. The basic difficulty encountered when attempting to solve this problem can be traced to the non-linearity of the governing equations in conjunction with the "mixed" type of differential equation which must be solved. The first notable advancement, which brought a clearer insight to the nature of the solution, was made by von Karman[31] in his paper on the transonic similarity laws. This work indicated that certain invariants could be defined which allowed the correlation of forces and pressures, experienced in transonic flow, for geometrically similar bodies. The laws set forth by von Karman were established on the basis of perturbational theory, the solution of the reduced equation of motion (for the perturbational concept) being obtained with due consideration for the boundary conditions of the compressible flow field and the body in this moving flow field taken into account.

The range of validity of these laws was established experimentally, and as is now known, these similarity conditions are applicable for the range of free-stream Mach numbers below unity, at unity, and above unity.

Subsequent to the above work, other investigators such as Spreiter[49], Oswatitsch[41] and Brandt[30], and Perl and Klein[50] extended and modified the similarity laws so that their application is in better agreement with experiment for the two- and three-dimensional flow cases.

At about this same period the experimental apparatus and techniques, which allowed wind tunnel investigations to be carried out at sonic speeds, were perfected and reliable experimental data were then obtainable. One of the necessary requirements for wind tunnel work was found to be a modification of the wind tunnel test section; this modification involved redesigning the working section so that, by partially opening the walls, the pressure accumulation experienced at near sonic speeds could be alleviated, thereby eleminating the choking of the tunnel. Such modifications are employed universally today on closed transonic tunnels. They allow testing of aerodynamic shapes through the entire transonic range of free stream Mach numbers. With the perfection of the transonic wind tunnel, Whitcomb was able to establish his now famous "Area Rule", by which the transonic drag rise is reduced for many present day aerodynamic vehicles. This empirical rule may be stated as, "Near the speed of sound, the rise in zero-lift drag of thin low-aspect ratio wing-body

combinations is primarily dependent on the axial distribution of cross-sectional area normal to the air stream''. Thus, in essence, if the area distribution for an aircraft is made the same as a geometrically similar slender body of revolution, the wave drag for the aircraft should be in close agreement with that of the body of revolution. Significantly this work was pure hypothesis, the analytical verification of the theorem being established only after the experimental justification had been demonstrated by Whitcomb.

Shortly after Whitcomb's discovery, several investigators published results which are considered significant contributions to the further understanding of the transonic problem. The work by Leipmann, Ashkenas, and Cole[51], by Leipmann and Bryson[52], and by Bryson[53], for the two-dimensional case; the investigations of Cole, Solomon and Willmarth[58], and by Solomon[42] on the axially symmetric flow over simple body types are notable experimental investigations in transonic flow. The theoretical work by Vincenti and Wagoner[54,55], and by Guderley and Yoshihara[56,57], on two-dimensional transonic flow over wedge shaped bodies; and the theoretical studies presented by Yoshihara[24], Heaslet and Lomax[59], by Berndt[60], by Heaslet and Spreiter[61], and by Miles[62], have all extended the knowledge of transonic theory. Most of these papers deal with the two-dimensional case, and even though three-dimensional flow would appear to be of more practical interest, the available published material on this phase of transonic theory is quite limited. The practical solution for a cone-cylinder at Mach number One[24], and the experimental work on

the same body type[42] at subsonic speeds close to Mach Number One is substantially the only available material with which comparisons can be made. It appears then that in proportion to its importance, transonic flow is not understood as well as any other phase of high-speed compressible flow.

As previously indicated, the nature of the governing equation imposes the greatest restriction on the solution of the transonic problem. It is well known, for instance, that the reduced form of the differential equation for the subsonic case is elliptic, and for the supersonic case is hyperbolic. Since transonic flow is a mixture of both subsonic and supersonic flow, the differential equation typical of this case is parabolic. This can be seen if the governing equation, reduced according to perturbation concepts, is inspected. It is readily seen that the equation is non-linear even in its reduced form. From equation (3.20) it follows that the coefficient of the streamwise gradient of the axial velocity component will acquire different values for different flow types. These differences clearly indicate the character of the differential equation, and hence indicate the type of equation which must be dealt with for each case indicated. That is, the appropriate coefficient

$$(1 - M_\infty^2) - \frac{(\gamma + 1) M_\infty^2}{U} u \quad \begin{cases} > 0, \text{ (elliptic), for subsonic flow} \\ = 0, \text{ (parabolic), for sonic flow} \\ < 0, \text{ (hyperbolic), for supersonic flow} \end{cases}$$

The general method of approach to the solution of the compressible flow problem has been to assume a first order approximation obtained

from the solution of the linearized equation of motion. To reduce the degree of approximation subsequent refinements are made by iterative processes being applied to this first solution, thereby obtaining second and higher order approximations and refinements. It is generally agreed now that such a procedure for transonic flow does not yield acceptable results since this series type solution does not generally converge. It should be mentioned that a subsequent effort described in reference 61 was carried out in a manner which overcame this discrepancy, and in fact the problem was approached not from the usual standpoint of attempting to refine the first order solution, but rather to evaluate the integral equation for the flow on a momentum basis. The results obtained in this paper were then checked against other existing solutions to ascertain the reliability of the method. The equations obtained from this work (reference 61) will be compared with the results of this thesis; these comparisons will be noted in a following section and comments made at that time.

Before passing to an outline of the present work a few comments on the method of reference 24 should be made. In this paper by Yoshihara, a solution for the pressure distribution over a cone-cylinder body of revolution in steady, sonic compressible potential flow is obtained. The problem was solved by relaxation techniques with due consideration being given to boundary conditions and the physics of the flow field. The author indicates that considerable time is required to complete his solution since, aside from the usual

rigors of relaxation, one of the required conditions is the determination of the shape of the Mach wave emanating from the shoulder, or body junction of the cone and the cylinder. The boundary conditions here are known but the wave shape is not. This solution, which is said to have experimental verification, cannot be extended to all similar bodies at all Mach numbers in the transonic range. Hence, to obtain the pressure distribution for another cone-cylinder at a Mach number different from that of the presented results, it would be necessary to repeat the complete process. Though the author makes use of the similarity law of reference (30) to obtain approximate pressures for other cone-cylinder bodies at the sonic Mach number (unity), it must be recalled that the use of the similarity condition is restricted under the conditions of the derivation. That is, since the concept of small perturbations was employed, only a limited range of cone apex angles may be assumed if a good approximation is desired. (As the results of Yoshihara[24] were used, in conjunction with the similarity law[30], in establishing the working equations of reference 61, the inability of these working equations to give satisfactory agreement with other results, and the results in this thesis, can be traced to the limitations indicated in this last paragraph).

The work given in the following sections of this study deals with the transonic problem from a different point of view. In an effort to give a wider range of applicability to the solution, considerable emphasis has been placed upon the physical aspects of the problem rather than the formal mathematics (and the restrictions which

must necessarily follow). Use of known and well established laws concerning compressible flow phenomena will be employed in the formulation of the solution procedure.

The body considered here is to be a body of revolution consisting of a conical head and a cylindrical afterbody. The problem will be treated for the case where the remote free stream is at all times directed along the body axis. The choice of flow direction and body configuration was made first, because of the geometric simplicity of the shape, and second, so that there would be a surface region for the cone-cylinder combination which would be shock free for all free-stream Mach numbers. That is, the conical head, which is the aerodynamic surface of primary interest in this study, does not experience any velocity or surface discontinuities for the entire range of transonic speeds. In this case, then, the hypothesis employed here will not have to be given special treatment to overcome the conditions associated with local discontinuities of the velocities or the body geometry. This is quite evident since any discontinuities which might occur on the combined body can only occur at the apex of the cone and/or at the plane of contact for the cone and the cylinder. And since the body region of interest, here, is the conical head, this region is free from these discontinuities. The cone body will also exhibit a favorable pressure gradient and hence the body should not experience large viscous effects which could lead to discrepancies between measured and predicted results.

In this investigation Gothert's Rule, which is the three-dimensional counterpart of the well known Prandtl-Glauert Rule in two-dimensional compressible flow, is applied to the incompressible pressure distribution for a cone-cylinder body of revolution in axially symmetric flow to obtain the compressible pressure distribution for the same body at subsonic Mach numbers. Now, before such a procedure is carried out, it is mandatory that a good approximation for the incompressible problem be available. Since for the most part any such solution, available in the literature, has been determined along the lines of the classical method of source-sink distribution, and since this method does not give a degree of accuracy felt adequate for this investigation, it has been necessary to incorporate a more acceptable method in this study. It is for this reason that one of the following sections has been devoted to the development of the "Vortex-Ring Distribution Method"[18], for determining the incompressible pressure distribution over a cone-cylinder body of revolution. The vortex ring method does not suffer from the usual inadequacies of the axially distributed source-sink approach (referred to as the "classical" approach) in that no restriction is made on the size of the conical head which may be employed in the problem. This may plausibly be explained as follows: for a source, located on the body axis, the disturbance produced at a body surface element varies inversely with the radial distance from the source to the surface element. But, if the surface is not in close proximity, the contribution to the resultant flow at the point of investigation will become

small. This diminishing velocity contribution indicates the inability of such a method to provide acceptable results. Of course it immediately becomes apparent that this discrepancy may be eliminated by locating the distributed sources on the surface elements proper; i.e., by employing source rings or disks. Though it is true that such an alternate procedure is required for other than very slender bodies, it is also quite true that such a problem requires an overwhelming amount of work before it can be solved completely. Hence, a method which is not restricted by either of the above arguments could certainly be employed to great advantage - - and, such a method is that employing distributed vortex rings.

In applying Gothert's Rule to predict compressible pressure distributions over a body, it is necessary that the range of applicability be known, and that the form of the rule be established. A study of this rule and the range of Mach numbers for which it may be used to predict results comparable with experiment is contained herein. It will be shown that the upper bounds on free-stream Mach number is the so-called "lower critical Mach number". This is that value of free-stream Mach number for which sonic conditions first occur locally at some point on the body surface. Throughout this investigation it is assumed that such a critical point for the cone-cylinder is the plane of the shoulder, or junction of the cone and the cylinder. Physically this is a very close approximation for the critical cross-section since, neglecting viscous effects, the local velocity will have its greatest magnitude there. In fact, if incompressible

inviscid theory is considered, the local velocity at the cone shoulder will necessarily be infinite. It can be argued that due to viscous boundary layer action the real fluid will tend to "round-off" the shoulder region, and in so doing will allow the local velocities to remain finite but still large. Since the largest local velocity occurs at the body junction it is then apparent that local sonic speed will occur here first on the body.

Now, knowing the limitation on the methods used to estimate the body pressures in the subsonic Mach number range, these pressure distributions are then known for the full range of subsonic Mach numbers. This makes known the solution of the compressible flow problem up to the threshold of the present investigation. All that now remains is to define the procedure by which the transonic solution may be given.

In the following analysis the transonic problem is studied under the condition of stationarity of local Mach number[58]. This may be defined on the premise that once local sonic conditions have been reached, the body does not experience any appreciable change in local Mach number with increasing free-stream Mach numbers, throughout the entire transonic speed range. Such a phenomenon appears to have been first noted by Cole, et al[58], and verified experimentally for both the two- and three-dimensional flow cases by several other investigators. The mathematical equivalence of the stationarity concept may be stated as

$$\left.\frac{dM_L}{dM_\infty}\right|_{M_\infty = 1} = 0.$$

The physical reasoning behind this is that as the free-stream Mach number approaches unity the free-stream shock wave is located infinitely far ahead of the body. As is well known, such a shock is fundamentally a normal wave form and hence the Mach number behind the shock is subsonic. Thus, if $M_\infty^2 = 1 + \epsilon$ (where $\epsilon << 1$), then the Mach number downstream of the shock is approximately given by $M_1^2 \approx 1 - \epsilon$. For such a condition the Mach number of the fluid approaching the body does not vary appreciably and therefore the local Mach number likewise does not change. This condition exists not only for subsonic free-stream values of Mach number, but also exists for a range of speeds which are slightly supersonic.

Having established the physical nature of the transonic compressible flow the body pressures may then be determined and the body forces defined. For the present study, the body axis being aligned with the direction of the free-stream, the only body force to be considered will be a drag force. Since the fluid media is assumed inviscid the drag force will be that due to pressure differences acting on the body surface. In this investigation no consideration is given to base pressures, or the drag associated therewith, hence the drag force will only be that defined from the pressures acting on the conical head. This drag force is usually referred to in the literature as wave drag.

In the initial stages of this investigation it was thought that the results might be correlated under one of the existing laws of similarity for transonic flow; however, when such laws were applied

to these results it was found that no such similarity existed. Undoubtedly a part of the difficulty can be explained by the fact that the range of body sizes investigated here far exceeded the limitations imposed on the similarity derivations. As the semi-apex angles for the conical heads studied extend to a value of 25 degrees, the perturbational values for such a blunted body can no longer be considered as "small". This alone rules out the application of the "small disturbance" similarity law, but does not explain the reasons why the smaller sized bodies also fail to fit the correlation. The explanation of this failure is given in reference 63 and will not be restated here.

In one of the latter sections a correlation of the drag coefficients for all cones studied, for the transonic range of free-stream Mach number, will be established and presented. In this, and in a following section, the agreement between the present results and existing data will be compared. It is believed that the data obtained here, and the correlation of these data, are the first such available in existing literature. Due to the unique approach used to establish the correlation parameter, the arguments[63] presented against the existence of similarity factors are not violated. Through the essence of the similarity conditions is still retained in the present development, the direct use of the similarity parameters are not employed explicitly and hence do not detract from the validity of the present results. The very simplicity of the definition for the

correlation parameter makes it surprising that such an approach has not been previously adopted. However, a search of the literature seems to indicate that this approach has been completely ignored until now.

Having outlined the problem to be studied and the manner in which it will be approached, a systematic development will be presented in the topics which follow with appropriate evidence and arguments to substantiate the results. The first such topic will deal with the development of the basic equation to be employed under the assumptions made for the problem.

3. BASIC EQUATIONS AND ASSUMPTIONS

3.1. Basic Equations and Assumptions

Consider the complete Navier-Stokes equation for a general fluid motion wherein the static pressure at a point is presumed to be defined by the mean value of the pressure in the immediate neighborhood of the point. Thus the equation of motion for such a fluid element is written vectorially as:

$$\rho\left(\frac{\partial\bar{V}}{\partial t}+\frac{\partial\bar{V}}{\partial\bar{r}}\bar{V}\right)=-\frac{\partial p}{\partial\bar{r}}+\rho\bar{g}+\frac{\mu}{3}\bar{\nabla}a_I\left(\frac{\partial\bar{V}}{\partial\bar{r}}\right)+\mu\bar{\nabla}^2\bar{V} \qquad (3.1)$$

where p = pressure, in average value, for the fluid element at $\bar{r}$.

$\rho\bar{g}$ = external forces acting on the fluid element.

$a_I\left(\frac{\partial\bar{V}}{\partial\bar{r}}\right)$ = first (scalar) invariant of the velocity tensor, $\frac{\partial\bar{V}}{\partial\bar{r}}$.

The left hand term of equation (3.1) represents the inertia force (per unit volume) of the fluid element; and, the right side of the equation defines the pressure, external, and viscous (or frictional) forces (per unit volume) acting upon the fluid element as demanded by the conservation of momentum.

Recognizing the vectorial identities

$$\begin{aligned}\bar{\nabla}^2\bar{V}&=\text{grad div }\bar{V}-\text{curl curl }\bar{V}\\ \bar{\nabla}a_I\left(\frac{\partial\bar{V}}{\partial\bar{r}}\right)&=\text{grad div }\bar{V}\end{aligned} \qquad (3.2)$$

equation (3.1) simplifies to,

$$\rho\left(\frac{\partial\bar{V}}{\partial t}+\frac{\partial\bar{V}}{\partial\bar{r}}\bar{V}\right)=-\frac{\partial p}{\partial\bar{r}}+\rho\bar{g}+\frac{4}{3}\mu\ \text{grad div}\ \bar{V}-\mu\ \text{curl curl}\ \bar{V}. \quad (3.1a)$$

A further simplification is available through the identity,

$$\frac{\partial\bar{V}}{\partial\bar{r}}\bar{V}=\text{grad}\frac{V^2}{2}-\bar{V}\times\text{curl}\ \bar{V} \quad (3.3)$$

allowing (3.1a) to be written as,

$$\rho\left(\frac{\partial\bar{V}}{\partial t}+\text{grad}\frac{V^2}{2}-\bar{V}\times\text{curl}\ \bar{V}\right)=-\text{grad}\ p+\rho\bar{g}+$$

$$+\frac{4}{3}\mu\ \text{grad div}\ \bar{V}-\mu\ \text{curl curl}\ \bar{V}\ . \quad (3.1b)$$

The usual treatment for a physical flow problem will entail the following assumptions:

(1) $\bar{g}$, the external forces, acting on the fluid element are conservative; namely $\bar{g}$ is the gravitational force, and as such, the conservative field will possess a scalar potential: hence, $\bar{g}=\text{grad}\ gz$.

(2) The motion of the element is considered to be steady, hence all time derivatives vanish.

(3) The fluid motion can possess a potential, and thus will be of an inviscid nature; hence curl $\bar{V}=0$, or $\mu=0$.

(4). The pressure being dependent on position only can be expressed in terms of a potential P.

Under these assumptions, equation (3.1b) takes the form

$$\rho(\text{grad}\frac{V^2}{2})=-\text{grad}\ P+\rho\ \text{grad}\ gz\ . \quad (3.1c)$$

In addition to the equation of motion, since there is a minimum of three unknowns to be evaluated, two additional equations need to be specified. These relationships can be expressed by, (1) the continuity equation or statement of conservation of mass, and, (2) a thermodynamic relationship between the pressure and density for the general fluid element. These relationships may be stated as;

(1) the continuity equation

$$\frac{\partial \rho}{\partial t} + \text{div } (\rho \bar{V}) = 0, \tag{3.4a}$$

and, (2) the thermodynamic (barotropic) relationship

$$p = p(\rho), \quad \text{or } \rho = \rho(p). \tag{3.4b}$$

Identically, equation (3.1d) may be written as

$$\frac{\partial \rho}{\partial t} + \rho \text{ div } \bar{V} + \bar{V} \text{ grad } \rho = 0 \tag{3.1e}$$

which, for steady motion (assumption (2) above), reduces to

$$\rho \text{ div } \bar{V} + \bar{V} \text{ grad } \rho = 0 \, . \tag{3.1f}$$

Digressing, it is of interest to note that for the fluid to possess a potential, i.e. for curl $\bar{V} = 0$, the velocity $\bar{V}$ may then be written as the gradient of some scalar potential function. Thus, under assumption (2)

$$\bar{V} = \text{grad } \phi, \quad \text{where} \quad \phi = \phi(\bar{r}) \tag{3.5}$$

From the Newtonian definition of the speed of a finite disturbance through a compressible medium

$$c^2 = \frac{dp}{d\rho} \quad , \tag{3.6}$$

the following identity is written after separating this relationship and describing the gradient on both sides;

$$\text{grad } p = c^2 \text{ grad } \rho \quad . \tag{3.7}$$

Using equation (3.6), equation (3.1f) may be rewritten as

$$\rho \text{ div } \bar{V} + \frac{\bar{V}}{c^2} \text{ grad } p = 0 \quad . \tag{3.1g}$$

Combining (3.1c) and (3.1g), considering the fluid to be gaseous, thereby neglecting the external forces (i.e. assuming grad gz = 0), the result is

$$c^2 \text{ div } \bar{V} - \bar{V} \text{ grad } \frac{V^2}{2} = 0 \quad . \tag{3.8}$$

Or, in terms of the so called velocity potential, equation (3.5),

$$c^2 \text{ div grad } \phi - \text{grad } \phi \cdot \text{grad } \frac{V^2}{2} = 0 \tag{3.8a}$$

which is the basic equation of motion for a steadily flowing compressible inviscid gaseous fluid.

Equation (3.8) still needs to have the definition for c^2 specified. If it is assumed, as has been verified by experiment, that the value of the sonic speed can be determined from the Poisson state equation for an adiabatic flow, i.e.,

$$p = k \rho^{\gamma} \qquad \text{where } k = \text{a constant} \quad , \tag{3.9}$$

then from (3.6) the relationship for the speed of sound is found to be

$$c^2 = \frac{\gamma p}{\rho} \, . \tag{3.6a}$$

3.2. Potential Equation for Compressible Flow.

It is now desired to write equation (3.8) in its scalar form prior to the setting down of the potential compressible equation. If equation (3.8) is expanded, by the rules of vectors, the following equation results,

$$(c^2 - u_1^2)\ \frac{\partial u_1}{\partial x_1} + (c^2 - u_2^2)\ \frac{\partial u_2}{\partial x_2} + (c^2 - u_3^2)\ \frac{\partial u_3}{\partial x_3} - u_1 u_2 \left(\frac{\partial u_2}{\partial x_1} + \frac{\partial u_1}{\partial x_2} \right) - u_1 u_3 \left(\frac{\partial u_3}{\partial x_1} + \frac{\partial u_1}{\partial x_3} \right) - u_2 u_3 \left(\frac{\partial u_3}{\partial x_2} + \frac{\partial u_2}{\partial x_3} \right) = 0 \, . \tag{3.8b}$$

From assumption (3), (specifying that the field is irrotational; i.e., curl $\bar{V} = 0$), the following scalar equalities are apparent:

$$\frac{\partial u_2}{\partial x_1} = \frac{\partial u_1}{\partial x_2}, \quad \frac{\partial u_1}{\partial x_3} = \frac{\partial u_3}{\partial x_1}, \quad \frac{\partial u_3}{\partial x_2} = \frac{\partial u_2}{\partial x_3} \, . \tag{3.9}$$

If equation (3.8b) is divided by c^2, and if the results (3.9) are incorporated, then (3.8b) becomes

$$\left(1 - \frac{u_1^2}{c^2}\right)\frac{\partial u_1}{\partial x_1} + \left(1 - \frac{u_2^2}{c^2}\right)\frac{\partial u_2}{\partial x_2} + \left(1 - \frac{u_3^2}{c^2}\right)\frac{\partial u_3}{\partial x_2} - 2\left[\frac{u_1 u_2}{c^2}\ \frac{\partial u_2}{\partial x_1} + \frac{u_1 u_3}{c^2}\ \frac{\partial u_1}{\partial x_3} + \frac{u_2 u_3}{c^2}\ \frac{\partial u_3}{\partial x_2} \right] = 0 \tag{3.8c}$$

From assumption (3), whereby the flow field is assumed to be defined in terms of the scalar potential ϕ, the following velocity -

potential derivative equalities are defined as:

$$u_1 = \frac{\partial \phi}{\partial x_1} = \phi_{x_1}$$

$$u_2 = \frac{\partial \phi}{\partial x_2} = \phi_{x_2} \qquad (3.10)$$

$$u_3 = \frac{\partial \phi}{\partial x_3} = \phi_{x_3} \quad .$$

Inserting the quantities (3.10) into (3.8c) yields

$$\left(1 - \frac{u_1^2}{c^2}\right)\phi_{x_1x_1} - \left(1 - \frac{u_2^2}{c^2}\right)\phi_{x_2x_2} - \left(1 - \frac{u_3^2}{c^2}\right)\phi_{x_3x_3} -$$

$$- 2\left[\frac{u_1u_2}{c^2}\phi_{x_1x_2} + \frac{u_2u_3}{c^2}\phi_{x_2x_3} + \frac{u_1u_3}{c^2}\phi_{x_1x_3}\right] = 0 \; . \qquad (3.8d)$$

Equation (3.8d) is now the non-linear governing equation of motion for a steady compressible potential flow, meeting all the assumed requirements set forth in the above argument. It should be mentioned that equation (3.8d) is general in that no stipulation is placed on the definition of c, the speed of sound; c^2 as associated with (3.8d) is not as yet confined to a definite thermodynamic relationship. After specifying the state equation governing the flow, equation (3.8d) will then be rewritten to suitably define the nature of the governing equation's variables compared to the physical phenomena of the flow process.

3.3. Thermodynamic Relations for an Isentropic State (Poisson Flow).

Let equation (3.1c) be examined under the conditions that the flow is steady, the media is a compressible gas following the isentropic law, and that the effects of gravity are negligible. Then, if (3.1c) and (3.4a) are combined, and if the reduced governing equation of motion is integrated along a characteristic line of the flow (i.e. a streamline), the result is

$$\int d\left(\frac{V^2}{2}\right) + \int \frac{dp}{\rho} = \text{constant} \quad . \tag{3.11}$$

In general, for Poisson steady flow, (3.11) takes the form

$$\frac{V^2}{2} + \left(\frac{\gamma}{\gamma - 1}\right) \frac{p}{\rho} = \text{constant} \tag{3.12}$$

and, from (3.6a) equation (3.12) may also be written as,

$$\frac{V^2}{2} + \frac{c^2}{\gamma - 1} = \text{constant} \quad . \tag{3.13}$$

Applying to (3.13) the condition that the flow originates at a state $(\ )_o$, denoting a rest condition, and flows into a region where the flow velocity is V, then (3.13) becomes

$$\frac{V^2}{2} + \frac{c^2}{\gamma - 1} = \frac{c_o^2}{\gamma - 1} \quad . \tag{3.13a}$$

If in (3.13a) the left hand member is to describe a region in which $c = 0$, that is, the maximum value of flow velocity attainable (or $V = V_{max}$), then, it follows that

$$\frac{V^2_{max}}{2} = \frac{c_o^2}{\gamma - 1} \, . \tag{3.14}$$

If now (3.13a) is to define a flow condition wherein the local flow velocity $\overline{V}$, and the local sonic speed c, are equal (or, in nature, the concept of a sonic throat[28] as defined by the continuity relation for steady Poisson flow of a streamtube), then

$$V = c = c^* \quad \text{(the critical flow condition)}$$

and

$$c^{*\,2} = \frac{2c_o^2}{\gamma + 1} \, . \tag{3.15}$$

It can readily be shown that c^* separates the regions of local subsonic and local supersonic flow. Specifically if $c^* > c$, then $\overline{V}^* > \overline{V}$, and thus the Mach number ($M_L = V/c$) is less than one or the flow is locally subsonic. Conversely, if $c^* < c$, then $\overline{V}^* < \overline{V}$ and hence $M_L > 1$ (the flow is locally supersonic), then the condition necessary for supersonic flow is that $V > c^*$.

It should be mentioned that equation (3.14) represents a physical situation which is for all practical purposes unattainable. A necessary condition that $c = 0$, is that $\rho = 0$, and therefore that $p = 0$. This is the condition for a flow in contact with, or flowing into, a region of perfect vacuum. Equations (3.14) and (3.15) are not intended to indicate that two such physical conditions exist for an arbitrary streamline, but merely state that two such conditions could possibly occur for the arbitrary streamline. $\overline{V}_{max}$ represents the maximum attainable flow velocity, under the assumptions provided, which could possibly occur and thus can nowhere be exceeded.

On combining (3.14) and (3.13a) the following relationship is obtained,

$$c^2 = \frac{1}{2}(\gamma - 1)(V^2_{max} - u_1^2 - u_2^2 - u_3^2) \qquad (3.16)$$

or, in terms of the rest condition, defined through the value of sonic speed c_o,

$$c^2 = c_o^2 - \frac{\gamma - 1}{2} V^2 = c_o^2 - \frac{\gamma - 1}{2}(u_1^2 + u_2^2 + u_3^2) . \qquad (3.16a)$$

Taking the ratio of (3.14) to (3.15) the following relationship is obtained

$$\frac{V^2_{max}}{c^{*2}} = \frac{\gamma + 1}{\gamma - 1} \qquad (3.17)$$

and, (3.16) has the alternate form,

$$c^2 = \frac{\gamma + 1}{2} c^{*2} - \frac{\gamma - 1}{2}(u_1^2 + u_2^2 + u_3^2) . \qquad (3.16b)$$

3.4. Potential Equation of Motion for Axially Symmetric Flow.

For the case of axially symmetric flow, for example flow about a body of revolution at zero yaw and zero pitch, the governing equation is defined in its simplest form by writing the equation of motion in cylindrical coordinates.

In place of equations (3.10) and (3.4a), with the restriction of steady motion placed on (3.4a), write

$$u_1 = \frac{\partial \phi}{\partial x}, \quad v_1 = \frac{\partial \phi}{\partial r}, \quad w_1 = \frac{1}{r}\frac{\partial \phi}{\partial \omega} \qquad (3.10a)$$

and

$$\frac{\partial}{\partial x}(\rho u_1) + \frac{1}{r}\frac{\partial}{\partial r}(r\rho v_1) + \frac{1}{r}\frac{\partial}{\partial \omega}(\rho w_1) = 0 \qquad (3.4c)$$

from the geometrical considerations of the coordinate system as pictorially presented below.

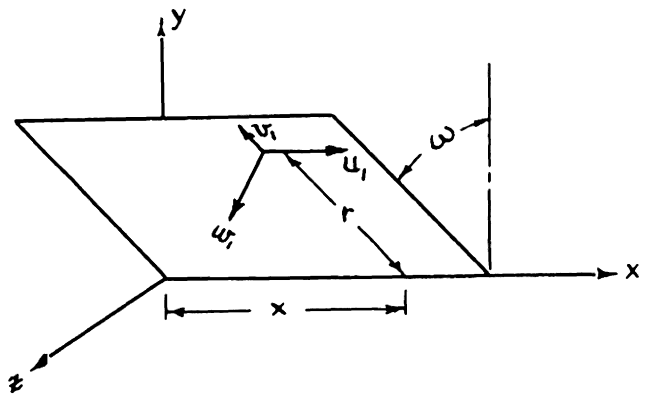

Rewriting equation (3.8d), to conform with the cylindrical coordinate notation, the governing potential equation obtained is,

$$(1-\frac{u_1^2}{c^2})\,\phi_{xx}+(1-\frac{v_1^2}{c^2})\,\phi_{rr}+(1-\frac{w_1^2}{c^2})\,\frac{\phi_{\omega\omega}}{r^2}-2\left[\frac{v_1w_1}{r^2c^2}\,\phi_{r\omega}+\right.$$

$$\left.+\frac{u_1w_1}{r^2c^2}\,\phi_{x\omega}+\frac{u_1v_1}{c^2}\,\phi_{xr}\right]+(1+\frac{w_1^2}{c^2})\,\frac{\phi_r}{r}=0\,. \qquad (3.8e)$$

For the special case of axial symmetry, deduced from the cylindrical coordinate relationship just defined, the condition of flow is such that the general velocity vector $\overline{V}=\overline{V}(x,r)$. That is, flow is not dependent upon the spatial rotational component ω ; rather, the flow is identical for all meridian planes (planes containing the axis of generation, or the x-axis), and study need be made only for variations in the x- and r- directions. Thus, by the hypothesis of such a flow, equations (3.4c) and (3.8e) are reduced to

$$\frac{\partial}{\partial x}(r\rho u_1)+\frac{\partial}{\partial r}(r\rho v_1)=0 \qquad (3.4d)$$

and

$$\left.\begin{aligned}&\left(1-\frac{u_1^2}{c^2}\right)\phi_{xx}+\left(1-\frac{v_1^2}{c^2}\right)\phi_{rr}-\frac{2u_1v_1}{c^2}\phi_{xr}+\frac{\phi_r}{r}=0\\ \text{or,}\quad&\left(1-\frac{u_1^2}{c^2}\right)\frac{\partial u_1}{\partial x}+\left(1-\frac{v_1^2}{c^2}\right)\frac{\partial v_1}{\partial r}+\frac{v_1}{r}=\frac{2u_1v_1}{c^2}\frac{\partial u_1}{\partial r}\end{aligned}\right\}\quad(3.8f)$$

It is readily noted that equation (3.8f), like (3.8e) and (3.8d), is a nonlinear differential equation due to the presence of terms like $\frac{u_1^2}{c^2}\phi_{xx}$, which, due to the existence of a velocity potential, can be written as $\frac{\phi_x^2}{c^2}\phi_{xx}$.

The nature of equations (3.8d) and (3.8e) depend upon the physical nature of the flow. In the subsonic compressible case ($M_L < 1$) the governing equation is of the elliptic type; for supersonic compressible flow ($M_L > 1$) the equation is of the hyperbolic type; and for transonic compressible flow ($M_L \approx 1$), the equation is of the parabolic or mixed type. Due to the inherent mathematical difficulties encountered in solving non-linear differential equations (like the aforementioned) the usual treatment is to linearize the governing equation, thereby simplifying the mathematics and readily minimizing the difficulty of solution.

3.5. Linearization of the Equations of Motion by Small Perturbation Concepts.

The concept of perturbation theory is based upon the assumption that the steady undisturbed flow field, characterized by the velocity

components

$$u_1 = U$$
$$v_1 = 0 \qquad (3.17)$$
$$w_1 = 0$$

is disturbed by the presence of a body, in the flow field, such that new velocity componants must be described. These are given as

$$u_1 = U + u$$
$$v_1 = v \qquad (3.18)$$
$$w_1 = w$$

where the velocity components u, v, w are the so-called "perturbational velocities". It is assumed here that these velocity components are in general small, or

$$\frac{u}{U}, \frac{v}{U}, \frac{w}{U} \ll 1 \, . \qquad (3.19)$$

For the case of axially symmetric flow these equations are reduced by the condition that the component of velocity w = 0 in all cases.

With the assumption of equation (3.19) the non-linearity of the governing equation (3.8f) may be removed, or the equation of motion may be linearized. To accomplish this linearization let all powers of the perturbations, greater than the first, be deleted, thus allowing the equation of motion to reduce to

$$(1 - M_\infty{}^2)\frac{\partial u_1}{\partial x} + \frac{\partial v}{\partial r} + \frac{v}{r} = \frac{M_\infty u}{c_\infty}\left[(\gamma + 1)\frac{\partial u_1}{\partial x} + (\gamma - 1)\frac{\partial v}{\partial r}\right] \qquad (3.20)$$

or

$$(1 - M_\infty^2)\frac{\partial u}{\partial x} + \frac{\partial v}{\partial r} + \frac{v}{r} = \frac{M_\infty u}{c_\infty}\left[(\gamma + 1)\frac{\partial u}{\partial x} + (\gamma - 1)\frac{\partial v}{\partial r}\right] \qquad (3.20)$$

where: $M_\infty = \frac{U}{c_\infty}$, and from (3.13) for a free-stream condition (U, c_∞),

$$c^2 = c_\infty^2 + \frac{\gamma - 1}{2}(U^2 - V^2) \; . \qquad (3.21)$$

It is quite apparent that equation (3.20) is as yet non-linear, due to the presence of the terms on the right. A complete linearization is afforded only if the right hand member vanishes. Thus the linearization of (3.8f) is accomplished only if

$$(1 - M_\infty^2)\frac{\partial u}{\partial x} + \frac{\partial v}{\partial r} + \frac{v}{r} = 0 \; . \qquad (3.20a)$$

Of these equations, the condition (3.20a) may be applied for purely subsonic and supersonic flow types, while equation (3.20) must be used for the near sonic case. In a section to follow an investigation will be brought forth to show in what range of subsonic flow this linearization is applicable, and for what range the linearized theory will have to be replaced by another approach.

The usual manner of solving the linearized equation is to show that such an equation can be related to known solutions, and information then extracted from these solutions. Actually, equation (3.20a) can be shown to exhibit a marked similarity to the Laplace equation, the principle difference being that a modified coordinate system will be indicated for the compressible case. To illustrate, if

$$\beta^2 = 1 - M_\infty^2 \qquad (3.22)$$

and if the perturbation flow is described in terms of a potential (see equation (3.5)), then the flow field may be represented by the potential function

$$\phi = Ux + \varphi \ , \tag{3.23}$$

where φ is the perturbation potential, bearing the relations

$$u = \frac{\partial \varphi}{\partial x}$$

and

$$v = \frac{\partial \varphi}{\partial r} \ . \tag{3.24}$$

If these relations are employed in (3.20a) the resulting equation is

$$\frac{\partial^2 \varphi}{\partial x^2} + \frac{1}{\beta^2} \frac{\partial^2 \varphi}{\partial r^2} + \frac{1}{\beta^2 r} \frac{\partial \varphi}{\partial r} = 0 \ , \tag{3.25}$$

which may be rewritten as

$$\frac{\partial^2 \varphi}{\partial x^2} + \frac{\partial^2 \varphi}{\partial r_1^2} + \frac{1}{r_1} \frac{\partial \varphi}{\partial r_1} = 0 \ . \tag{3.25a}$$

Equation (3.25a) is the Laplace equation for a coordinate system (x, r_1) where r_1 and r are related by

$$r_1 = \beta r = \sqrt{1 - M_\infty^2}\, r \ . \tag{3.26}$$

Physically, it is seen that the coordinate r_1 is a reduced coordinate compared to r for subsonic flow. Thus the body described by (x, r_1) will have the same length as a body described by (x,r), but the former body will be more slender than the original body (x,r). Such a

coordinate relationship is said to be affinely related; or, one body may be affinely transformed into another body (similar in shape) by the affine transformation

$$x \rightarrow x$$
$$r \rightarrow r_1 = \beta r \quad . \tag{3.27}$$

3.6. Linearized Pressure Coefficient

To describe the pressure distribution over the body as influenced by the dynamic action of the flow stream, recourse is made to the pressure coefficient defined as

$$C_p = \frac{p_L - p_\infty}{q_\infty} = \frac{(p_L - p_\infty)}{\frac{\gamma\, p_\infty\, M_\infty^2}{2}} = \frac{2}{\gamma\, M_\infty^2}\left(\frac{p_L}{p_\infty} - 1\right). \tag{3.28}$$

If the pressure ratio p_L/p_∞ is taken from the isentropic flow relations (and written as a function of Mach number), and if c is related to c_∞ through the Bernoulli equation then

$$\frac{p_L}{p_\infty} = \left(\frac{c}{c_\infty}\right)^{\frac{2\gamma}{\gamma - 1}} , \tag{3.29}$$

and (3.28) becomes

$$C_p = \frac{2}{\gamma\, M_\infty^2}\left\{\left[1 + \frac{\gamma - 1}{2} M_\infty^2 \left(\frac{U^2 - V^2}{U^2}\right)\right]^{\frac{\gamma}{\gamma - 1}} - 1\right\}. \tag{3.28a}$$

And, in terms of the perturbation components (3.18),

$$C_p = \frac{2}{\gamma\, M_\infty^2}\left\{\left[1 - \frac{\gamma - 1}{2} M_\infty^2 \left(\frac{2u}{U} + \frac{u^2 + v^2}{U^2}\right)\right]^{\frac{\gamma}{\gamma - 1}} - 1\right\}. \tag{3.28b}$$

Before complete linearization is carried out, equation (3.28b) needs to be expanded and the order of magnitude of the velocities inspected.

From the continuity relationship, specialized for axially symmetric steady flow, it is seen from (3.4c) that

$$\frac{\partial(\rho u_1)}{\partial x} + \frac{\partial(r\rho v)}{r\partial r} = 0 \quad . \tag{3.30}$$

Linearization is carried through on the basis that the boundary conditions may be evaluated near the axis due to the smallness of the perturbation quantities and the consequent slenderness of the body. With this in mind it follows that the second term of (3.30) should be of the same order of magnitude as any other term, or

$$r \frac{\partial u}{\partial x} \propto \frac{\partial(rv)}{\partial r}$$

Since $\partial u/\partial r$ is finite it follows that the boundary conditions consistent with small quantities will demand that

$$\lim_{r \to 0} \frac{\partial(rv)}{\partial r} \approx 0 \quad .$$

This in turn implies that in the vicinity of the body axis

$$rv = f(x) \quad . \tag{3.31}$$

Let v be represented by a series expansion, say

$$v = \frac{f_0}{r} + f_1 + f_2 r + \cdots \tag{3.32}$$

evaluated in the region of the axis. Then with u having small gradients

throughout, it follows that this component may likewise be expressed as a series. That is

$$u = g_o + g_1 x + g_2 x^2 + \cdots ,$$

where the $g_i = g_i(r)$. The correlation between these expansions may be defined from the condition of irrotationality

$$\frac{\partial u}{\partial r} = \frac{\partial v}{\partial x}$$

leading to the relationship,

$$\frac{\partial u}{\partial r} = \frac{f_o'}{r} + f_1' + f_2' r + \cdots$$

after differentiating (3.32). This expression may be integrated to yield

$$u = f_o' \ln r + f_1' r + f_2' r^2 + \cdots \qquad (3.33)$$

Since (3.32) and (3.33) show the perturbation components to be of different order, then the linearization of C_p will require that to the first order of approximation*

$$C_p = -\frac{2u}{U} - \frac{v^2}{U^2} \quad . \qquad (3.34)$$

Equation (3.34) is seen to be functionally dependent upon both perturbation velocity components. Thus the difference between the axially symmetric flow case and the two-dimensional flow case is indicated by the disappearance of the second term on the right side

---

* Note: A more rigorous approach to this first order approximation of the pressure coefficient is outlined in reference (48).

of (3.34) for linearized two-dimensional flow. This implies that the spatial flow case is more sensitive to variations of local speed than is the corresponding two-dimensional case. Also, it is recognized that the radial velocity component can assume a magnitude as great or greater than the axial component of perturbational velocity. (It is noted in the literature that (3.34) gives closer agreement to experiment than the simpler linear relation $C_p = -\frac{2u}{U}$.)

Since the body of revolution could be assumed to experience a variety of flow types, a description of these will be presented next.

4. FLOW TYPES ABOUT A BODY OF REVOLUTION

A body of revolution placed in a moving stream of steady, compressible fluid will have forces acting upon it dependent upon the Mach number classification of the flow. In a general sense such classifications could be described as potential incompressible, subcritical compressible, supercritical and transonic compressible flow. The differences in these flow types will be discussed under their respective headings in the following paragraphs, with the additional stipulation that the body is at zero angle of yaw and pitch.

4.1. Incompressible Flow.

The classical study of fluid flow problems is primarily concerned with this classification of flow. Generally, unless boundary layer phenomenon and/or heat transfer is to be considered, this approach to the problem demands the flow field be irrotational (thus inviscid). It is here that Mach number effects are completely ignored, for in this classification the concept of sonic velocity is deleted, and in fact the free-stream Mach number is considered to be infinite. A physical comparison to this flow regime is approximated in experimental work when investigations are carried out at low speeds in a wind tunnel. It is of interest to note that there exists a general and fundamental difference in the two- and three-dimensional types of flow under this classification. In the two-dimensional case the fluid is constrained to move about the body with all such

constraints being laterally defined. That is, the fluid can only deviate from the body in one lateral direction relative to the body proper. In the three-dimensional case this restriction is not present in that the fluid is free to flow about the body in any fashion desired. That is the restraints on flow direction relative to the body are removed. It follows immediately that for bodies of similar cross-section, the three-dimensional streamwise gradient of velocity is not so great as in the two-dimensional case. This is easily recognized if the two-dimensional case of the circular cylinder, whose axis is normal to the flow direction, is compared to the corresponding case of a sphere in a three-dimensional flow. As is well known, the maximum local velocity over the circular cylinder occurs at the maximum thickness station and has a magnitude equal to twice that of the undisturbed stream. For the sphere the maximum velocity occurs at the same streamwise position but has a magnitude of only 1.5 times the free-stream speed. This difference in maximum values clearly indicates the effects of constraint on the fluid flow. Since the unrestrained flow does not attain the same acceleration over the body, it therefore follows that the three-dimensional flow has a "relieving effect" not given to the constrained two-dimensional case.

It is of course obvious that the fluid flow for a compressible subsonic case retains most of the characteristics of the incompressible case but must experience the effect of compressibility as well.

4.2. Subcritical Flow

Removing the assumption of an incompressible fluid leads next to the case of a fluid motion at speeds less than near sonic, or the subcritical flow case.

Here, in addition to the body thickness effect, which can be described fundamentally by an incompressible study, the so-called Mach number effect must also be included to more fully describe the nature of flow patterns in the vicinity of a body. It is in this study that the linearized equation of motion is utilized to predict the aerodynamic pressures and forces acting on a body shape. Generally the problem is approached on the perturbational velocity concept, this leading either to the technique of solving the problem by an affined transformation of the body coordinates (such as the Prandtl-Glauert Rule in two-dimensional flow), or by more direct means though such solutions might require numerical, or graphical analyses. No matter what the ultimate approach may be, the effects of both body thickness and compressibility must be included in the procedure.

It is now well known, and irrefutibly demonstrated by experiment, that any solution technique has only limited applicability in the subsonic Mach number range - - and, that though the techniques are similar for both two and three-dimensional flow cases there is a distinct difference between them. It is for this reason that the Prandtl-Glauert, or Karman-Tsien, method does not apply in the three-dimensional flow case. Though it was argued for some time that these

rules were applicable to the axially symmetric flow case, it has since been proven (and demonstrated experimentally) that there does exist this distinct difference. The proper form of the linearized-affined transformation approximation to be used for three-dimensional flow is the Gothert Rule[39], as was pointed out by Sears, in his second note on compressible flow[45].

Granting that such approximations exist, and that there are differences in flow types dictating their proper use, little has been said about the range of Mach numbers for which they apply. Assumptions have been made and conclusions have been drawn from experiment that these rules do have upper limits of applicability; in fact the very assumption of the linearized equation of motion in their derivation indicates the restriction. This follows from the known condition that linearized theory fails completely at sonic speeds, and from the necessity of retaining non-linear terms in the transonic equation. Still with these known restrictions nothing definite has been stated concerning the upper limit as such. One of the topics in this thesis concerns an argument which defined this upper limit as the lower critical free-stream Mach number. The conclusion drawn from this study is that the linear theory can be applied up to and including, but not beyond, the value of free-stream Mach number for which local sonic conditions first occur on the body. Then, for the three-dimensional flow case, Gothert's Rule is a good approximation for predicting pressures, forces, etc. acting on a three-dimensional body in a subsonic compressible flow.

Since the problem dealt with herein is a three-dimensional problem, Gothert's Rule is employed to obtain the approximate values of pressures, etc. through the subsonic speed range. To assure the most accurate results it has been necessary to establish the form of the rule to use for this work and to establish the range of application.

Before describing the flow field type which next most logically occurs a discussion of the supercritical fluid will be presented.

4.3. Supercritical Flow

The supercritical flow case considers the problem of supersonic flow over the body under investigation. Though this regime may be classified in several categories, the descriptions here will be limited to those applicable to the lower range of free-stream Mach numbers.

In a study of this type the linearized approximation may be employed to advantage for obtaining results which show good agreement with physical measurements. Differences exist for the two-dimensional and three-dimensional flows as for instance the Ackeret solution in the two-dimensional case and the solution of Taylor and Maccoll[65] in the other. The basic differences previously mentioned are still apparent in the supercritical range, and these differences are shown in the theories which apply. For this type of flow the free-stream, and the body flow, are both characterized by Mach numbers which are greater than unity; shock waves (discontinuities) are present in the field of flow, and expansion regions occur where geometric

configurations so dictate. The shape of the bow shock is initially straight at the nose of the body, provided the body is pointed. These last statements are exact for the two-dimensional case, though for the three-dimensional case there may be some exceptions. Depending upon the value of the free-stream Mach number, there can exist an imbedded region of subsonic flow at the conical surface, even with an attached shock wave. Though conical flow theory is presumed to exist, this subsonic flow condition is present for a range of free-stream Mach numbers just slightly greater than the attachment value. In tracing the flow history from attachment on, the surface Mach number (or local Mach number) is first subsonic and later supersonic. This condition is evident from the solution as given by reference 65 - - at attachment the flow downstream of the shock is completely subsonic, and as the free stream Mach number increases, this subsonic region diminishes and becomes imbedded between a supersonic region behind the shock wave and the body surface. The explanation of such an action is given in several references (see, for instance, reference 66). Some points of the above arguments will be altered if the body shape is blunted, but for pointed bodies the generalities just described are applicable.

The transonic flow case remains to be discussed. It is presented next.

4.4. The Critical Flow Case.

Categorically the transonic regime is defined by that range of Mach numbers between the sub- and super-critical flow types.

At the upper limit of the subcritical range of Mach number, local sonic speed has been attained on the body. Let it be assumed that the body is pointed and that at least the forward tip of the body is conical in shape. After reaching sonic flow conditions on the body, and recognizing that disturbances can only be transmitted through the fluid at sonic speed, this acoustical region acts like a barrier to stop downstream disturbances from being transmitted upstream to the body surface. Thus it follows that as long as a sonic zone is present the conditions of flow upstream of this region are not influenced by the conditions downstream. If this is coupled with the argument presented in the Introduction concerning stationarity of Mach number on the body surface, then it becomes apparent that the local pressures experienced by the body cannot change until the character of the surrounding fluid changes. Hence, until the bow shock reaches the body the flow adjacent to the body cannot alter its characteristics. Or, if the local pressures are taken in ratio to the local sonic pressure, that is the ratio p_L/p^*, an invariant will be established which holds so long as the bow wave does not attach. Attachment will alter this argument due to the effect on the flow in the immediate vicinity of the body proper. It follows that ideally there exists a range of Mach numbers, from the lower free-stream critical value to at least some value slightly below attachment Mach number, for which the local body conditions are fixed. Hence, the concept of stationarity of local Mach number spans this range of free-stream values

which extends from a subsonic, through sonic, to a supersonic value of free-stream Mach number. In the case of a real fluid this concept is not exact, but is certainly a very close approximation to the true physical picture. This phenomenon is not entirely new; Prandtl recognized the likelyhood of such in his earlier works on compressible flow. There is also experimental evidence which verifies the stationarity concept, as is indicated in the following quotation from reference 63 on the problem of transonic flow past a conical nose:

> "Some features of this problem are similar to the transonic wedge flow . . . For example, the sonic line passes through the shoulder point, and the principle of stationarity at $M_\infty = 1$, that is $(dM_L/dM_\infty)\big|_{M_\infty = 1} = 0$, applies as well for a conical tip".

Throughout all of the discussion on flow types it has been assumed that the flow fields are potentially defined. In other words the premise that the flow is irrotational has been taken for granted. In the first two cases this assumption is quite reasonable and approximately true even for a real fluid if the region of the boundary layer and the region of downstream separation are excluded from the investigation. However, for the transonic flow case this assumption cannot be utilized for the entire range of Mach numbers. So long as the head shock remains nearly normal, that is as long as its radius of curvature is large, the irrotational premise is a reasonable assumption. But, once the curvature reaches the order of

magnitude of the body length the flow field behind the head shock alters significantly and the assumption of potential flow fails. The fluid then begins to act as if it originated from a source downstream of the body with varying lateral intensity, each outward layer being greater in speed than its neighbor lying closer to the body surface. One consequence of this condition is that the constancy of p_L/p^* no longer holds, and thus any prediction depending on this invariancy is no longer true. A study of this rotational field has been made by Vincenti and Wagoner[54,55] for the two-dimensional flow about a wedge shaped profile. This rotational condition for the flow puts a restriction on the governing equation, such that due to the complex nature of the resulting problem the solution requires a step-by-step calculation. As yet such a problem for the case of a cone (or other three-dimensional body) has not appeared in the literature to the author's knowledge.

It has previously been pointed out that the use of the linearized equation of motion will not suffice for the critical flow case; also it has been stated, and can be seen from equation (3.20a), that the theory fails at $M_\infty = 1$. The degeneracy of linear theory in transonic flow clearly indicates the inadequacy of retaining only linear terms in the equation of motion. In fact the theory predicts a continual accumulation of pressure, until finally an infinite pressure appears to exist locally. In order to obtain a solution, it is therefore necessary to retain non-linear terms in the governing equation since

the linear equations fails. Which terms should be held in the equation can only be justified according to the physical structure of the flow field. Since strong gradients exist in the streamwise direction, and smaller ones exist in the lateral directions, the larger derivative quantities are necessarily retained due to their superiority. It has been shown that only a single term needs to be retained for the transonic solution, not that the single term improves the accuracy of the solution, but rather that it keeps the solution from degenerating completely. The retaining of a single quadratic term allows for the dependency of local pressures on local conditions. This then prevents the accumulation of infinite disturbances, leading to infinite pressures, for the body at sonic and near sonic speeds.

The very non-linear nature of the governing equation indicates the difficulty encountered in solving the transonic problem. Though much of this difficulty has been overcome by the approach made in reference 61, only limited applicability persists for the theory developed there.

In the interest of experimental testing, the discrepancy of linear theory closely parallels the difficulty encountered in testing at near sonic speeds. With conventional wind tunnel construction it was found that as the free stream approached sonic speed the local supersonic zone on the body expanded until finally it reached the tunnel boundaries. Once this happened, the tunnel became choked and no further acceleration of the stream could be produced. It was the

realization that the pressure increase, associated with the expanding supersonic imbedded region, which was choking the flow that led to the transonic vented section design. Recognizing that transonic testing would be possible if the pressure accumulation could be eliminated led naturally to the design of slotted and perforated walls for the working section. The ultimate results of such designs have been pointed out in the introductory remarks.

Much of the above discussion has been devoted to the physical aspects of the flow field and the associated phenomena which occur there and in the neighborhood of a pointed body located therein. The present analysis depends to a large extent on these physical happenings. A basic premise in this method of approach, for transonic flow about the cone-cylinder, is the constancy of local Mach number with increasing free-stream Mach number through the critical range. In the formulation of the solution the fluid is assumed to be isentropic throughout its extent so long as shock waves are not present upstream of the body. Once such discontinuities are apparent, the isentropic assumption is assumed to prevail for the region of flow up to the wave, and downstream of the wave, but not across the wave itself. Since initially the wave is nearly normal it will be presumed that the normal shock relations may be utilized to cross the wave structure proper. It is recognized that such an assumption fails to hold once the wave has appreciable curvature, and for this reason the analysis will be stopped before the free-stream Mach number has reached the attachment value. Thus the range of Mach numbers

considered is not the complete critical span, but does include subsonic, sonic and supersonic values. To this end the analysis will afford a continuous solution for such variables as the drag coefficient from subsonic to some supersonic speed - - a range not covered in general by other existing theories.

One final point needs to be discussed before leaving the discussion on the transonic flow range. That point concerns the value of Mach number which will be considered as the upper limit of applicability for the present analysis. That is, it is necessary to identify the "upper critical Mach number", or that value of free-stream Mach number for which the stationarity of local Mach number ceases to be applicable.

Under the stationarity concept it has been assumed that the free stream lower critical value was the onset of the constancy of local Mach number. Granting that the upper limit will be given as a free-stream supersonic value, then if the Mach number behind a bow wave is as much below unity as the value ahead of the wave is above unity, an approximation can be made from the normal shock relation for Mach numbers. This relation is

$$M_2^2 = \frac{2 + (\gamma - 1) M_1^2}{2\gamma M_1^2 - (\gamma - 1)} \tag{4.1}$$

where M_1 is now the free-stream upper critical value and M_2 is the value of Mach number behind a normal wave. Identifying M_2 as the lower critical value of M_∞, then M_1 will be approximately the upper

critical value of free-stream Mach number. Thus the assumed range for critical flow will be, according to the above equation, $(M_1 < 1 < M_2)$; this being the range of free-stream Mach numbers for which the Principle of Stationarity of local Mach number is valid.

Bryson[53] offers an argument that a better approximation to this range is given by modifying equation (4.1) as follows:

$$1 - M_2^2 = 1 - \frac{2 + (\gamma - 1) M_1^2}{2\gamma M_1^2 - (\gamma - 1)} \tag{4.2}$$

or, after manipulation, retaining only first order terms in M^2, this reduces to

$$1 - M_2^2 \approx M_1^2 - 1 \tag{4.3}$$

which, for M_1, $M_2 \approx 1.0$, further reduces to

$$1 - M_2 \approx M_1 - 1 \, . \tag{4.4}$$

The last equation would certainly hold for small slender bodies where the lower critical Mach number is quite close to unity, but for bodies of more blunted profile the approximation to the upper critical value given by equation (4.1) would be more nearly correct. For this reason the upper limit value will be described by the first equation (4.2) rather than the subsequent approximations (4.3) or (4.4).

5. LIMITATIONS OF THREE-DIMENSIONAL LINEAR THEORY FOR COMPRESSIBLE FLOW

5.1. Introduction

Linear aerodynamic theory can be defined from acoustic theory, wherein disturbances propagate away from an acoustic center at a rate equal to the speed of sound for the fluid in which the center is located. Thus, in aerodynamics, a body creating disturbances, by its presence in a gaseous fluid, will have these disturbances propagate at the sonic speed of the gas. If the gas is at rest, and if the body has motion, the disturbances will move away from the body, or be left behind the body, or remain with the body depending upon the speed. When the body travels at, or near to, the speed of sound these disturbances remain with the body, causing an increase in pressure, and thus rendering linear theory inapplicable since such a simplified theory fails to indicate correctly the pressure increase. It is known that local disturbances being dependent on local flow conditions are defined by variations of a non-linear nature; hence only when these non-linearities become unimportant can the simpler theory apply. In the transonic range, where local conditions are not closely related to stream conditions, non-linear terms become important thereby forcing a departure from linear considerations; and, making the solution of the governing equation more complicated since a solution cannot be constructed by simply adding elementary solutions.

One of the most frequent attempts at defining compressible phenomena has been the "correcting" of incompressible quantities wherein the correction factors are defined by relating similar geometric configurations to each other. One such well-known method is the Prandtl-Glauert Rule, applicable to slender geometrically similar two-dimensional bodies. Several papers in the past have attempted to use this method for the three-dimensional case, without good result. This is especially true for very slender bodies where, for instance, the pressures are practically independent of Mach number. In this rule, the pressures are seen to be more dependent on Mach number than on body thickness. However, in the spatial case the converse is true, and hence, this rule will overpredict the pressures for the body of revolution. Gothert[39] has shown the proper method for treating the spatial case which, though similar to the two-dimensional case, is less dependent on Mach number. Neither case, unfortunately, indicates where the practical limit of correction should cease. Therefore, to more adequately define the limit of applicability, the following discussion is presented.

5.2. Limit of Linear Theory

For axially symmetric potential flow of a compressible, steady, irrotational fluid the equation of motion is given by equation (3.8f),

$$\left(1 - \frac{u_1^2}{c^2}\right) \frac{\partial u_1}{\partial x} + \left(1 - \frac{v^2}{c^2}\right) \frac{\partial v}{\partial r} + \frac{v}{r} = \frac{2u_1 v}{c^2} \frac{\partial u_1}{\partial r} \qquad (3.8f)$$

where

$$u_1 = U + u = \frac{\partial \phi}{\partial x} \qquad u = \frac{\partial \varphi}{\partial x}$$

$$v = v = \frac{\partial \phi}{\partial r} \quad \text{and} \quad v = \frac{\partial \varphi}{\partial r}$$

for $\phi = Ux + \varphi$

and

$$\frac{u_1}{c} \approx M_L \ , \quad \frac{U}{c_\infty} = M_\infty \ .$$

It will now be assumed, as before, that the disturbance values are of a magnitude such that the products and powers greater than the first of these quantities are vanishingly small. Such a consideration is the linearization process, necessary to delete the nonlinearity of (3.8f) typified by terms like $\frac{u_1^2}{c^2} \frac{\partial u_1}{\partial x}$.

The continuity equation for the axially symmetric flow case is

$$\frac{\partial}{\partial x}(r\rho u_1) + \frac{\partial}{\partial r}(r\rho v) = 0 \ . \tag{3.4f}$$

From the Bernoulli equation the velocity of sound, in terms of the stream conditions is given as (see equation (3.16a),

$$c^2 = c_\infty^2 + \frac{\gamma - 1}{2}(U^2 - V^2) = c_\infty^2 - \frac{\gamma - 1}{2}(2uU + u^2 + v^2) \ .$$

In linearizing the components of (3.8f), the following approximations are made

$$\frac{u_1^2}{c^2} \approx \frac{U^2 + 2uU}{c^2} \approx M_\infty^2 + \frac{(\gamma - 1) M_\infty^2 + 2}{c_\infty^2} \, u \, U =$$

$$= M_\infty^2 \left[1 + \left((\gamma - 1) M_\infty^2 + 2 \right) \frac{u}{U} \right] \tag{5.1}$$

$$\frac{v^2}{c^2} \approx 0 \tag{5.1}$$

$$\frac{u_1 v}{c^2} \approx \frac{M_\infty v}{c_\infty} = \frac{M_\infty^2 v}{U} \quad .$$

When a slender symmetric body produces the disturbances, the values (5.1) may be further reduced if it is assumed that the body flow must remain tangent to the body. Thus the velocity v is of order of magnitude of the body thickness which is considered small compared to the body length. Now, through (5.1) equation (3.8f) can be restated as

$$\left[1 - M_\infty^2 - M_\infty^2 \left((\gamma - 1) M_\infty^2 + 2\right) \frac{u}{U}\right] \varphi_{xx} + \varphi_{rr} + \frac{\varphi_r}{r} = 2M_\infty^2 \frac{v}{U} \varphi_{xr} \tag{5.2}$$

which is non-linear due to the nature of the first term and the right hand member of the equation. This equation is equivalent to stating that

$$1 - M_L^2 \approx 1 - M_\infty^2 \left((\gamma - 1) M_\infty^2 + 2\right) \frac{u}{U} - M_\infty^2 \tag{5.3}$$

if it is assumed that the local Mach number is predominately dependent on the velocity component u_1 for the slender body. Since the velocity component v is small (of the order of body thickness) then the right member of (5.2) is of lesser order of magnitude than the remaining members of the equation. From these arguments equation (5.2) is reduced and approximated by

$$(1 - M_L^2)\,\varphi_{xx} + \varphi_{rr} + \frac{\varphi_r}{r} = 0 \,. \qquad (5.2a)$$

Though the linearization process has been applied to the governing equation (3.8f), under small perturbation concepts, this equation remains non-linear in view of (5.2a) and the relationship (5.3). This non-linear equation is suggested as being applicable to the case where local flow conditions are not closely approximated by the undisturbed stream conditions. If now the ratio of the non-linear part of (5.3) is taken to the linear part, i.e.,

$$\Lambda = \frac{\text{non-linear term}}{\text{linear term}} = \frac{\left[(\gamma - 1)\, M_\infty^2 + 2\right] M_\infty^2 \frac{u}{U}}{1 - M_\infty^2} \qquad (5.4)$$

a measure of the effect of non-linearity can be investigated.

From (5.4) it is seen that if $\Lambda < 1$ the linear term is predominant, while if $\Lambda > 1$ the non-linear term is of greater significance. It is then apparent that the division between linear and non-linear predominance for (5.4) can be described for the condition $\Lambda = 1$. This condition is seen to be the definition of local Mach number from (5.3); hence it appears that simple linear theory (obtained by approximating $1 - M_L^2 \approx 1 - M_\infty^2$ in (5.2a)) should give reasonably accurate predictions for the range of free-stream Mach numbers up to that value of Mach number for which local conditions, somewhere on the body, become sonic. That is, linear theory could be applied up to the critical undisturbed free-stream Mach number, where the critical Mach number is that value of the

undisturbed stream Mach number for which sonic conditions first occur on the body.

To illustrate that the above hypothesis is a reasonable approximation, a specific problem will be investigated and substantiating experimental evidence presented. This will be carried out and commented upon following the development in the next topic. This next investigation is needed to describe the proper compressibility correction which is required for this class of three-dimensional bodies in axially symmetric linearized potential fluid flow.

5.3. Linearized Compressible Correction for Three-Dimensional Symmetric Flow.

A slender body of revolution in axially symmetric compressible flow is governed approximately by the linearized equation (5.2a) reduced to

$$(1 - M_\infty^2)\, \phi_{xx} + \phi_{rr} + \frac{\phi_r}{r} = 0 \qquad (5.5)$$

for the condition that $M_\infty < M_{\infty_{cr}}$. Here the body pressures are assumed to be but slightly different from that of the undisturbed stream. These pressures in turn are related to the density through the square of the sonic speed (see equation (3.6a)).

The stream function (ψ) is now introduced (see Reference 40, pg. 28) by the relations

$$\rho_L\, u_l = \frac{\rho_\infty}{r}\, \frac{\partial \psi}{\partial r}\,, \quad \rho_L\, v = -\frac{\rho_\infty}{r}\, \frac{\partial \psi}{\partial x} \qquad (5.6)$$

which have been normalized to account for the density. From these

the following velocity - stream function approximations can be made:

$$\frac{1}{rU}\frac{\partial\psi}{\partial r} = \frac{\rho_L}{\rho_\infty}\frac{u_1}{U} \tag{5.7a}$$

$$\frac{1}{rU}\frac{\partial\psi}{\partial x} = -\frac{\rho_L}{\rho_o}\frac{v}{U} \quad . \tag{5.7b}$$

From the barotropic condition for isentropic flow

$$p = (k\rho\gamma),$$

it follows from (3.6a) that

$$\frac{\rho_L}{\rho_\infty}\left(\frac{p_L}{p_o}\right)^{\frac{1}{\gamma}} = \left(\frac{c^2}{c_\infty^2}\right)^{\frac{1}{\gamma-1}} \quad . \tag{5.8}$$

Equation (5.8), under the considerations of linear perturbations can be approximated by

$$\frac{\rho_L}{\rho_\infty} \approx \left(1 - (\gamma - 1) M_\infty^2 \frac{u}{U}\right)^{\frac{1}{\gamma-1}}$$

and, after expansion by the binomial theorem, again deleting the higher order terms,

$$\frac{\rho_L}{\rho_\infty} \approx 1 - M_\infty^2 \frac{u}{U} \quad . \tag{5.8a}$$

Now if (5.8a) is used in (5.7a) and (5.7b), the approximations are given by

$$\frac{1}{rU}\frac{\partial\psi}{\partial r} \approx \left(1 - M_\infty^2 \frac{u}{U}\right)\left(\frac{u+U}{U}\right) \approx 1 + (1 - M_\infty^2)\frac{u}{U} = 1 + \beta^2\frac{u}{U} \tag{5.7c}$$

$$\frac{1}{rU}\frac{\partial\psi}{\partial x} \approx -\left(1 - M_\infty{}^2\,\frac{u}{U}\right)\frac{v}{U} \approx -\frac{v}{U} \quad . \qquad (5.7d)$$

Through equations (5.7a), (5.7b), and (5.8) the stream function may be defined by means of the Cauchy-Reimann relations. A physical interpretation of this function is obtained if it is recalled that the surfaces ψ = constant are stream surfaces, each such surface being made up of characteristic lines for the flow field (streamlines). According to the definition of streamlines and stream surfaces it follows that any arbitrary surface (ψ = constant) of the family of surfaces could be thought of as a solid boundary. In this manner one such surface can be chosen as the disturbance body in a uniform field of flow. Then, the potential for this combination can be given as

$$\phi = Ux + \varphi(x,r) \qquad (5.9)$$

where $\varphi(x,r)$ is the disturbance potential previously mentioned.

It is now desired to obtain a suitable transformation which will define a second similar body significantly placed in an incompressible flow. In this manner, similar to the Prandtl method, a new incompressible flow field is defined which has the character of the compressible flow field. It should be noted that such a transformation will transfer the compressible effects to the coordinates rather than to the flow field proper. The transformation obtained will require that no discontinuities exist in the field, otherwise the projections will induce errors not consistent with the limitations of the method.

The proper form of the transformation will be defined through solutions of equation (5.5), since it has been shown that this equation is a form of the Laplace equation (see (3.25a)).

According to the Cauchy-Riemann conditions,

$$\frac{\partial \varphi(x,r)}{\partial x} = \frac{1}{r} \frac{\partial \tau(x,r)}{\partial r}, \quad \frac{\partial \varphi(x,r)}{\partial r} = -\frac{1}{r} \frac{\partial \tau(x,r)}{\partial x}, \tag{5.10}$$

thus the stream function corresponding to (5.9) can be shown to be

$$\psi = \frac{Ur^2}{2} + \tau(x,r), \tag{5.11}$$

with the requirements that $\lim_{r \to 0} \tau(x,r) \neq 0$, and $\tau(-\infty, r) = 0$.

Now, a general potential function will be chosen so that by comparing the solution of (5.5) with a known incompressible solution, the necessary transformation is obtained.

In place of (5.9) write a general potential function

$$\phi = Ux + \lambda_s \varphi(x_1, r_1) \tag{5.12}$$

where $x_1 = \lambda_1 x$ and $r_1 = \lambda_2 r$. The λ's are constants which will be adjusted to obtain the required transformation. Differentiating (5.12), and substituting into (5.5), gives

$$\beta^2 \lambda_s \lambda_1^2 \varphi_{x_1 x_1} + \lambda_s \lambda_2^2 \varphi_{r_1 r_1} + \frac{\lambda_s \lambda_2^2}{r_1} \varphi_{r_1} = 0 \tag{5.5a}$$

Since (5.9) must satisfy the incompressible ($\beta^2 = 1$) solution of (5.5), then on comparing (5.5a) with the incompressible equation,

$$\varphi_{xx} + \varphi_{rr} + \frac{\varphi_r}{r} = 0 \quad ,$$

indicates that the derivative coefficients must have the following relations if consistent solutions are to exist:

$$\beta^2 \lambda_s \lambda_1^2 = 1 \quad \text{and} \quad \lambda_s \lambda_2^2 = 1, \quad \text{or} \quad \beta^2 \lambda_1^2 = \lambda_2^2 \ . \tag{5.13}$$

Equation (5.13) is the necessary condition that (5.12) is a solution of (5.5a). It is also noted that two of the constants (λ) may be chosen arbitrarily.

Without loss of generality it is evident that the velocity relations (5.7c) and (5.7d) may be defined when $\varphi(x_1, r_1)$ and $\tau(x_1, r_1)$ are substituted for $\varphi(x,r)$ and $\tau(x,r)$ respectively. Thus, employing the conditions (5.10),

$$\frac{1}{rU}\frac{\partial \psi}{\partial r} \approx 1 + \frac{\beta^2}{U}\lambda_1\lambda_s \varphi_{x_1}(x_1,r_1) \left[= 1 + \frac{\beta^2 \lambda_1 \lambda_s \tau_{r_1}(x_1,r_1)}{U \lambda_2 r} \right] \tag{5.14}$$

$$\frac{1}{rU}\frac{\partial \psi}{\partial x} \approx -\frac{\lambda_s \lambda_2 \varphi_{r_1}(x_1,r_1)}{Ur} \qquad \left[= -\frac{\lambda_s \tau_{x_1}(x_1,r_1)}{Ur} \right] .$$

After partially integrating the relations (5.14), the stream function is obtained as

$$\psi + \frac{U r^2}{2} + \frac{\lambda_s}{\lambda_1} \tau(x_1, r_2) \ . \tag{5.15}$$

It is readily seen that (5.15) does not allow a direct transformation of stream surfaces due to the inconsistency of coordinates. However, if (5.15) is rewritten as

$$\psi = \frac{\lambda_s}{\lambda_1}\left[\frac{U\,(\lambda_2 r)^2}{2}\,\frac{\lambda_1}{\lambda_s\,\lambda_2^2} + \tau(x_1,\, r_1)\right] \qquad (5.15a)$$

then stream surfaces should map into stream surfaces. Thus, on comparing (5.15a) and (5.11) it is required that

$$\frac{\lambda_1}{\lambda_s\,\lambda_2^2} = 1 \qquad (5.16)$$

if such similar solutions are to exist. Now, from the condition that $\lambda_2^2 = \beta^2\,\lambda_1^2$, (5.16) yields the result that

$$\lambda_s = \frac{1}{\lambda_2\,\beta} \quad .$$

Now having an arbitrary choice of only a single constant (λ), and choosing $\lambda_1 = 1$, it follows that

$$\lambda_2 = \beta \quad \text{and} \quad \lambda_s = 1/\beta^2 \quad .$$

The consequence of these results, when applied to (5.15a), gives

$$\psi = \frac{U r^2}{2} + \frac{\tau(x,\, \beta r)}{\beta^2} \quad . \qquad (5.15b)$$

The interpretation of (5.15b) is that now an incompressible flow has been described which corresponds to the compressible flow through a coordinate transformation. The equivalent body is described by the second member of the right side of the equation. It is seen that the compressible equivalent body has coordinates $(x,\, \beta r)$, and that though the bodies have the same length the equivalent body has its radial

dimension reduced in the ratio β: 1. The first member on the right shows that both bodies are subjected the same undisturbed stream (U). It can be shown, by proper differentiation, that the velocity components over the equivalent body are greater in the following ratios: for the perturbation axial component, $1/\beta^2$: 1; and for the radial perturbation component, $1/\beta$: 1. Thus it follows that for the linearized pressure coefficient, equation (3.34), the proper relationship for the related flows is given by

$$C_{p_c}\Big|_{x,r} = \frac{1}{\beta^2}\ C_{p_i}\Big|_{x,r\beta}$$

or, since the semi-apex angle for a conical head is defined as

$$\text{tn}\ \delta = x/r\ ,$$

then

$$C_{p_c}\Big|_{\delta} = \frac{1}{\beta^2}\ C_{p_i}\Big|_{\beta\delta}\ . \qquad (5.17)$$

Further examination of (5.15b) shows it to meet the requirements stipulated originally for the problem: namely, it has defined the effects (approximately) for compressibility through a proper coordinate transformation. The nature of the compressible correction has been imposed on the perturbation component of the stream function only - - and this result is capable of describing either compressible ($\beta^2 < 1$) or incompressible ($\beta^2 = 1$) phenomena. Of course it still must be presumed that no flow discontinuities are present in the field of flow; that is, the flow is shock free and meets the usual requirements of a potential field.

The foregoing results are those obtained by Gothert[39], in his original paper on the extension of the Prandtl Rule to the three-dimensional flow case.

Equation (5.17) should not be interpreted too literally since the effects of body thickness and Mach number do not have the same weight in the expression. It has been brought out by several authors[46,40] that for the spatial case of axially symmetric flow the effects of body thickness are more pronounced in (5.17) than the effects of Mach number for slender bodies. For example, in the case of ellipsoids of revolution, use of Gothert's Rule is made by applying the relationship given symbolically in (5.17) to the hydrodynamic equation for the fluid flow. Thus a reduced equation for the linearized compressible pressure coefficient (see Ref. 46, for example) is obtained in the form

$$\frac{C_{p_c}}{C_{p_i}} = 1 + \frac{\ln \beta}{1 - \ln 2f} \tag{5.18}$$

where f is the actual body fineness ratio $\frac{\ell/2}{r_{max}}$. This equation has all the variations indicated by the symbolic equation (5.17), including then both Mach number and thickness effects.

With the development of the preceding section on the limits of applicability of linear theory, and the result of the present section, a verification of these sections can be investigated.

5.4. Experimental Verification on the Limit of Linear Theory.

In this section it will be shown that the argument on the upper

limit of linear theory is verified with good approximation by experimental results.

Reviewing the previous discussion briefly, it has been stated that the appropriate linearized compressible correction can be used to predict the pressure distribution over bodies of the same family for only a limited range of Mach number. Due to the nature of the linearization, the correction may be applied to the case of slender bodies only. And, as has been shown, the upper limit of applicability of such linear approximations is the so-called "free-stream critical Mach number".

To illustrate that these results are acceptable a comparison is made for the actual and predicted pressure distributions on an ellipsoid of revolution. Since linear theory has been shown to give adequate results for low subsonic Mach numbers by other investigators (see, for instance, references 26, 39, 44, 46), the considerations here shall only be to substantiate the arguments made previously. Data for ellipsoids of revolution are used in this comparison since no known compressible data exist for the class of bodies of primary interest to this thesis. These data are taken from reference 46.

First, to illustrate that (5.18) is the correct form of Gothert's Rule, consider Figure 1. The graph shows a comparison of the predicted and experimental pressure distributions over the front half of a 16.7 percent thick ellipsoid of revolution. The results presented

in the figure clearly illustrate that the correct form of Gothert's Rule is given by equation (5.18); that the symbolic equation (5.17) cannot be literally applied for the best possible predictions, and lastly, the figure shows the discrepancy when using the Prandtl-Glauert (two-dimensional) Rule, $C_{p_c} = C_{p_i}/\beta$, for the three-dimensional flow. (According to equation (5.17), the compressible pressure distribution for an ellipsoid of revolution can be obtained by correcting the incompressible pressure distribution for a similar ellipsoid of smaller thickness. For instance, at a free-stream Mach number of 0.8, an estimation of the pressure distribution for the 16.7 percent ellipsoid is obtained from the incompressible pressure data of an ellipsoid of thickness $\beta\delta$ (where $\beta = \sqrt{1 - M_\infty^2} = \sqrt{1 - (0.8)^2}$). In this case the affinely related ellipsoid has a thickness ratio of 10 percent. And, finally the desired pressure data is obtained by correcting the incompressible values according to the relationship $C_{p_c} = \frac{C_{p_i}}{\beta^2}$ (see equation 5.17). This procedure was employed in plotting the curve denoted by $M_\infty = 0.8$, corrected.) In each case incompressible data were corrected by use of Gothert's Rule and the Prandtl-Glauert Rule, as indicated on the figure.

Now, to show that the upper limit of linear theory corresponds to the critical free-stream Mach number, attention is called to Figure 2. The plot is presented for two free-stream Mach numbers, namely $M_\infty = 0.90$ and 0.94. The choice of Mach number is dictated by the experimental data available in reference 46. From the experimental pressure distributions it was found that the free-stream critical Mach

number, $M_{\infty_{cr}} = 0.916$.

In Figure 2 a comparison of the predicted and experimental pressure distributions is made, for the two Mach numbers indicated, over the front half of the ellipsoid of revolution. In both cases the predicted data are obtained by correcting the pressure distribution, for $M_\infty \approx 0$, by equation (5.18).

Examination of the plot indicates that (5.18) over-predicts the supercritical pressure distribution ($M_\infty = 0.94$); while the agreement for the slightly subcritical case affords very good agreement between experiment and theory. Since $M_\infty = 0.90$ is quite close to the critical value of Mach number ($M_{\infty_{cr}} = 0.916$), it is believed that the agreement substantially validates the argument on the upper limit of linear theory.

5.5. Estimation of the Lower Critical Mach Number

It is of interest to note that equation (5.18) may also be used to predict the critical free-stream Mach number. Since the equation has the effect of compressibility incorporated in it, an estimate of when local sonic conditions are first reached on the body can be made. It will be seen that only the maximum negative pressure acting on the body in incompressible flow is required to be known. To illustrate this, consider the definition of pressure coefficient for compressible flow (3.28)

$$C_p = \frac{2}{\gamma M_\infty^2} \left(\frac{p_L}{p_\infty} - 1 \right) \qquad (3.28)$$

If the pressure ratio p_L/p_∞ is expressed in terms of Mach number, through the isentropic relationship

$$\frac{p_L}{p_\infty} = \left[\frac{2 + (\gamma - 1)\, M_\infty^2}{2 + (\gamma - 1)\, M_L^2}\right]^{\frac{\gamma}{\gamma - 1}} \tag{5.19}$$

then

$$C_p = \frac{2}{\gamma\, M_\infty^2}\left(\left[\frac{2 + (\gamma - 1)\, M_\infty^2}{2 + (\gamma - 1)\, M_L^2}\right]^{\frac{\gamma}{\gamma - 1}} - 1\right). \tag{5.20}$$

Now, if the critical condition is assumed; i.e. $M_\infty = M_{\infty_{cr}}$, for which $M_L = 1$, then (5.20) becomes

$$C_{p_{cr}} = \frac{2}{\gamma\, M_{\infty_{cr}}^2}\left(\left[\frac{2 + (\gamma - 1)\, M_{\infty_{cr}}^2}{\gamma + 1}\right]^{\frac{\gamma}{\gamma - 1}} - 1\right). \tag{5.20a}$$

Now if the critical pressure coefficient in (5.20a), is replaced by equation (5.18), where for critical values (5.18) is

$$C_{p_{cr}} = C_{p_i}\left(1 + \frac{\ln\,(1 - M_{\infty_{cr}}^2)}{1 - \ln 2\, f}\right),$$

then (5.20a) may be written as

$$C_{p_i} = \frac{\dfrac{2}{\gamma\, M_{\infty_{cr}}^2}\left(\left[\dfrac{2 + (\gamma - 1)\, M_{\infty_{cr}}^2}{\gamma + 1}\right]^{\frac{\gamma}{\gamma - 1}} - 1\right)}{1 + \dfrac{\ln\sqrt{1 - M_{\infty_{cr}}^2}}{1 - \ln 2\, f}} \tag{5.20b}$$

In (5.20b) C_{p_i} is the lowest value of pressure coefficient for the body in near incompressible flow. The lowest value of C_{p_i} is required since this corresponds to the point of highest velocity; i.e., the point at which local sonic conditions are to first occur. The equation cannot be solved explicitly for $M_{\infty_{cr}}$; hence it is plotted in Figure 3. Obtaining the lowest value of C_{p_i} from experiment, the value of $M_{\infty_{cr}}$ may be determined from this figure. A comparison of the experimental and estimated values of $M_{\infty_{cr}}$ for the bodies investigated in reference 46 is tabulated below.

BODY	$M_{\infty_{cr}}$ EXP	EQ. (5.20b)
Ellipsoid of Revolution (f = 10)	0.947	0.95
Ellipsoid of Revolution (f = 6)	0.916	0.918
Ogival body of Revolution (f = 6)	0.898	0.905

The tabulated results show a good correlation between the critical Mach number predicted by equation (5.20b) and those values obtained from experiment. In all cases the percent error of prediction is of the order of one percent.

Though the expression for the pressure coefficient, corrected by use of Gothert's Rule (as given by equation (5.18)) is for ellipsoids of revolution, it appears that the expression may give good results for nearly similar body types also. For example the ogival body of revolution in the above table is not too different in shape from an ellipsoid of revolution. In this case the body curves in the meridian

planes are intersecting circular arcs, giving the body pointed ends. With the agreement experienced in predicting critical Mach number it follows that (5.18) could be used to estimate the effect of compressibility on pressure distributions for this body as a first approximation. Certainly these predicted values should be reasonable for the central portion of the body, though discrepancies are expected near the nose and tail where these sections are nearly conical.

A general expression for bodies of revolution has been developed by Laitone[3], wherein Gothert's Rule has been applied in the same manner as that leading to equation (5.18). In his work Laitone, has obtained an expression which gives the pressures, at points along the body, in terms of body geometry and β. In a later section this expression will be used as a means of estimating the critical Mach number for the class of bodies considered in this thesis.

The preceding sections have been devoted to ascertaining the limits of the Mach number range of applicability of linear theory, the proper compressible correction applied to axially symmetric flow about bodies of revolution, and some experimental justification of these results. As has been shown, the upper limit for linearized theory (small perturbation theory) is the critical Mach number of the undisturbed stream; Gothert's Rule may be applied to the linearized governing equation to give the necessary corrections on the incompressible flow for compressible flow, to the upper limit of

applicability of linear theory; and a means of defining the free-stream critical Mach number has been established for a particular class of bodies. The justification of these statements and hypotheses has been achieved by comparing the approximations with actual experimental data. In the following sections the class of bodies to be considered in this investigation will be investigated along the same lines of reasoning.

In the next section a discussion and description of some experimental investigations, carried out at the Virginia Polytechnic Institute, will be presented. These studies were necessary to determine whether known theories could adequately predict the pressure distribution over a cone-cylinder body of revolution in axially symmetric fluid flow. The findings and agreements will be fully discussed in that section.

6. EXPERIMENTAL INVESTIGATION

The pressure distributions determined experimentally, and described below, represent the results obtained from measurements made in the Virginia Polytechnic Institute subsonic wind tunnel. For a description of this wind-tunnel and its basic characteristics attention is directed to reference 37.

The models used in these experiments were designed and constructed at the Virginia Polytechnic Institute. All necessary equipment for measurement purposes was either available or constructed prior to the testing.

6.1. Model Description

The models tested were bodies of revolution consisting of a conical head and a cylindrical afterbody. The heads of two of the models were turned from brass bar stock, and the afterbodies of these were turned from hardwood. The third model (consisting of a 20° semi-apex angle cone and cylindrical afterbody) was made from hardwood, with the exception of the apex tip which was turned from brass bar stock. Each model was drilled so that pressure measurement tubes could be inserted flush with the body surface. All such measurement tubes were soldered to the brass cone heads and forced into drilled openings in the hardwood afterbodies after a hard setting glue had been applied to the base of each tube to prevent leakage around the drilled holes. The tubing used for pressure measurements was copper tubing, 1/16-inch O.D., having an opening of approximately 1/32-inch

in diameter. Two of the models, the 5°- and 10°-semi-apex angle cone heads, were ten inches in axial length, while the 20°- semi-apex angle cone head had an axial length of 5.15 inches. Each cylindrical afterbody was constructed in two halves so that each half could be fitted over the sting support attached to the cone head, and which carried the pressure measurement tubes. Each sting support for each model was fitted with adjustment lugs used to align the model with the wind stream in the tunnel. A schematic drawing of a typical model and sting arrangement is shown in Figure 4.

6.2. Testing Procedure

Prior to the actual measurement of pressures exerted on any model, the body was aligned in the wind tunnel at zero angles of yaw and pitch. Each conical head contained two sets of "alignment orifices" to insure proper alignment of all models. These orifices, four in number, were spaced 90° apart around the periphery of the body at approximately the 50 percent and 90 percent axial stations of the cone. To align the bodies for zero yaw and pitch, each diametrically opposite pair of orifices was connected to the manometer board and the pressure readingsfor the pair balanced by correcting the body position relative to the wind stream. Body position was corrected by adjusting the alignment screws fitted into the alignment lugs on the sting support. The alignment procedure was carefully carried out in all cases to insure as near true streamwise orientation as possible.

The procedure was repeated for each model test in the wind-tunnel so that no supposition of alignment was made for any particular test.

Once the alignment of the model was insured the actual pressure measurements were made. All tests were conducted at a constant wind tunnel speed with appropriate notations of temperature, etc. being made for the test. To insure against possible inherent testing errors a complete set of measurements was made on each body combination in four orientations. That is, each body was tested with the principal measurement orifices at four different peripherial positions (90° rotational increments) so that a pressure envelope was obtained in each body quadrant. The purpose of such a procedure was to eliminate, as far as possible, any effects which may have been present due to unsymmetrical tunnel flow, support blockage, and manufacturing misalignment. In all cases it was found that only small variations in measurements were noted for each such peripherial survey. The data presented from this experimental investigation are the average of all such survey measurements. These data have no other corrections applied to them. Due to the small size of each model in comparison to the size of the tunnel, any additional corrections (such as buoyancy) are of negligible magnitude.

Prior to the actual model testing several preliminary tests were conducted for the purpose of determining the desired afterbody length, and the effect of body imperfections on the pressure measurements. During these initial studies it was observed that the conical head pressures were affected by any misalignment present, any body

imperfections, and the relative size of the sting support. In order that such discrepancies could be minimized an optimum size cylindrical afterbody was defined (from testing) and the lengthy alignment procedure outlined above was adopted for the actual testing procedure.

To determine an optimum length of afterbody each model was tested with the cylindrical afterbody being increased in length by adding circular disks. With each increase in length the pressures on the conical head were measured, and the afterbody influence noted from these measurements. A typical investigation is presented in Figure 5, this graph representing the measurements made on the 10° semi-angle cone body. The data of Figure 5 show the effect of afterbody length on pressure measurements, each curve representing the measurements made at a particular orifice for increasing cylinder length. It is readily seen that the region most greatly affected is the under pressure region near the after end of the conical head. As the overall body length is increased, pressure measurements tend to show smaller and smaller variation. As a result of this investigation it was concluded that a four-inch long cylindrical afterbody ($L_{cyl}/L_{cone} = 0.4$) was adequate to insure negligible influence of afterbody on the head measurements. Similarily, the 5°- semi-angle cone was found to require four-inch afterbody, but it was deemed necessary to use a six-inch afterbody on the 20° semi-angle cone-cylinder combination.

It is interesting to note here that Figure 5 indicates that a 10 percent cylinder ($L_{cyl}/L_{cone} = 0.10$) shows the greatest pressure

measurement variation (or greatest afterbody effect) for the conical head. It can be seen that any increase over this 10 percent value indicates a recovery of pressures, and that subsequent lengthening tends to the negligible change in pressure measurements for the 40 percent cylinder length.

In addition to the above mentioned effects, it was noted that the relative sting size could also cause measureable differences in head pressures. To better define the magnitude of such an effect a wooden plug was manufactured for the 10° cone which has the same relative diameter ($d_{sting}/D_{cyl} = 0.47$) as the actual sting diameter ($d_{sting}/D_{cyl} = 0.47$) of the 5° cone. This plug was placed over the sting of the 10° cone body in the test. The results of this investigation are presented in Figure 6. As is seen in the figure, the differences in measured pressures for this body configuration compared to the original body ($d_{sting}/D_{cyl} = 0.24$) are relatively slight. As a consequence of this study it was concluded that the effect of the sting could be disregarded since the error in measurement is within acceptable experimental limits. In addition, these preliminary studies indicated that any imperfection of fit between the conical head and cylindrical afterbody could also influence the pressure measurements. To minimize this effect, all body junctions were carefully fitted and any imperfections removed prior to the actual testing of the body combinations.

It can be said that a conical body having rather small pressures exerted on it is influenced by all downstream body imperfections, etc.

In order that the data obtained from this investigation could be representative, care was taken to reduce all effects to a minimum throughout the testing procedure. As a check on consistancy of the data, the experimental investigations on the cone-cylinder bodies were repeated, and the data collected were found to agree within negligible limits.

6.3. Data Representation

The data presented in Figures7 represent the average of all data obtained from the experimental investigation carried out in the V.P.I. Aeronautical Laboratory. It is felt that these curves represent the true nature of the pressure distribution over a cone-cylinder body combination in axially symmetric "near incompressible" fluid flow. The tests were conducted at as low a speed as practicable for reliable pressure measurements. The test Reynold's number and Mach number is indicated on each curve in Figure 7. These values of Reynold's number are based on body diameter and have been corrected for wind tunnel turbulence level.

At the time these investigations were carried out no known experimental data was available by which the results could be compared. After this study had been completed some data were found (see reference 23) for similar body types taken from water tunnel investigations made at the Iowa State University. Though the two tests are not actually comparable throughout, the marked similarity of the results gives a high degree of confidence in the reliability of the

present tests. The data of reference 23 indicate that the shoulder region of the conical head is a low pressure region, and that variations due to viscous phenomena will certainly occur in this region. Due to the instability of such a flow type (at the shoulder) there exists a marked tendency for separation to occur there. The effect of such a separation phenomenon would be to effectively "round-off" the body at the shoulder, thus increasing the resulting equivalent cylindrical afterbody in size over the actual body size. Such a "rounding-off" of the body is quite noticeable from a study of the comparable data[23] which indicates that the effects of cavitation show a marked influence on the measurements.

The care and caution with which the present investigation was conducted are mentioned, and are justified, since this work represents the only tests known to the author. Apparently little interest in this class of bodies at low subsonic flow speeds has existed prior to this time, or else similar data have long since been forgotten if indeed they ever existed. It seems odd that with the fundamental interest in axially symmetric flow exhibited in the literature, and with the challenge this particular case poses, that so little has been done about it. In all probability this problem has been neglected in the past since classical analytical methods fail to predict comparable results adequately.

Lastly, it should be mentioned that this laboratory study was conducted to ascertain the degree of accuracy which could be expected from existing analytical treatments. As was feared, it became apparent

that the classical axially distributed source-sink method did not give acceptable agreement with experiment. Inspection of Figure 9 will indicate the comparison between such a theory[3] and the experimental study.

Though other analytical methods are known to exist, the labor involved in applying them was prohibitive. Recently data* have been made available to the author which were calculated on an electronic computor. This analytical procedure could only have been carried out on such an automatic device due to the complex and rigorous mathematical manipulations required. The accuracy of these results may be seen in Figure 8, which is a plot of these data against experiment. It is noted that the agreement is very good in general.

In a next section of this thesis a method will be presented by means of which the pressure distribution for a cone-cylinder-body in incompressible axially symmetric flow may be calculated. Though this method is time consuming, it is not impractical to employ. The agreement for this method with experiment is most gratifying and is justifiable from the standpoint of time required.

---

* Unpublished data for cone-cylinder bodies computed on an IBM 701 calculator by Douglas Aircraft Co., 1957.

7. DETERMINATION OF THE FLOW FIELD ABOUT A BODY OF REVOLUTION IN AN AXIALLY SYMMETRIC PERFECT FLUID BY THE METHOD OF VORTEX RING DISTRIBUTION

7.1. Historical Sketch

It is well known that a slender streamlined body in a uniform axially symmetric flow closely approximates a potential flow type[1]. This has led many authors to search for a convenient method for obtaining numerical solutions of such a potential flow problem.

Rankine[2] showed that by using potential theory a family of bodies of revolution could be obtained when sources and sinks were spaced along an axis parallel to a uniform flow. This general method, was extended and used by several authors[4,5,6,7,9] where in all cases the problem was to describe a body shape for a specified velocity or pressure distribution; i.e., an indirect approach to the problem.

In 1927, von Karman[10] presented the solution for the flow about a specified body of revolution. This problem embodied an approximate solution of an integral equation using simultaneous linear equations. This method, though widely used, has limited accuracy due to the labor required in refinement of the simultaneous equations.

Weinig[12] formulated the same problem using doublet distributions and effected the solution by an iterative process. Since this method of solution was presented in a divergent form, it was necessary to extrapolate backwards to obtain the desired result.

Kaplan[13] and Smith[14] made a different approach to the problem by determining the velocity potential for the flow field about a body of revolution in an axially symmetric uniform stream. Their solutions required the solving of a finite number of an infinite set of linear equations; giving the potential expression (approximately) from which the required axial source-sink distribution could be described. A further simplification of the basic method has been presented by Young and Owen[15].

In all the above cases the laborous calculations and limited accuracy have severely hampered investigations, as is typified by the following statement[15]:

> "In every case, however, the methods proposed are laborious to apply, and the labor and heaviness of the computations increase rapidly with the rigour and accuracy of the process. Inevitably, a compromise is necessary between the accuracy aimed at and the difficulties of computation. All the methods reduce, ultimately, to finding in one way or another the equivalent sink-source distribution, and it is this part of the process which in general involves the heaviest computing."

Also, these methods have been limited to a special class of bodies of revolution, not applicable to a general body shape, and specifically not applicable to the case of a pointed body. The fundamental difficulty lies with the assumption of axially distributed sources and sinks as the following quotation[10] indicates:

"This (referring to axially distributed sources and sinks representation) is possible only in the exceptional case when the analytical continuation of the potential function, free from singularities in the space outside the body, can be extended to the axis of symmetry without encountering singular spots."

The statements quoted above describe the basic difficulties encountered when using the source-sink distribution method, and are the fundamental reasons behind the continued work in the investigation of this problem in aerodynamics.

In recent years several methods have been developed which tend to give more accurate predictions of the flow field about a body of revolution in axially symmetric uniform potential flow. One of the first such methods was developed by Kaplan[16], though this method is not in general use due to the complexity of its application. Landweber[17] has developed two methods, one exact and one approximate; the first requires a numerical solution of an integral equation, with the gauss quadrature formula recommended for the numerical work. The integral equation is found from the assumption of a continuous axial distribution of doublets, in a uniform stream, used to describe a desired body of revolution in an axially symmetric potential flow field. The second (approximate method) again requires numerical evaluation of an integral equation, but here the solution is for the surface velocity over the desired body of revolution. Both of these methods, though more easily applied than the Kaplan[16] method, are still difficult to apply to the so-called blunted body shape.

Vandrey[18] presented a method which eliminates the body bluntness restriction through the use of vortex ring distributions in a uniform stream. This method again requires the numerical solution to an integral equation for the determination of the flow field, with the only restriction being that the body shape must have continuous tangents. The same author[19] has also developed a method for determining the flow field about a general body of revolution through the distribution of sources and sinks on the body surface. The latter method is general in that it may be applied to a body not aligned with a remote uniform stream, though in general the calculations are more lengthy than those of the former method. In a later paper[20], a special problem, related to a torpedo in a general curved path of motion, was solved wherein the flow field was again described from the numerical solution of an integral equation.

In all these last methods the so called "direct" approach is made to the problems investigated. That is, the body is given, and the solution is made for the velocity components, etc., experienced by the specified body in the particular remote potential flow field stated.

7.2. Introduction

As has been noted in the preceding discussion, the description of the flow field about a body of revolution by source-sink distribution, spaced along the body axis, presents difficulties of such a nature that only approximate results are obtainable. The method to be developed in this section does not exhibit the failings of the more

classical approach, and will be shown to exhibit very close agreement with experiment.

It should be noted that the failings of the axial source-sink distribution could be alleviated by use of a surface distribution; i.e., spacing the sources and sinks along the body surface. However, it has been found that such a distribution leads to considerable mathematical complexity when attempting to evaluate the necessary distribution strength for a general surface contour. The present method[18] has the ability of representing the flow field to a large degree of accuracy, and it also is found to present only minor complexity of mathematical manipulation. In the main, most calculations can be carried out by slide rule, the only exception being that in the region where the body junction is made (i.e. cone-cylinder junction) considerable care must be exercised regarding the accuracy of calculation.

The vortex-ring, introduced by Helmholtz, leads to a method of describing the flow field about a body comprised of vortex-rings. The circulation associated with these rings is used to describe the velocity at the body surface, and the surface discontinuity associated with this fluid mechanism introduces into the body interior a velocity at which the entire system moves through an undisturbed fluid. The necessary condition that a steady flow which will bring the body system to rest is met by the superposition of a uniform flow, equal and opposite to that generated in the body interior. With this formulation a relationship for the vortex-density is described, and from

this, for an arbitrary body shape, a solution of the equation will yield the necessary density of vortex-rings required to define the arbitrary body in the uniform stream.

The necessary conditions imposed on this problem are those usually associated with perfect fluid problems, the requirement that the body normal velocity component vanish, and the additional requirement that the body have continuous tangents (though not necessarily continuous curvature). This last condition demands that the body be described by analytic curves (straight lines, arcs of circles, etc.), and that these curves then have identical tangents at their junction points. To meet this stipulation throughout it is demanded that the nose of the cone be considered spherical in nature; this does not introduce an unrealistic condition if one considers that a "point" is never physically realized and can only exist as a mathematical concept. Also, the junction of the cone-cylinder shall be described by a circular arc, in the meridinal planes, and the body shall be considered semi-infinite in extent downstream. By so doing, any undue influence of the finite afterbody on the conical section is deleted and the final results will exhibit the character of the real fluid in experiment.

There exists a need for the semi-infinite body other than that need given above. Originally the method of Laitone[3] was thought to be sufficient to describe the flow field for the conical body; however, this method was found to exhibit too great an error when compared with

the results of experiment (See Figure 9). The method was applied to the case of an infinite cone in a stream with a finite velocity far ahead of the body. It has since been found that such a situation is unlikely to exist for the following reasons:

Consider a slender cone of semi-angle θ_c described by a linear axial source distribution of strength

$$dQ = 2\pi U \theta_c^2 \xi \, d\xi, \text{ where } d\xi = \text{element of axial length.} \quad (7.1)$$

The axis extends from $x = 0$ to $x = +\infty$. At any point $x < 0$, a disturbance is produced by such a distribution of magnitude

$$\frac{\partial \varphi}{\partial x} = \frac{1}{2} U \theta_c^2 \int_0^{+\infty} \frac{\xi \, d\xi}{(x - \xi)^2} \, . \quad (7.2)$$

Since the integral is divergent; i.e.,

$$\lim_{l \to \infty} \int_0^l \frac{\xi \, d\xi}{(x - \xi)^2} = \lim_{l \to \infty} \left[\frac{l}{x - l} + \ln \frac{x - l}{x} \right] = -\infty \, ,$$

there is no solution for the infinite cone in a uniform stream of speed U at $x = -\infty$.*

Though Laitone's method is in error, for the same reasons that any source-sink method is in error, it has been found that the error is almost of constant magnitude for the major portion of the cone. Possibly, through viewing experimental results, some measures could be taken which would empirically correct his results; however, no attempt is made herein since this method is not employed for the solution.

---

* This was pointed out by Dr. F. Vandrey in a private communication.

7.3. Formulation of the Vortex-Ring Distribution Problem

A cone-cylinder body of revolution, comprised of a cone having a 10° semi-apex angle and a cylinder of unit radius, having the coordinate origin at the nose of the cone is described as follows:

$$\begin{aligned} r &= x \tan 10^{\circ} && 0 \leq x \leq 5.471 \\ r &= -2.3663 + \sqrt{-25.2299 + 12.0933\,x - x^2}, && 5.471 \leq x \leq 6.04663 \\ r &= 1 && 6.04663 \leq x < +\infty \end{aligned} \tag{7.3}$$

where r is the cylindrical coordinate normal to the axis of symmetry (x-axis), see Figure 10a. The intermediate limits, $x = 5.471$ and $x = 6.04663$, describe the region wherein the cone and the cylinder are joined by a circular arc in the meridinal plane. These points represent, in terms of the cone length, $0.95L_{cone}$ and $1.05L_{cone}$ respectively. The choice of such points was arbitrary. No special attempt was made to qualitatively ascertain if such points were descriptive of the real fluid action due to boundary layer rounding of the sharp body junction in the experiment. Due to the good agreement between theory and experiment, it is felt that this arbitrary choice is adequate, and further that any closer agreement for the rounding of the body would produce only negligible improvement between theory and experiment.

The body described in equation (7.3) is seen to be a single valued function of the coordinate x with the additional geometric restrictions that

$$r(0) = 0$$

$$r(\infty) = R_o = 1 \ . \tag{7.4}$$

The body surface S will be regarded as separating the entire flow field into two regions, R_{int} and R_{ext}, such that S represents a surface of velocity discontinuity. A requirement on the velocity components at S is that the normal component shall vanish at all points while the tangential component shall in general be finite. With this requirement it follows that the tangential component will be the resultant velocity over the body surface. Letting w(s) be the resultant velocity at any point s, the circulation associated with any such point, for an element of arc length ds along the body contour, will be

$$d\Gamma = - w(s)\, ds \ , \tag{7.5}$$

where the negative sign is to describe the direction of the circulation velocity in accordance with this definition. Thus, w(s) may be described as the strength of an elementary vortex ring per unit length of arc.

The vortex rings, distributed along the body surface, will induce a velocity - U in the interior of the body. Hence, the system of vortex rings would then tend to move with this velocity in the direction - x in an undisturbed unbounded fluid. By superposition, if a parallel stream of velocity + U is imposed on the ring system, the fluid in the interior region would be brought to rest thereby meeting the requirement for steady motion in potential theory. Such a flow would possess a potential function

given by;

$$\phi_{ext} = + Ux. \tag{7.6}$$

The problem may now be postulated as follows:

To find the distribution of vortex rings such that the velocity induced in the region R_{int} is given by the potential function $\phi_{int} = - Ux$, where - U is the velocity parallel to the body axis produced by this system of rings. (See Figure 10b).

Consider two points, $P_1(x,r)$ and $P_2(x + \Delta x, r + \Delta r)$, separated by an infinitesimal arc length Δs, on the body surface in a characteristic meridinal plane. Since the vortex rings distributed over the body surface S produce an internal velocity (- U), the approximate difference in potential between these two points is given by

$$d\phi_{int} = - U \, d \, x \quad . \tag{7.7}$$

This potential difference is contributed to in a two-fold manner: (1) by the vortex ring(s) between P_1 and P_2, and (2) by all other vortex rings along the body surface S (except those between P_1 and P_2). That is,

$$d\phi_{int} = \phi_1 + d \, \phi_2 \quad . \tag{7.8}$$

From elementary considerations, knowing the vortex strength per unit arc is - w(s) ds,

$$\phi_1 = - \frac{w(s)}{2} ds \tag{7.9}$$

and, for all other vortex elements the contribution to the potential difference is described from the Biot-Savart Law as

$$d\phi_2 = -\sum_S \frac{w(\sigma)\, d\sigma}{2\pi\, \eta(\sigma)} \left(u^* dx + v^* dr\right) \tag{7.10}$$

where: $-w(\sigma)$ is the strength of a variable vortex ring element; $\eta(\sigma)$ is the normal ($r^{\underline{th}}$) coordinate at the variable point (see Figure 10a). The quantities u^* and v^* are non-dimensional velocity components derived from proper differentiation of the stream function for a vortex ring, as given by Lamb*. That is

$$u^* = \frac{\eta}{\sqrt{(x-\xi)^2 + (r+\eta)^2}} \left(K(k^2) - \left[1 + \frac{2\eta(r-\eta)}{(x-\xi)^2 + (r-\eta)^2} \right] E(k^2) \right)$$

$$v^* = \frac{-(x-\xi)\,\eta}{\sqrt{(x-\xi)^2 + (r+\eta)^2}} \left(K(k^2) - \left[1 + \frac{2r\eta}{(x-\xi)^2 + (r-\eta)^2} \right] E(k^2) \right) \tag{7.11}$$

where

$$K(k^2) = \int_0^{\pi/2} \frac{d\psi}{\sqrt{1 - k^2 \sin^2 \psi}}, \quad E(k^2) = \int_0^{\pi/2} \sqrt{1 - k^2 \sin^2 \psi}\, d\psi$$

and

$$k^2 = \frac{4r\eta}{(x-\xi)^2 + (r+\eta)^2} \quad .$$

On substitution of (7.7), (7.9), and (7.10) into (7.8) the following result is obtained:

---

* Hydrodynamics, Lamb, Art 161.

$$- U\,dx = -\frac{w(s)}{2}\,ds - \frac{1}{2\pi}\int^{S}\frac{w(\sigma)}{\eta}\,(u^{*}dx + v^{*}dr)\,d\sigma \qquad (7.12)$$

Non-dimensionalizing (7.12) by introducing the non-dimensional velocity $w^{*}(s) = \frac{w(s)}{U}$, and dividing by $-\frac{U}{2}\,ds$, it becomes

$$w^{*}(s) = 2\frac{dx}{ds} - \frac{1}{\pi}\int^{S}\frac{w^{*}}{\eta}\,(u^{*}\frac{dx}{ds} + v^{*}\frac{dr}{ds})\,d\sigma\ . \qquad (7.13)$$

The vortex density (non-dimensionalized) may now be referred to the axial length (dx) by introducing the definition of arc length

$$ds = \sqrt{dx^2 + dr^2} \quad \text{or} \quad \frac{ds}{dx} = \sqrt{1 + r'^2} \qquad (7.14)$$

giving, from (7.13)

$$\gamma^{*}(x) = 2 - \frac{1}{\pi}\int_{o}^{\infty}\frac{\gamma^{*}(\xi)}{\eta}\,(u^{*} + v^{*}\,r')\,d\xi \qquad (7.15)$$

where $\gamma^{*}(x) = w^{*}(s)\sqrt{1 + r'^2}$.

Equation (7.15) is a linear integral equation of the second kind solvable for the vortex density (γ^{*}) necessary to describe the flow field about the cone-cylinder body in a uniform potential flow parallel to the body axis. The integral equation is seen to demand that the body have a continuous tangent for the region of integration; and, it is further seen that this equation is not readily solved by elementary methods.

7.4. Solution of the Linear Integral Equation of the Second Kind[21]

The linear integral equation of the second kind

$$f(x) = F(x) + \lambda\int_{a}^{b}K_{o}(x,\xi)\,f(\xi)\,d\xi \qquad (7.16)$$

where λ = a parameter

$K_o(x,\xi)$ = the kernel of the equation,

has non-trivial solutions corresponding to characteristic values of λ (i.e., values of λ for which Det $(\lambda) = 0$), which are in the form of the sum of $F(x)$ and arbitrary multiples of the characteristic functions. If at least one of the expanded algebraic equations for the right hand side of (7.16) does not vanish, a unique non-trivial solution exists. This non-vanishing equation leads to a non-trivial solution of the integral equation only if the determinant, Det (λ), does not vanish. However, in the case where Det (λ) does vanish then these algebraic equations in the expansion are either incompatible and no solution exists, or they are redundant and an infinite number of solutions exist.

In general the characteristic values (λ) are difficult to determine, thus most practical solutions of the integral equation are obtained by an iterative process.

Suppose $f(\xi)$ is replaced by an initial approximation $f^{(0)}$ in (7.16). Then a first approximation to the solution is given by

$$f^{(1)}(x) = F(x) + \lambda \int_a^b K_o(x,\xi)\, f^{(0)}(\xi)\, d\xi \,. \qquad (7.17)$$

Substituting $f^{(1)}$ into the right-hand member of (7.16) yields a second approximation $f^{(2)}$. By continuing this procedure, successive approximations are determined as indicated by the formula

$$f^{(n)}(x) = F(x) + \lambda \int_a^b K_o(x,\xi)\, f^{(n-1)}(\xi)\, d\xi \,. \qquad (7.18)$$

To determine the conditions under which this process tends to a solution of (7.16), these results are written explicitly. To avoid ambiguity, the dummy variable ξ_1 is used in place of ξ in the first approximation, etc. Hence,

$$f^{(1)}(x) = F(x) + \lambda \int_a^b K_o(\xi, \xi_1)\, f(\xi_1)\, d\xi_1 \qquad (7.19a)$$

and

$$f^{(2)}(x) = F(x) + \lambda \int_a^b K_o(x,\xi) \left[F(\xi) + \lambda \int_a^b K_o(\xi,\xi_1)\, f^{(0)}(\xi_1)\, d\xi_1 \right] d\xi,$$

or (7.19b)

$$f^{(2)}(x) = F(x) + \lambda \int_a^b K_o(x,\xi)\, F(\xi)\, d\xi + \lambda^2 \int_a^b \int_a^b K_o(x,\xi)\, K_o(\xi,\xi_1)\, f^{(0)}(\xi_1)\, d\xi_1\, d\xi,$$

and

$$f^{(3)}(x) = F(x) + \lambda \int_a^b K_o(x,\xi)\, F(\xi)\, d\xi + \lambda^2 \int_a^b K_o(x,\xi) \int_a^b K_o(\xi,\xi_1)\, d\xi_1\, d\xi + \lambda^3 \int_a^b K_o(x,\xi) \int_a^b K_o(\xi,\xi_1) \int_a^b K_o(\xi_1,\xi_2)\, f^{(0)}(\xi_2)\, d\xi_2 d\xi_1\, d\xi \qquad (7.19c)$$

Introducing the integral operator

$$\mathcal{K} f(x) = \int_a^b K_o(x,\xi)\, f(\xi)\, d\xi \qquad (7.20)$$

then (7.16) is given symbolically as

$$f(x) = F(x) + \lambda \mathcal{K} f(x)\,, \qquad (7.16a)$$

and (7.18) takes the form

$$f^{(n)}(x) = F(x) + \lambda \mathcal{K} f^{(n-1)}(x), \tag{7.18a}$$

while (7.19a), (7.19b), (7.19c) become

$$\left.\begin{aligned} f^{(1)}(x) &= F(x) + \lambda \mathcal{K} f^{(0)}(x) \\ f^{(2)}(x) &= F(x) + \lambda \mathcal{K} F(x) + \lambda^2 \mathcal{K}^2 f^{(0)}(x) \\ f^{(3)}(x) &= F(x) + \lambda \mathcal{K} F(x) + \lambda^2 \mathcal{K}^2 F(x) + \lambda^3 \mathcal{K}^3 f^{(0)}(x) \end{aligned}\right\} \tag{7.20}$$

Or, in general,

$$f^{(n)}(x) = F(x) + \lambda \mathcal{K} F(x) + \lambda^2 \mathcal{K}^2 F(x) + \cdots + \lambda^{n-1} \mathcal{K}^{n-1} F(x) + R_n(x), \tag{7.21}$$

where

$$R_n(x) = \lambda^n \mathcal{K}^n f^{(0)}(x). \tag{7.22}$$

Hence, as $n \to \infty$, there is a possible expansion for $f(x)$ as the infinite series

$$f(x) = F(x) + \sum_{n=1}^{\infty} \lambda^n \mathcal{K}^n F(x). \tag{7.23}$$

Now it should be established under what conditions the series (7.23) converges, and for what conditions $R_n \to 0$.

Suppose that for all values of x and ξ in the interval (a,b) the kernel $K(x,\xi)$ is less, in absolute value, than some fixed positive constant M; i.e.,

$$\left|K(x,\xi)\right| < M. \tag{7.24a}$$

Also, that the prescribed constant $F(x)$ is bounded in (a,b), or,

$$\left| F(x) \right| < m \; ; \tag{7.24b}$$

and, the initial assumption $f^{(0)}(x)$ is bounded in (a,b), or,

$$\left| f^{(0)}(x) \right| < \phi \quad . \tag{7.24c}$$

These bounds are certain to exist if $f^{(0)}(x)$, $K(x,\xi)$ and $F(x)$ are continuous in the closed interval $\left[a,b\right]$. Now, assuming $b > a$, it follows that $\left| \mathcal{K} f^{(0)}(x) \right| = \left| \int_a^b K(x,\xi)\, f^{(0)}(\xi)\, d\xi \right| < \int_a^b M\phi \, d\xi = M\phi\,(b-a)$.

Thus, from iteration it is observed that

$$\left| \mathcal{K}^n f^{(0)}(x) \right| < M^n \phi\, (b-a)^n \; , \tag{7.25a}$$

and likewise that

$$\left| \mathcal{K}^n F(x) \right| < M^n m (b-a)^n \quad . \tag{7.25b}$$

Hence from (7.22) and (7.25a) it follows that

$$\left| R_n(x) \right| < \left| \lambda \right|^n M^n \phi\, (b-a)^n \quad . \tag{7.26}$$

Finally, it is seen that $R_n(x) \to 0$ if

$$\left| \lambda \right| < \frac{1}{M(b-a)} \; ; \tag{7.27}$$

and thus it follows from (7.25a) that

$$\left| f(x) \right| \leq \left| F(x) \right| + \sum_{n=1}^{\infty} \left| \lambda \right|^n \left| \mathcal{K}^n F(x) \right|$$

which, according to (7.25b), is dominated by the constant series

$$m \left[1 + \sum_{n=1}^{\infty} \left| \lambda^n \right| \left| M^n (b-a)^n \right| \right] \quad .$$

Since this constant geometric series converges for all λ's satisfying the inequality (7.27), then (7.23) converges absolutely and uniformly in the interval (a,b) when (7.27) is satisfied.

Since (7.23) is a power series, and as the solution for the integral equation generally fails when λ takes on a characteristic value, it appears certain that (7.23) will fail to converge at least as soon as $|\lambda|$ becomes equal to the absolute value of the smallest characteristic number λ_1. It can be shown that (7.23) converges, when, and only when $|\lambda| < |\lambda_1|$. Noting that (7.27) is conservative, in the sense that (7.23) may converge even though (7.27) is not satisfied, leads to the useful result that

$$|\lambda_1| \geq \frac{1}{(M(b-a))} \cdot \tag{7.28}$$

This expression describes a lower bound for the magnitude of the smallest characteristic number λ_1.

In practice it is usually more desirable to merely evaluate the successive terms in (7.23) by iteration rather than actually to pursue the method of successive substitutions which motivated (7.23). If this latter method is used, the initial approximation $f^{(0)}(x) = F(x)$ is usually a convenient one and may be used unless advanced information concerning the nature of the solution is available.

Throughout this entire section it has been presumed that the integral equation is not singular; i.e. that the range of integration

is finite and that the kernel, $K(x,\xi)$, does not possess any discontinuities in the interval (a,b). Since both these conditions are violated in the present case, special considerations must be given to the integral equation and its subsequent evaluation.

7.5. Singularities of the Integral Equation

The kernel of equation (7.15)

$$K_o(x,\xi) = \frac{u^* + r' v^*}{\eta} \tag{7.29}$$

can be expanded in terms of the coordinates of the problem into the form,

$$K_o(x,\xi) = \frac{1}{\sqrt{(x-\xi)^2 + (r+\eta)^2}} \left(\left[1 - \frac{r'(x-\xi)}{r} \right] \left[K(k^2) - E(k^2) \right] - \right.$$

$$\left. - \frac{2\eta \ (r-\eta) - r'(x-\xi)}{(x-\xi)^2 + (r-\eta)^2} \ E(k^2) \right) \ . \tag{7.29a}$$

The complete elliptic integrals of the first kind may be expanded in terms of the modulus, and the complimentary modulus, where the complimentary modulus[36]

$$k'^2 = 1 - k^2 = \frac{(x-\xi)^2 + (r-\eta)^2}{(x-\xi)^2 + (r+\eta)^2} \ . \tag{7.30}$$

That is,

$$E(k^2) = \pi/2 \left[1 - 2\frac{k^2}{8} - 3\left(\frac{k^2}{8}\right)^2 - 10\left(\frac{k^2}{8}\right)^3 - .... \right] \tag{7.31a}$$

$$E(k^2) = 1 + \frac{1}{2}\left(\Lambda - \frac{1}{2}\right) k'^2 + \frac{3}{16}\left(\Lambda - \frac{13}{12}\right) k'^4 + \cdots \qquad (7.31a)$$

and

$$K(k^2) = \pi/2\left[1 + 2\frac{k^2}{8} + 9\left(\frac{k^2}{8}\right)^2 + 50\left(\frac{k^2}{8}\right)^3 + \cdots + \cdots\right] \qquad (7.31b)$$

$$= \Lambda + \frac{1}{4}(\Lambda - 1) k'^2 + \frac{9}{64}\left(\Lambda - \frac{7}{6}\right) k'^4 + \cdots$$

where

$$\Lambda = \ln \frac{4}{k'} \quad .$$

The principal singularity of the integral equation (7.15) is for the point $x = \xi$. To ascertain the behavior of the integral at this point, the kernel is investigated below.

For $x \approx \xi$, the modulus, k^2, of the elliptic integrals approaches unity and the complimentary modulus approaches zero. If, for the present case, the coordinate η is expressed in a Taylor series

$$\eta \approx r - r'(x - \xi) + r''/2\,(x - \xi)^2 + \cdots$$

and if the expansions (7.31a) and (7.31b) are substituted into (7.29a) it can be shown that

$$K_o(x,x) \approx \frac{1}{2r}\left[\frac{rr''}{1 + r'^2} - 1 + \ln \frac{8r}{|x - \xi|\sqrt{1 + r'^2}}\right] \qquad (7.32)$$

Thus, for the case of $\xi \to x$, ($k^2 \to 1$, $k'^2 \to 0$) the singularity is logarithmic in nature and thus is integrable. From (7.32) it is likewise seen that the non-singular part of $K_o(x,x)$ is discontinuous if the point x has a discontinuity in curvature. In general, as for

the case considered here, it will be necessary to evaluate the integral by its so-called principal value at such a singular point.

The previously mentioned condition of continuous tangency needs some investigation in the region of the cone tip, and the infinite extent of integration should be investigated to ascertain the behavior of the kernel for these cases.

For the case of an intermediate pivotal point, with the special case of the variable point at the nose and the downstream end of the body; i.e.

$$x \neq 0,\infty; \quad \xi = 0,\ \eta = 0 \text{ and } \xi = +\infty,\ \eta = R_o$$

the kernel (29a) gives the results, by direct substitution, that

$$K_o(x,0) = K_o(x,\infty) = 0 \ . \tag{7.33}$$

For the case of the pivotal point at the nose of the cone, (i.e., $x = 0$) the first expansions (7.31a, 7.31b) will be used since k^2 is small for the region of the nose. Thus, deleting higher order terms in k^2 from equation (7.29a) leads to the result that

$$K_o(0,\xi) \approx \frac{\pi\eta^2}{(\xi^2 + \eta^2)^{3/2}} \left[1 - \frac{2\xi}{\xi^2 + \eta^2} \lim_{x \to 0} rr' \right] . \tag{7.34}$$

In the following paragraphs the behavior of the integral equation will be shown to be asymptotic for the case of a pivotal point far downstream on the cylindrical portion of the body.

To show the nature of the kernel for this condition, again consider the equation

$$K_o(x,\xi) = \frac{u^* + r' v^*}{\eta} \quad . \tag{7.29}$$

From the physical considerations of this case it is readily seen that $r' = 0$, and thus the kernel is given by

$$K_o(x,\xi) = \frac{u^*}{\eta} \quad . \tag{7.35}$$

Likewise, for the position defined by $x \rightarrow +\infty$, the local body velocity will approach the free-stream velocity (U) and hence equation (7.15) will yield

$$1 = 2 - \frac{1}{\pi} \int_o^{+\infty} \frac{\gamma^*(\sigma)}{\eta} u^* \, d\xi \quad . \tag{7.15a}$$

This immediately requires that

$$\frac{1}{\pi} \int_o^{+\infty} \frac{\gamma^*(\sigma)}{\eta} u^* \, d\xi = 1 \, , \tag{7.36}$$

further signifying the asymptotic behavior of the integral expression for a pivotal point far downstream on the body. Actually, this particular solution is exactly the solution for an infinite cylinder whose axis is aligned with the parallel stream (+U).

To alleviate the difficulty of an infinite range of integration, it is desirable to express the integral equation as a series summation (see equation (7.23)), and to evaluate this infinite series, approximately, by a finite series plus an additive constant. The constant will account for the infinite range of integration, being the remainer term added to the finite series sum. Now consider

equation (7.29) specialized for a pivotal point on the cylindrical portion of the body; the kernel is again given by

$$K_o(x,\xi) = \frac{u^*}{\eta} \tag{7.35}$$

but, if the variable point is likewise on the conical portion of the body, then for

$$|x - \xi| \gg 1, \text{ and } |r - \eta| \ll |x - \xi|$$

$$K(k^2) \approx E(k^2) \approx \pi/2 \ .$$

For this case the order of magnitude of (7.35) is given as

$$K_o(x,\xi) = \frac{u^*}{\eta} \approx \left| x - \xi \right|^{-3} \ . \tag{7.35a}$$

This result leads to the approximate evaluation of the integral as

$$1/\pi \int_c^\infty K_o(x,\xi)\, d\xi = \text{a constant,}$$

where c is a finite position coordinate for the cylindrical portion of the body.

The proper choice of the point "c" may be defined after viewing the graphical representation of the integral equation for some assumed iterated value of $\gamma^*(\sigma)$. Since $K_o(x,\xi)$ decreases rapidly in magnitude as $|x - \xi|$ becomes large, the contribution to $K_o(x,\xi)$ for a position $|x - \xi| >> 1$ is small (see Figure 11).

In a similar manner it is easily shown that for the case of both the pivotal and variable points located on the cylindrical portion of the body, or

$$|x - \xi| \gg 1, \quad r = \eta = R_o = 1$$

$$K(k^2) \approx E(k^2) \approx \pi/2$$

then

$$K_o(x,\xi) = \frac{u^*}{\eta} \approx 0 \quad . \tag{7.35b}$$

This result clearly indicates the asymptotic behavior of the kernel and shows that for significantly large values of $|x - \xi|$ the contribution from such points to the value of the integral may be neglected.

7.6. Numerical Solution of the Integral Equation

Following the development of section 7.4, a series expansion for $\gamma^*(x)$ may be written from equation (7.23) as

$$\gamma^*(x) = 2 + \sum_{n=1}^{\infty} \lambda^n \mathcal{K}^n \gamma^*(\xi) \tag{7.23a}$$

and, if the recursion formula (7.18) is incorporated into (7.23a), then the series expansion may be restated as

$$\gamma^*(x) = \sum_{n=0}^{\infty} \lambda^n \gamma^{*n}(x) \tag{7.23b}$$

which is a series expansion in the parameter $\lambda = -1/\pi$, and the $\gamma^{*n}(x)$ are the iterative values of $\gamma^*(x)$ necessary for this numerical solution. That is, the first few values of $\gamma^{*n}(x)$, are, for instance,

$$\gamma^{*(0)}(x) = (F(x)) = 2$$

$$\gamma^{*(1)}(x) = \int_a^b \mathcal{K}\, \gamma^{*(0)}(\xi)\, d\xi \qquad (7.37)$$

$$\vdots$$

$$\gamma^{*(n)}(x) = \int_a^b \mathcal{K}\, \gamma^{*(n-1)}(\xi)\, d\xi$$

and $\gamma^{*}(x) = \lim_{n \to \infty} \gamma^{*(n)}(x)$.

It follows from equations (7.27) and (7.28) that the series (7.23b) converges if the parameter $1/\pi < |\lambda_1|$, where λ_1 is the smallest characteristic of the kernel.

The above statements have been based on the first iterative assumption $\gamma^{*(0)} = (F(x)) = 2$, such that the iterative process is written as

$$\gamma^{*(0)}(x) = 2 - 1/\pi \int_0^\infty 2\, K_0(x,\xi)\, d\xi$$

$$\gamma^{*(1)}(x) = 2 - 1/\pi \int_0^\infty \gamma^{*(0)}(\xi)\, K_0(x,\xi)\, d\xi \qquad (7.38)$$

etc.,

and

$$\gamma^{*}(x) = \lim_{n \to \infty} \gamma^{*(n)}(x) \quad .$$

Since the solution for $\gamma^{*}(x)$ is the limit of an infinite sequence of iterations, it has been shown[18] that a more rapid convergence is afforded if the iterative sequence if given by

$$\gamma^{*(01)}(x) = 0;\ \gamma^{*(02)}(x) = 2 - \tfrac{1}{\pi} \int_0^\infty \gamma^{*(01)}(\xi)\, K_0(x,\xi)\, d\xi = 2$$

$$\gamma^{*(0)}(x) = \frac{\gamma^{*(01)} + \gamma^{*(02)}}{2} = 1 \qquad (7.39)$$

$$
\left.
\begin{aligned}
\gamma^{*(11)}(x) &= 2 - \frac{1}{\pi}\int_0^{\infty} \gamma^{*(0)}(\xi)\, K_0(x,\xi)\, d\xi; \\
\gamma^{*(12)}(x) &= 2 - \frac{1}{\pi}\int_0^{\infty} \gamma^{*(11)}(x)\, K_0(x,\xi)\, d\xi \\
\gamma^{*(1)}(x) &= \frac{\gamma^{*(11)} + \gamma^{*(12)}}{2} \\
&\vdots \\
\gamma^{*(n1)}(x) &= 2 - \frac{1}{\pi}\int_0^{\infty} \gamma^{*(n-1)}(\xi)\, K_0(,\xi)\, d\xi; \\
\gamma^{*(n2)}(x) &= 2 - \frac{1}{\pi}\int_0^{\infty} \gamma^{*(n1)}(x)\, K_0(x,\xi)\, d\xi \\
\gamma^{*(n)}(x) &= \frac{\gamma^{*(n1)} + \gamma^{*(n2)}}{2}
\end{aligned}
\right\} \quad (7.39)
$$

which converges to the same limit $\gamma^{*}(x)$. Due to the rapidity of convergence of this iterative process, the method outlined above (equations (7.39)) will be used for this problem. For the present case the first iterative assumption will employ the estimated $\gamma^{*(0)}(x) = 1$, with the procedure to follow, as given above, from that point in the iteration. At the end of each successive "step" procedure an evaluation of $\gamma^{*(i)}$ will be made; in this manner the rate of convergence will be noted, and when insignificant changes in $\gamma^{*(i)}$ are found to exist, the iteration will be stopped with the then available value of $\gamma^{*}(x)$ assumed to be the correct solution.

Since special consideration must be given to the case of $x \approx \xi$, it is advisable that this case be investigated now.

As has previously been shown, the kernel possesses a singularity, logarithmic in nature, for the variable point located at approximately the pivotal point. Thus, as this singularity is integrable, though evaluated by its so-called principal value, the integral may be written as

$$\int_0^\infty \gamma^*(\xi)\, K_o(x,\xi)\, d\xi = \underset{(1)}{\int_o^a} + \underset{(2)}{\int_a^x} + \underset{(3)}{\int_x^b} + \underset{(4)}{\int_b^\infty} \qquad (7.40)$$

where a and b are arbitrary values of ξ within the range of integration. The second and third parts of (7.40) still retain the singularity at $\xi = x$, but this singularity may be removed by a coordinate transformation. That is, if the transformation is given by

$$x - \xi = \chi^2 \quad \text{for integral (2) of (7.40), with } d\xi = -2\chi d\chi$$

$$\xi - x = \chi^2 \quad \text{for integral (3) of (7.40), with } d\xi = +2\chi d\chi$$

then integrals (2) and (3) become

$$\int_o^{\sqrt{x-a}} \gamma^*(\xi)\, K_o(x,\xi)\, 2\chi d\chi \text{ and } \int_o^{\sqrt{b-x}} \gamma^*(\xi)\, K_o(x,\xi)\, 2\chi d\chi \qquad (7.41)$$

respectively. The behavior of these integrals now being

$$\gamma^*(\xi)\, K_o(x,\xi)\, 2\chi = \gamma^*\, K_o^*\, \propto \text{constant} \cdot \chi \cdot \ln \chi$$

which approaches zero as χ approaches zero (i.e., for the position $\xi = x$). By use of this coordinate transformation the integrals are

now treated by the usual numerical methods (see Figure 11 for the relative graphical relation of K_o and K_o^*). For the present problem the interval (a,b) will, in general, be chosen as the length of the conical portion of the body.

At this point sufficient information is available to allow the integration of the linear integral equation (7.15) according to the iterative scheme (7.39). The procedure will entail the plotting of the kernel functions and evaluation of the graphical plot by mechanical, graphical, or numerical means. One advantage to plotting the result is that information regarding the trend of the convergence, for each successive iteration, can readily be seen. Too, the relative number of required pivotal points, which most accurately describe the change of the plot for the kernels, can be determined as the process is carried forth. It has been found that, in general, three or four pivotal points are required in the region where the body has constant curvature; that several (3 or 4) additional points are needed around the point(s) where the curvature is discontinuous; and several points needed on the afterbody. If any unusual trends begin to appear on the running plots for the successive iterations, additional pivotal points should be taken in these regions in order that these unusual occurences may be more adequately defined.

7.7. Application of the Trapezoidal Rule to the Numerical Integration

In applying the General Trapezoidal rule[35] to the numerical integration of the integral equation (7.15), it is necessary to

develope the equation in a manner such that the singularities of the kernel function are degenerated and taken into account[20]. Primarily, consideration must be made of the point $\xi = x$ which bears the significant singularity of the equation.

In principal the idea here is to replace the integral

$$I(x) = \int_0^\infty \gamma^* (\xi)\, K_0(x,\xi)\, d\xi \qquad (7.42)$$

by a finite sum of the ordinates $\gamma^* K_0$ multiplied by suitable weighted values p_μ, such that

$$I(x) = \sum_\mu \gamma^* (\xi_\mu) \cdot p_\mu \cdot K_0(x,\xi_\mu) \qquad (7.43)$$

In order that a good approximation may be obtained for equation (7.42) with a minimum number of chosen variable points, ξ_μ, these points should be chosen so that each term of (7.43) should contribute approximately the same to that sum.

This may be done by a suitable integral variable transformation (see reference 8), such as

$$h = h(\xi), \text{ and thence } d\xi = \frac{1}{h'(\xi)}\, dh(\xi) \quad .$$

Using this transformation equation (7.42) may be written as

$$I(x) = \int_{h(0)}^{h(\infty)} \gamma^*(\xi)\, K_0(x,\xi)\, \frac{1}{h'(\xi)}\, dh(\xi), \qquad (7.44)$$

where $h'(\xi)$ is the derivative of $h(\xi)$ with respect to ξ.

The requirements on this transformation are that it remove the singularities as much as possible, and either transform the interval of integration into a finite interval, or allow the series to converge rapidly enough so that the infinite interval may be described by a sum plus an additive constant (see the preceding section). These requirements are given as

(a) $h(x) = 0$

(b) $\lim_{\xi \to x} K_0(x,\xi) \frac{1}{h'(\xi)}$ = finite value (specifically for the logarithmic singularity).

(c) $h(\infty)$ = finite value (for the infinite integral consideration).

It will also be advantageous to choose the $h(\xi)$ in such a manner that the variable points (ξ_μ) are symmetrically placed with respect to the pivotal point; i.e.,

$$\frac{\xi_\mu + \xi_{-\mu}}{2} = x ,$$

indicating that $h(x - \xi) = - h(\xi - x)$.
These conditions will then show the weights (p_μ) to bear the relationship

$$p_\mu = p_{-\mu} .$$

These requirements are readily seen to be satisfied by the simple function

$$h(\xi) = \operatorname{sgn} (\xi - x) \sqrt{\frac{|x - \xi|}{|x - \xi| + 1}} \qquad (7.45)$$

and, it follows immediately that

$$\frac{1}{h'(\xi)} = 2\sqrt{|x-\xi|\left(|x-\xi| + 1\right)^3} \qquad (7.46)$$

It can be shown that the conditions on the transformation are satisfied: i.e., condition (a) is obviously met; condition (b) is

$$\lim_{\xi \to x} K_o(x,\xi)\,\frac{1}{h'(\xi)} = 0$$

(an indeterminate form requiring some manipulation);

and condition (c) is

$$h(\infty) = \lim_{\xi \to \infty} \sqrt{\frac{|x-\xi|}{|x-\xi| + 1}} = 1 .$$

Thus, when equations (7.46) and (7.45) are substituted into (7.44), the result is that

$$I(x) = \int_{h(o)}^{h(\infty)} 2\gamma^{*}(\xi)\, K_o(x,\xi) \cdot \cdot\sqrt{|x-\xi|\left(|x-\xi| + 1\right)^3}\, d\left[\operatorname{sgn}(\xi - x)\sqrt{\frac{|x-\xi|}{|x-\xi| + 1}}\right]. \qquad (7.47)$$

When the general trapezoidal rule for integration

$$\int_a^b f(x)\,dx \approx \frac{1}{2}\left[f(a)\,(x-a) + \sum_1^{n-1}\left[f(x_\mu)\,(x_{\mu+1} - x_{\mu-1})\right] + + f(b)\,(b-x)\right]$$

is used to evaluate the integral for a general point x, the expression

involves only the central sum if $f(a) = f(b) = 0$. It will be recalled that this situation exists for the present case (when the trapezoidal rule is applied to the integral of equation (7.15)) since, for $x \neq 0,\infty$, $K_o(x,0) = K(x,\infty) = 0$. Actually, this same result may be applied to a finite interval of integration (with the addition of a small constant) without inducing significant error. This becomes apparent when it is recognized that $K_o(x,\xi)$ approaches zero for $|x - \xi| \gg 1$ (this is given in equation (7.35b) and can be seen from the plot of Figure 11). Thus, the application of the trapezoidal rule reduces to

$$I(x) \approx \sum_{1}^{n-1} \gamma^{*}(\xi_\mu)\, K_o(x,\xi_\mu) \cdot$$

$$\cdot \sqrt{|x - \xi_\mu|\,(\,|x - \xi_\mu| + 1)^3}\,\Big[h(\xi_{\mu+1}) + h(\xi_{\mu-1})\Big] \qquad (7.48)$$

for any general point ($x \neq 0,\infty$). On identifying (7.48) with (7.43) it is immediately seen that

$$p_\mu = \frac{h(\xi_{\mu+1}) + h(\xi_{\mu-1})}{2h'(\xi)} = \operatorname{sgn}(\xi_\mu - x)\,\sqrt{|x - \xi_\mu|\,(|x - \xi_\mu| + 1)^3} \cdot$$

$$\cdot \left[\sqrt{\frac{|x - \xi_{\mu+1}|}{|x - \xi_{\mu+1}| + 1}} - \sqrt{\frac{|x - \xi_{\mu-1}|}{|x - \xi_{\mu-1}| + 1}}\right] \qquad (7.49)$$

It is now necessary that the points, ξ_μ, be specified for the evaluation of the weights p_μ. As previously stated, these points

should be so chosen that each part of the summation contributes approximately the same to the final sum. Thus, the ξ_μ should be chosen so that they are numerically convenient and so that Δ h would be nearly constant. On plotting $h(\xi)$ the following set of variable points are specified, these giving as nearly constant values of Δ h as is convenient. (It is noted that constant increments in $h(\xi)$ would dictate fractional values of ξ, and thus are not suitable for easy arithmetic). It has been found that small variations in the intervals $\Delta\, h(\xi)$ do not cause appreciable errors in the numerical work.

$\mu = 0$	± 1	± 2	± 3	± 4	± 5
$\frac{(x - \xi_\mu)^*}{L_{cone}} = 0$	$\pm .01$	$\pm .04$	± 0.1	± 0.20	± 0.40
$^* p_\mu =$	$\pm .1112$	$\pm .2393$	$\pm .4417$	$\pm .7687$	± 1.466

μ	± 6	± 7	± 8	± 9	± 10	± 11	± 12
$\frac{(x - \xi_\mu)^*}{L_{cone}}$	± 0.7	± 1.0	± 1.5	± 2.5	± 4.0	± 9	∞
$^* p_\mu$	± 1.96	± 2.14	± 3.82	± 7.28	± 13.01	± 57.4	

Finally, for the case of $x = 0$, the procedure is the same as before except that here the $\lim_{\xi \to x} K_o(x,\xi) \sqrt{(|x + \xi_\mu|)(|x - \xi_\mu| + 1)^3} \neq 0$.

* These values are for a cone of semi-apex angle $\theta_c = 10^o$.

For this case the integral is evaluated as the sum

$$I(0) = \gamma^{*}(0)\sqrt{\frac{\xi_1}{\xi_1 + 1}} \lim_{\xi \to 0} K_o(0,\xi)\sqrt{\xi} + \sum_{1}^{\infty} \gamma^{*}(\xi_\mu)\, K_o(0,\xi_\mu)\, P_\mu \qquad (7.50)$$

The first value of $P_\mu = p_o = \sqrt{\frac{\xi_1}{\xi_1 + 1}} = 0.0995\, L_{cone}$, the remaining weights being given in the table above.

Basically the procedure recommended for the calculations here is the same as that previously stated, with the caution that the selection of pivotal points must be carefully made (as per the previously noted selection), and that a running plot of the results should be made so that all variations in the iterative procedure can be noted as the work progresses. Since each numerical integration must be iterated, it is recommended that the scheme (equations (7.39)) be used with the addition of pivotal points as needed. It will be advisable to choose points spaced more closely to each other in the regions where changes in body contour occur, since these regions will generally exhibit peculiar variations not consistent with points for the more "regular" body contour.

It is truly unfortunate that the labor involved here is rather extensive; however, a far greater degree of accuracy is given by this method than by the so-called "classical approach" of axially distributed sources and sinks. At the same time it should be mentioned that this method, though tedious, is not as complicated as other methods (such as distributed diapoles, or surface distributed sources and sinks[17]).

7.8. Determination of the Pressure Distribution

The procedures just outlined give the vortex density, $\gamma^*(x)$, to the desired degree of accuracy, for a specified body of revolution in a parallel potential flow. From this result the velocity distributed over the body may now be obtained and from that the required pressure distribution. Since the flow field considered is that of a perfect fluid, the relationship between pressure and velocity is given by the incompressible Bernoulli equation.

In determining the local velocity at any point on the body surface, equation (7.14) is utilized where, from (7.14)

$$w^*(s) = \frac{w(s)}{U} = \frac{\gamma^*(x)}{\sqrt{1 + r'^2}} \quad . \tag{7.51}$$

Through the Bernoulli equation, the pressure distribution, expressed in terms of the pressure coefficient, is

$$C_p = \frac{p_L - p_o}{q} = 1 - w^*(s)^2 \tag{7.52}$$

where: p_o is the free-stream static pressure, p_L is the local static pressure and q is the free-stream dynamic pressure ($\rho U^2/2$). Thus from (7.51), the pressure coefficient is immediately given in terms of the local vortex density and body slope as

$$C_p = 1 - \frac{\gamma^*(x)}{\sqrt{1 + r'^2}} \quad . \tag{7.52a}$$

Equation (7.52a) yields the desired result for the problem.

7.9. Comparison of Theory and Experiment

The relative degree of accuracy of the theoretical development just outlined may be seen in Figure 12, where the experimental results, obtained in the V.P.I. subsonic wind tunnel, are compared to the theory. The agreement exhibited here is good, the greatest variation being in the region of the body junction point (or the plane where the cone and the cylinder join). Some discrepancy in results was expected since the experiment was performed in a real fluid while the theory considered a perfect fluid. It is seen that the apparent choice of the arc joining the cone and cylinder, for theory, is certainly adequate for comparative purposes. In the case of the real fluid, some rounding of the junction was expected due to boundary layer effects.

The next section will be concerned with the calculation of pressure coefficient for each class of fluid flow considered in this investigation.

8. CALCULATION OF THE PRESSURE COEFFICIENT

In order to indicate the methods by which pressure distributions were calculated for each type of flow considered, the procedures will be outlined below according to the classification of flow.

8.1. Incompressible Potential Flow.

The ideal case has been presented with the method used to define the local velocity distribution over the body for incompressible potential flow. After determining the velocities the incompressible form of the Bernoulli equation was used to obtain the local body pressures (see section 7).

8.2. Subcritical Flow.

A description of the flow field classed as a subcritical flow has been given in section 4. It is in this range of Mach number that linear theory may be employed to define the flow properties about the body, and makes the calculation of the pressure distribution possible.

With the data of the incompressible case available, either from systematic experimental studies or from a suitable potential flow analysis, the proper application of the linearized compressible correction formula may be applied to obtain the pressure envelope at values of subcritical Mach number. It has been established that the proper method to be utilized for approximating the compressible effect on pressures is the Gothert Rule. In section 5, the form of Gothert's Rule is given by equation (5.17); this equation states that

the pressure coefficient for a given body of thickness δ, at a free stream Mach number of M_∞ may be defined as follows: the incompressible pressure distribution over a body of reduced thickness $\beta\delta$ is corrected according to the equation

$$C_{p_{c_\delta}} = \frac{C_{p_i}}{\beta^2}\Big|_{\beta\delta} \quad . \tag{5.51}$$

Here both the thickness effect and the compressible effect have been taken into account. Body thickness effect has been introduced through the affinely related goemetry of the bodies, and compressibility has been introduced through division by the Mach factor, β^2. The equation shows that for a complete definition of all pressure envelopes, for the full range of Mach number, this would require a large number of incompressible pressure distributions since each Mach number demands a new body thickness, $\beta\delta$. In an effort to reduce the amount of labor involved for the calculation of such a large number of incompressible solutions, the unpublished data referred to in section 6 have been utilized. This collection of results represents a systematic solution of the incompressible flow case for a large number of bodies carried out by automatic calculation on an electronic computer. Should these results not have been available a large number of man hours would have been required to compile the necessary data using the method of section 7.

Knowing the limiting Mach number for which the correction formula may be applied, the estimation of the pressure distributions can be given for the entire range up to the established lower critical speed.

8.3. Supercritical Flow.

The solution for the pressure distribution over a cone body in supercritical flow has been given by Taylor and Maccoll[65]. Though the authors give their results in mathematical form, with the numerical integrations indicated, a complete and accurate tabulation of these results is presented in reference 66. Great care and accuracy were reported to have been exercised in the calculation of these tables, and it is common practice today to utilize this publication whenever the conical solution is desired. Since both the method and theory are presented in this volume, no description of these will be given here. In part these results were used in the preparation of Figures 13a, b, c, d, and are indicated on the figures.

8.4. The Critical Flow Case.

In the range of Mach number describing critical flow, or transonic flow, the calculation of the pressure distribution follows the assumptions and concepts outlined in the description of this type of flow.

Once the pressure distribution has been established at the lower critical Mach number, which has been determined from the subcritical flow case, the local Mach number stationarity theorem is introduced to formulate the method for determining subsequent pressure distributions.

From equation (3.28), the general definition of pressure coefficient,

$$C_p = \frac{2}{\gamma M_\infty^2}\left(\frac{p_L}{p_\infty} - 1\right) \tag{3.28}$$

the pressure ratio can be defined more conveniently as

$$\frac{p_L}{p_\infty} = \frac{p_L}{p^*}\,\frac{p^*}{p_\infty} \quad . \tag{8.1}$$

If the flow field is considered to be isentropic throughout, and the free-stream Mach number taken to be less than one, then from the pressure - Mach number relation, the component ratios given in (8.1) may be evaluated separately. That is, for the general isentropic pressure ratio formula

$$\frac{p_1}{p_2} = \left[\frac{2 + (\gamma - 1) M_2^2}{2 + (\gamma - 1) M_1^2}\right]^{\frac{\gamma}{\gamma - 1}} \tag{8.2}$$

if subscript (1) is identified as the local condition (L), and subscript (2) is the local sonic (*) condition, then (8.2) may be rewritten as

$$\frac{p_L}{p^*} = \left[\frac{2 + (\gamma - 1) M^{*2}}{2 + (\gamma - 1) M_L^2}\right]^{\frac{\gamma}{\gamma - 1}} \quad . \tag{8.2a}$$

But, since the local sonic condition is characterized by a Mach number of unity, then

$$\frac{p_L}{p^*} = \left[\frac{\gamma + 1}{2 + (\gamma - 1) M_L^2}\right]^{\frac{\gamma}{\gamma - 1}} \quad . \tag{8.2b}$$

Now, introducing the stationarity of local Mach number, it follows that p_L/p^*, for any body station and for all free-stream Mach numbers in the transonic range, is an invariant. Letting

$$\frac{p_L}{p^*} = G = \left[\frac{\gamma + 1}{2 + (\gamma - 1) M_L^2}\right]^{\frac{\gamma}{\gamma - 1}} \tag{8.3}$$

equation (8.1) is rewritten as

$$\frac{p_L}{p_\infty} = G \frac{p^*}{p_\infty} \quad . \tag{8.1a}$$

If now in (8.2) condition (1) is to be the (*) condition, and if subscript (2) is to be identified with the free stream (∞), then

$$\frac{p^*}{p_\infty} = \left[\frac{2 + (\gamma - 1) M_\infty^2}{\gamma + 1}\right]^{\frac{\gamma}{\gamma - 1}} \quad . \tag{8.4}$$

Combining (8.2) and (8.4) through (8.1) yields,

$$\frac{p_L}{p_\infty} = \left[\frac{\gamma + 1}{2 + (\gamma - 1) M_L^2}\right]^{\frac{\gamma}{\gamma - 1}} \left[\frac{2 + (\gamma - 1) M_\infty^2}{\gamma + 1}\right]^{\frac{\gamma}{\gamma - 1}} \tag{8.1b}$$

or, in place of (8.1b) write the G from (8.3), so that,

$$\frac{p_L}{p_\infty} = G\left[\frac{2 + (\gamma - 1) M_\infty^2}{\gamma + 1}\right]^{\frac{\gamma}{\gamma - 1}} \quad . \tag{8.1c}$$

Writing (8.1c) for $\frac{p_L}{p_\infty}$ in (3.28), then the pressure coefficient is given by

$$C_p = \frac{2}{\gamma M_\infty^2} \left(G \left[\frac{2 + (\gamma - 1) M_\infty^2}{\gamma + 1} \right]^{\frac{\gamma}{\gamma - 1}} - 1 \right) , \qquad (8.5)$$

where $M_\infty \leq 1.0$.

Equation (8.5) defines the local pressure coefficient for any body station as a function of the free-stream Mach number and the invariant pressure ratio G.

The value of G is determined from the predicted pressure coefficients defined at the upper limit of the subcritical range of Mach numbers. Recalling that the onset of local Mach number stationarity occured for the lower critical Mach number, then G is defined from equation (8.5), where the C_p values are those obtained from the subcritical upper limit analysis. Thus, solving (8.5) for G, and writing for M_∞ the lower critical value, $M_{\infty_{cr}}$, then

$$G = \left(1 + \frac{\gamma M_{\infty_{cr}}^2}{2} C_{p_{cr}} \right) \left[\frac{2 + (\gamma - 1) M_{\infty_{cr}}^2}{\gamma + 1} \right]^{\frac{-\gamma}{\gamma - 1}} . \qquad (8.6)$$

Some experimental results[42] do exist from which estimates of p_L/p^* may be obtained. Figures 14 indicate the approximate shape of the p_L/p^* distribution as calculated from the material available in reference 42. An inspection of these curves show that the stationarity of local Mach number is a very reasonable approximation for free stream Mach numbers close to unity. Unfortunately the experimental results are given only for the subsonic range of Mach number

near unity, and therefore there are no (p_L/p^*) distributions on the supersonic side of this unity.

For the analysis carried out in this investigation it was necessary to obtain the p_L/p^* curves from the analytical evaluation of pressure coefficients described in this section. In the actual evaluation process it became apparent that the p_L/p^* curves required some adjustment in the vicinity of the cone's shoulder, since the theoretical prediction could not completely follow physical and experimental evidence. To make these curves fit the requirement that local sonic conditions occur at the body shoulder, and do so at the free stream lower critical Mach number, the theoretical values obtained by equation (8.6) had to be "rounded-off" to the value of $p_L/p^* = 1.0$ at the shoulder. This adjusting was accomplished by fairing the curves from their calculated values, at approximately an x/L_{cone} position of 0.85, to the value of unity at the shoulder position ($\frac{x}{L_{cone}} = 1.0$). The nature of this adjusting is seen in Figure 15. The curves in this figure represent a composite diagram for all body sizes investigated, and thus show the nature of the approximation for the entire study.

The determination of $M_{\infty_{cr}}$ has not as yet been described, but this will be discussed immediately following the next few paragraphs.

Equation (8.5) may be used for defining C_p so long as the free-stream Mach number is not greater than unity. Once the flow is defined by $M_\infty > 1.0$, there will be a shock wave present in the flow

upstream of the body and the isentropic assumption previously made cannot be used for the entire flow field. Specifically, the flow through the shock wave is non-isentropic, though the region of flow upstream and downstream of the shock may be considered isentropic. Since there exists a pressure change across the shock, then in order to use the definition (3.28), the pressure ratio p_L/p_∞ must be properly defined to take into account this change. The wave form will be considered to be basically that of a normal wave, and as such the pressure change will be defined from normal shock relations. In fact the pressure ratio will be defined in a manner such that the normal shock assumption will be quite reasonable. This is apparent from the following steps.

Writing the pressure ratio (equation (8.1)) as

$$\frac{p_L}{p_\infty} = \frac{p_L}{p^*} \cdot \frac{p^*}{p_{stag}} \cdot \frac{p_{stag}}{p_\infty} \tag{8.7}$$

the individual ratios will be evaluated separately as before. Considering the Mach number range to be that where $\frac{p_L}{p^*}$ is still constant, then this ratio is given by the constant value "G" obtained from (8.6).

To determine the value of p^*/p_{stag}, let the flow field depicting these pressures be confined to the region of the body. Since this region is isentropic then (8.2) may be used, where here subscript (1) refers to the local sonic value and subscript (2) refers to the

body stagnation point. Hence (8.2) is written for this case as

$$\frac{p^*}{p_{stag}} = \left[\frac{2}{\gamma + 1} \right]^{\frac{\gamma}{\gamma + 1}} \quad . \tag{8.1d}$$

Obviously (8.1d) is a constant for the range of Mach numbers considered here, and if this constant is defined as

$$\frac{p^*}{p_{stag}} = G_1$$

then, equation (8.7) may be written as

$$\frac{p_L}{p_\infty} = G \cdot G_1 \cdot \frac{p_{stag}}{p_\infty} \quad . \tag{8.7a}$$

To evaluate the remaining ratio (p_{stag}/p_∞), it must be recognized that this relates the body stagnation pressure to the free stream static pressure. Since there exists a head loss across the normal shock, as defined by the entropy increase, then the flow being non-isentropic will demand a relationship not previously indicated. The proper relationship between pressures and Mach number, across the shock, is given by the Rayleigh Equation[67], which states that

$$\frac{p_{stag}}{p_\infty} = \frac{\left[\frac{\gamma + 1}{2} M_\infty^2 \right]^{\frac{\gamma}{\gamma - 1}}}{\left[\frac{2\gamma}{\gamma + 1} M_\infty^2 - \frac{\gamma - 1}{\gamma + 1} \right]^{\frac{1}{\gamma - 1}}} \quad . \tag{8.8}$$

Now, equation (8.7a) can be completely expressed in terms of constants and the free-stream Mach number as

$$\frac{p_L}{p_\infty} = G \cdot G_1 \cdot \frac{\left[\frac{\gamma+1}{2} M_\infty^2\right]^{\frac{\gamma}{\gamma-1}}}{\left[\frac{2\gamma}{\gamma+1} M_\infty^2 - \frac{\gamma-1}{\gamma+1}\right]^{\frac{1}{\gamma-1}}}, \tag{8.7b}$$

and thus the proper form of (3.28) is

$$C_p = \frac{2}{\gamma M_\infty^2}\left\{ G \cdot G_1 \cdot \frac{\left[\frac{\gamma+1}{2} M_\infty^2\right]^{\frac{\gamma}{\gamma-1}}}{\left[\frac{2\gamma}{\gamma+1} M_\infty^2 - \frac{\gamma-1}{\gamma+1}\right]^{\frac{1}{\gamma-1}}} - 1 \right\}$$

or, when expanded this becomes

$$C_p = \frac{2}{\gamma M_\infty^2}\left\{ \left[\frac{2 + (\gamma-1) M_L^2}{\gamma+1}\right]^{\frac{\gamma}{\gamma+1}} \left[\frac{2}{\gamma+1}\right]^{\frac{\gamma}{\gamma-1}} \cdot \frac{\left[\frac{\gamma+1}{2} M_\infty^2\right]^{\frac{\gamma}{\gamma-1}}}{\left[\frac{2\gamma}{\gamma+1} M_\infty^2 - \frac{\gamma-1}{\gamma+1}\right]^{\frac{1}{\gamma-1}}} - 1 \right\} \tag{8.9a}$$

where $M_\infty \geq 1.0$.

Here again C_p has been given functionally in terms of the free-stream Mach number. Equations (8.5) and (8.9) are of different form due to the presence of the shock wave in the flow field.

Another method, which correctly relates the pressure coefficient to free-stream Mach number, and which involves less calculation if tabulated normal shock relations are available, is given by the following. Writing for p_L/p_∞ the ratio forms,

$$\frac{p_L}{p_\infty} = \frac{p_L}{p^*} \cdot \frac{p^*}{p_d} \cdot \frac{p_d}{p_\infty} \tag{8.10}$$

where $(\ )_d$ refers to flow conditions downstream of the normal shock, then the ratio (p^*/p_d), being isentropically defined, is

$$\frac{p^*}{p_d} = \left[\frac{2 + (\gamma - 1)M_d^2}{\gamma + 1} \right]^{\frac{\gamma}{\gamma - 1}} \tag{8.11}$$

from equation (8.2). The ratio p_d/p_∞, which relates the static pressure downstream of the shock to that upstream of the shock (the free-stream value), is given by[67]

$$\frac{p_d}{p_\infty} = \frac{1 + \gamma M_\infty^2}{1 + \gamma M_d^2} \quad . \tag{8.12}$$

The relationship between M_∞ and M_d is also given from normal shock relations. This expression is

$$M_d^2 = \frac{2 + (\gamma - 1) M_\infty^2}{2\gamma M_\infty^2 - (\gamma - 1)} \quad . \tag{8.13}$$

Substituting this into (8.12), and simplifying, then

$$\frac{p_d}{p_\infty} = \frac{2\gamma M_\infty^2 - (\gamma - 1)}{2 - \dfrac{(\gamma - 1)(1 - M_\infty^2)}{1 + \gamma M_\infty^2}} \quad . \tag{8.14}$$

Now, using equations (8.14) and (8.11) in (8.10), where equation (8.11) is written in terms of the free-stream Mach number (through equation (8.13)), then the pressure coefficient expression becomes

$$C_p = \frac{2}{\gamma M_\infty^2} \left\{ G \left[\frac{\gamma + 1}{2\gamma + \dfrac{1 - \gamma}{M_\infty^2}} \right]^{\frac{\gamma}{\gamma - 1}} \cdot \frac{2\gamma M_\infty^2 + (1 - \gamma)}{2 - \dfrac{(\gamma - 1)(1 - M_\infty^2)}{1 + \gamma M_\infty^2}} - 1 \right\} \tag{8.15}$$

(for $M_\infty \geq 1.0$).

When tabulated data for normal shock relations are available a more useful form of the equation for C_p is

$$C_p = \frac{2}{\gamma M_\infty^2} \left\{ G \left[\frac{2 + (\gamma - 1) M_d^2}{\gamma + 1} \right]^{\frac{\gamma}{\gamma - 1}} \cdot \frac{p_d}{p_\infty} - 1 \right\} \tag{8.16}$$

(for $M_\infty \geq 1.0$).

This expression is more applicable since the tables give the values of M_d and p_d/p_∞ for corresponding values of M_∞. Hence (8.16) and/or (8.15) again define the local pressure coefficient in terms of free stream Mach number and the invariant pressure ratio "G". It is easily shown that (8.16) and (8.5) give identical results when

$M_\infty = 1.0$ (sonic free-stream value). Thus the values of C_p are continuously defined through the entire transonic range with no discontinuities in value being exhibited.

8.5. Determination of the Lower Critical Free-Stream Mach Number

A necessary condition for the ascertaining of the transonic pressure distributions, etc. is the determination of the lower critical free-stream Mach number. It is of particular importance that this be defined since it is the principle parameter needed to establish the value of the invariant pressure ratio p_L/p^* defined in section 8.4.

Prior to this point the physical and theoretical arguments pertinent to this quantity have been stated, and the necessary interpretation of its role in the subcritical investigation has been given. But, in so far as the actual evaluation is concerned, it will now be necessary to rely on the experimental and/or theoretical works which are available in the literature.

Having established that this value of Mach number defines the upper limit of linear theory, and simultaneously the lower bound for the critical flow range, then the estimation of the value may be established from the physical evidence of either of the above boundaries. In this investigation the estimation will be made through the linear theory relations, and will be done in an indirect manner due to the lack of sufficient data necessary to making a direct evaluation.

Usually, as in the case of slender ellipsoids of revolution, the Gothert definition of compressible pressure coefficient together with the general definition of pressure coefficient (equation (3.28)) can be used to obtain a transcendental equation for the critical Mach number (see the development in section 5). But for the cone-cylinder it is difficult to apply the potential theory solution (required by Gothert's Rule) since the theory does not predict reliable minimum values of C_p with which to estimate $M_{\infty_{cr}}$ adequately. To alleviate this discrepancy a method has been devised which allows the fitting of this estimate to available data obtained from the literature. The manner in which the estimates are made is indicated below.

A value of the potentially defined pressure coefficient has been taken, which when extrapolated by Gothert's Rule, gives results that agree with the experimental data of reference 42. Once an initial agreement is established, a body position is defined which corresponds to the value of the incompressible pressure coefficient used to yield the lower critical Mach number. All subsequent critical values are then obtained by using the pressure coefficient taken for the same streamwise body position for the proper cone size. In order that the critical Mach number can be defined as directly as possible, the incompressible pressure coefficient is used to determine the corresponding fineness ratio for an equivalent ellipsoid of revolution. The data of minimum pressure coefficient for various ellipsoids of

revolution are given in reference 29. With the equivalent ellipsoidal fineness ratio established, the critical Mach number was estimated according to the method described in section 5. Though this procedure is somewhat artificial, it appeared to be the most logical one by which consistant values of the Mach number can be obtained. Actually, this procedure was found outlined in reference 67, with the comment that such was recommended when adequate physical measurements or other data were not available. The value of the incompressible pressure coefficient used to obtain the critical Mach number, by the procedure defined here, was that value taken for the 92 percent streamwise body coordinate.

Having defined the lower critical Mach number, the next step in the analysis is the evaluation of the pressure ratio p_l/p^* given by equation (8.1). The actual determination of this quantity was made using equation (8.6), and the pressure distribution on the conical head for the transonic range of Mach numbers was next obtained from equations (8.5) and (8.16). The upper limit on the range of Mach numbers, for which (8.16) was used, has been previously given by equation (4.1).

8.6. Presentation of Results

The results of the calculations as described in this and the previous sections are presented in Figures 13. These figures also have some results plotted from the material of reference 66. These results are presented only to indicate the differences in pressure

envelopes for the critical and supercritical flow cases. It should be noted that a wide range of conical heads have been studied by this method. The procedure used in this study has not been restricted, as have so many other analytical treatments wherein the transonic equation of motion was necessarily solved under the restraining slender body assumption. The nature of the solution carried out here, with emphasis placed more strongly on physical concepts than on analytical manipulations, has not been weakened by the perturbational restriction which becomes quite severe in the near sonic speed range. Though the method is only approximate the results obtained are quite gratifying, particularly for the close agreement which will be noted and discussed later.

One of the fundamental comparisons and predictions set as a goal for this problem was the ability of the method to estimate the wave drag experienced by the body in transonic flight. Sufficient knowledge and information may now be obtained from the method to carry out the calculations needed to define the wave drag coefficient. In the next topic this will be outlined and the present investigation compared with other studies.

9. DETERMINATION OF WAVE DRAG COEFFICIENT

9.1. Determination of the Drag Coefficient

The pressure envelope surrounding the body of revolution is continually changing as the free-stream speed increases; these changes are twofold in nature, being dependent upon both the increase in free-stream speed and the compressible nature of the fluid flow in which the body is immersed. In this analysis these effects are recognized and evaluated by noting the variation of forces developed on the body under conditions of a compressible fluid flow.

Presuming the body to be immersed in a uniform inviscid steady stream, flowing in the axial direction, pressure variations due to the kinetic action of the stream over the body are present at all body surface elements. It is immediately apparent that a body axially aligned with the remote stream direction, and of circular cross-section, will not experience forces normal to the direction of flow. But, there will be pressure variations present which will exert forces in the streamwise direction. Focusing attention only on the kinetic pressure effects, the forces under consideration will be those comprised only of those pressures which are dependent on local dynamic fluid action. Thus a general increment of pressure force is

$$dF = (p_L - p_\infty)\, dA$$

where dA is an element of wetted surface area. Resolving the force into normal and streamwise components, and considering only the

streamwise component, from the above argument, then

$$dD = (p_L - p_\infty)\, dA_d$$

where dA_d is an element of drag area (see Figure 16). Since the flow patterns are similar in all meridian planes, the total drag force due to pressure is

$$D = 2\pi \int_0^{R_o} (p_L - p_\infty)\, r\, dr \quad . \qquad (9.1)$$

To convert this force into a more useful (non-dimensional) form, consider the drag coefficient which is defined as

$$C_D = \frac{D}{q_\infty A_d} \quad ,$$

where q_∞ is the stream dynamic pressure, A_d is the body drag area, which for the present investigation will be taken as the maximum cross-sectional area for the body ($= \pi R_o^2$). Thus from (9.1),

$$C_D = \frac{4}{\gamma M_\infty^2} \int_0^{R_o} \frac{(p_L - p_\infty)}{p_\infty} \frac{r}{R_o^2}\, dr \quad . \qquad (9.2)$$

Evaluating the drag coefficient only over the conical head of the body, since the cylindrical afterbody will not have pressure force components in the stream direction; then, from the geometrical consideration,

$$r = x \text{ tn } \theta_c$$

and $$dr = (\text{tn } \theta_c)\, dx \, ,$$

(9.2) becomes

$$C_D = \frac{4}{\gamma M_\infty^2} \int_0^1 \left(\frac{p_L}{p_\infty} - 1 \right) \cdot \frac{x}{L} \cdot d\left(\frac{x}{L} \right) \qquad (9.2a)$$

where L is the conical head length in the stream direction and where the integration has been written in terms of body axial coordinate rather than the radial coordinate. From equation (3.28), the definition of pressure coefficient, alternate forms of (9.2a) are

$$C_D = 2 \int_0^{1.0} C_p \cdot \frac{x}{L} \cdot d\left(\frac{x}{L} \right) \qquad (9.2b)$$

and/or

$$C_D = \int_0^{1.0} C_p \cdot d\left(\frac{x}{L} \right)^2 \quad . \qquad (9.2c)$$

These last expressions (9.2b) and (9.2c) are useful forms to apply in the numerical and/or graphical integration of the pressure envelope when the pressures are not expressed as an analytic function of the variable of integration. Due to the complexity of the expressions for pressure coefficient, it is necessary in this work to do such an integration by informal means. The actual manipulations herein will be carried out according to the scheme (9.2b), though (9.2c) is equally applicable.

To successfully perform the integration for C_D it is necessary to express C_p in a manner whereby the compressibility effect on the local pressures is taken into account. This can be accomplished by

correctly expressing the pressure ratio $\frac{p_L}{p_\infty}$, in the pressure coefficient, in terms of Mach number.

In section 8, for the case of $M_\infty \leq 1.0$, the pressure coefficient was formulated and given by equation (8.5),

$$C_p = \frac{2}{\gamma M_\infty^2}\left(G\left[\frac{2 + (\gamma - 1) M_\infty^2}{\gamma + 1}\right]^{\frac{\gamma}{\gamma - 1}} - 1\right). \quad (8.5)$$

On substituting (8.5) into (9.2b) the drag coefficient is given as

$$C_D = \frac{4}{\gamma M_\infty^2}\left[\frac{2 + (\gamma - 1) M_\infty^2}{\gamma + 1}\right]^{\frac{\gamma}{\gamma - 1}} \int_0^{1.0} \frac{p_L}{p^*} \frac{x}{L}\, d\left(\frac{x}{L}\right) -$$

$$- \frac{4}{\gamma M_\infty^2} \int_0^{1.0} \frac{x}{L}\, d\left(\frac{x}{L}\right) \quad . \quad (9.3)$$

Or, after evaluating the last integral value on the right of (9.3),

$$C_D = \frac{4}{\gamma M_\infty^2}\left\{\left[\frac{2 + (\gamma - 1) M_\infty^2}{\gamma + 1}\right]^{\frac{\gamma}{\gamma - 1}} \int_0^{1.0} \frac{p_L}{p^*} \frac{x}{L} d\left(\frac{x}{L}\right) - \frac{2}{\gamma M_\infty^2}\right. \quad (9.3a)$$

$$C_D = \frac{4}{\gamma M_\infty^2}\left[\frac{2 + (\gamma - 1) M_\infty^2}{\gamma + 1}\right]^{\frac{\gamma}{\gamma - 1}} \int_0^{1.0} \frac{p_L}{p^*} \frac{x}{L} d\left(\frac{x}{L}\right) -$$

$$\left. - \frac{1}{2}\right\}, \ (M_\infty \leq 1.0) \quad (9.3b)$$

where p_L/p^* is recognized as the invariant pressure ratio (G) given by equation (8.3).

In equation (9.3b), for any free-stream Mach number within the range of values for which the local Mach number is constant, and for which $M_\infty \leq 1.0$, the integral

$$\int_0^{1.0} \frac{p_L}{p^*} \frac{x}{L} d\left(\frac{x}{L}\right) \tag{9.4}$$

is itself a constant, being only a function of local Mach number (see equation (8.3)). Likewise, for the analogous case where $M_\infty \geq 1.0$, but for which M_L is constant, it will be shown that this same integral value appears in the drag coefficient equation. Therefore, due to the invariant nature of this integral, the evaluation of C_D depends only upon the free stream Mach number, the explicit relationship being contained in the coefficient of the integral. Hence, the determination of C_D, for this range of free-stream Mach number, simply becomes a mathematical operation after one integration of the invariant pressure ratio integral (9.4).

In a similar fashion the equation for C_D, for $M_\infty \geq 1.0$, but in the range of constant local Mach number, follows the procedure outlined in the above paragraph. Here, however, due consideration must be given to the evaluation of C_p for the presence of a shock in the free stream. That is, the value of C_p to be used in equation (9.2b) is given by (8.9a) or (8.16). If (8.16) is to describe C_p, then

after following the same process just completed for the subsonic side of Mach number one, the following expression for C_D is obtained,

$$C_D = \frac{4}{\gamma M_\infty^2}\left\{\left[\frac{2 + (\gamma - 1) M_d^2}{\gamma + 1}\right]^{\frac{\gamma}{\gamma - 1}} \frac{p_d}{p_\infty} \int_0^{1.0} \frac{p_L}{p^*} \frac{x}{L} d\left(\frac{x}{L}\right) - \right.$$

$$\left. - \frac{1}{2}\right\}, \quad M_\infty \geq 1.0 \qquad (9.5)$$

where, as stated before, the integral in (9.5) will require only one evaluation for a given body in the range of Mach numbers considered.

If the value of the integral is defined by a single integration; that is, if

$$\int_0^{1.0} \frac{p_L}{p^*} \frac{x}{L} d\left(\frac{x}{L}\right) = K_\theta \qquad (9.6)$$

then the expressions for C_D can be stated as,

$$C_D = \frac{4}{\gamma M_\infty^2}\left\{\left[\frac{2 + (\gamma - 1) M_\infty^2}{\gamma + 1}\right]^{\frac{\gamma}{\gamma - 1}} K_\theta - \frac{1}{2}\right\} \text{ (for } M_\infty \leq 1.0) \qquad (9.3c)$$

and

$$C_D = \frac{4}{\gamma M_\infty^2}\left\{\left[\frac{2 + (\gamma - 1) M_d^2}{\gamma + 1}\right]^{\frac{\gamma}{\gamma - 1}} \frac{p_d}{p_\infty} K_\theta - \frac{1}{2}\right\} \text{ (for } M_\infty \geq 1.0). \qquad (9.5a)$$

The values of K_θ were determined for each conical head by numerical integration of the integral given in equation (9.6). To illustrate the relative magnitude of these numbers, the table below

lists the values as determined by using the trapezoidal rule for integration.

TABLE I. The value of the invariant integral for the range of cones investigated.

Cone θ_c (deg)	K_θ (Eq. 9.6)
25	0.6584
20	0.6292
14.033	0.5923
10	0.56597
8	0.5508
5	0.52814

Before discussing and comparing results, one further analysis is presented which is pertinent to the proper description of the drag coefficient - Mach number relations in the transonic region-- namely, the nature of the variation of C_p and C_D with free-stream Mach number at sonic conditions. This investigation is presented in the next subsection.

9.2. Slope of the C_p and C_D Curves at $M_\infty = 1.0$

To show the variation of pressure coefficient with free-stream Mach number, at $M_\infty = 1$, consider the definition (3.28)

$$C_p = \frac{p_L - p_\infty}{q_\infty} = \frac{2}{\gamma M_\infty^2} \left(\frac{p_L}{p_\infty} - 1 \right) . \qquad (3.28)$$

For the condition of free stream Mach number of unity any wave formations present in the upstream field of flow will be of the nature of Mach waves, or waves of very weak magnitude. Thus, as in the general case, the flow field up to and ahead of the cone cylinder junction will be considered to be isentropic. Therefore, the pressure ratio in (3.28) may be expressed by the familiar isentropic relation

$$\frac{p_L}{p_\infty} = \left[\frac{2 + (\gamma - 1) M_\infty^2}{2 + (\gamma - 1) M_L^2} \right]^{\frac{\gamma}{\gamma - 1}} \tag{9.7}$$

leading to

$$C_p = \frac{2}{\gamma M_\infty^2} \left(\left[\frac{2 + (\gamma - 1) M_\infty^2}{2 + (\gamma - 1) M_L^2} \right]^{\frac{\gamma}{\gamma - 1}} - 1 \right) \tag{9.8}$$

as previously seen.

If the slope of the graph of C_p versus M_∞ is to be determined, at $M_\infty = 1.0$, it is only necessary to take the appropriate derivative and evaluate the resulting equation for this condition. Of course, in the mathematical manipulation care must be exercised to recognize that this case is typical of the Mach number stationarity concept and utilization of the quantity $\left.\frac{dM_L}{dM_\infty}\right|_{M_\infty = 1.0} = 0$ is required. The definition for C_p at $M_\infty = 1$, from (9.8) is

$$C_p^{(1)} = \frac{2}{\gamma} \left(\left[\frac{\gamma + 1}{2 + (\gamma - 1) M_L^2} \right]^{\frac{\gamma}{\gamma - 1}} - 1 \right) . \tag{9.9}$$

Utilizing this definition in the derivative, the resulting expression for the slope is

$$\left.\frac{dC_p}{dM_\infty}\right|_{M_\infty = 1.0} = \frac{4 - 2C_p^{(1)}}{\gamma + 1} \quad . \tag{9.10}$$

This result shows that the nature of the slope, for any body surface pressure depends at least in part on the magnitude of the local pressure. Since local pressure is a function of body shape and position, it is clearly established that the curves for all stations will vary from one another. It is also recognized that since the local Mach number is fixed, for the range of free-stream values close to unity, the slope will primarily depend upon the free-stream Mach number only (for a given body position). This result (9.10) has also been given by Solomon[42].

Since, as has been shown previously, the pressure drag (or wave drag) depends upon the variation and orientation of the pressure envelope over the body, it is now desired to determine the slope of the drag coefficient - Mach number graph for $M_\infty = 1.0$.

From a previous development the drag coefficient due to pressure is given by

$$C_D = 2 \int_0^{1.0} C_p \cdot \frac{x}{L}\, d\left(\frac{x}{L}\right) .$$

Writing C_p as in equation (9.8), this expression may be rewritten as

$$C_D = \frac{4}{\gamma M_\infty^2} \int_0^{1.0} \left(\left[\frac{2 + (\gamma - 1) M_\infty^2}{2 + 9\gamma - 1) M_L^2} \right]^{\frac{\gamma}{\gamma - 1}} - 1 \right) \frac{x}{L} \cdot d\left(\frac{x}{L}\right) \tag{9.11}$$

To determine the appropriate slope it is necessary to apply a special form of Leibnitz's Rule (limits of integration being constants), with the understanding that the integrand is continuous within the range of integration. Experiment indicates that there are no discontinuities in the pressure envelope so long as the range of integration does not pass over any shock waves or other pressure discontinuities. Restricting the range of integration to the conical portion of the body deletes the possibility of such discontinuities in pressure. Likewise there will not be any surface, or body, irregularities so that straight forward use of the rule for differentiation under the integral sign may be employed.

At first glance it might appear that equation (9.10) could be utilized directly here, but it must be remembered that the pressure coefficient is dependent upon the body station (thus it is a point-wise function of coordinates, or point-wise function of local Mach number, which is the same). Hence this dependency requires that the pressure coefficient be expressed analytically in terms of body coordinates so that the proper use of equation (9.10) may be made. In the general case such a relationship is not known and the differentiation must follow the formal pattern.

Following the usual method of differentiation, using the concept of local Mach number stationarity, and defining $C_p^{(1)}$ as in equation (9.9), an intermediate step in the procedure gives

$$\left.\frac{dC_D}{dM_\infty}\right|_{M_\infty = 1.0} = \frac{4\gamma}{\gamma+1}\int_0^{1.0}\left[2\gamma\,\frac{(\gamma+1)^{\frac{\gamma}{\gamma-1}}}{(2+(\gamma-1)M_L^2)^{\frac{\gamma}{\gamma-1}}}\right]\frac{x}{L}\,d\left(\frac{x}{L}\right) -$$

(9.12)

$$-4\int_0^{1.0}\frac{2}{\gamma}\left(\left[\frac{\gamma+1}{2+(\gamma-1)M_L^2}\right]^{\frac{\gamma}{\gamma-1}}-1\right)\frac{x}{L}\,d\left(\frac{x}{L}\right).$$

If now the integral

$$\frac{\gamma}{\gamma+1}\int_0^{1.0}\frac{x}{L}\,d\left(\frac{x}{L}\right)$$

is added and subtracted from (9.12), then through the definition (9.9), (9.12) is reduced to

$$\left.\frac{dC_D}{dM_\infty}\right|_{M_\infty = 1.0} = \frac{4\gamma}{\gamma+1}\int_0^{1.0} C_p^{(1)}\cdot\frac{x}{L}\cdot d\left(\frac{x}{L}\right) -$$

(9.13)

$$-4\int_0^{1.0} C_p^{(1)}\cdot\frac{x}{L}\cdot d\left(\frac{x}{L}\right)+\frac{8}{\gamma+1}\int_0^{1.0}\frac{x}{L}\cdot d\left(\frac{x}{L}\right).$$

Now from (9.11) it follows that the value of C_D at a free-stream Mach number of unity ($C_D^{(1)}$) is given as

$$C_D\Big|_{M_\infty = 1.0} = C_D^{(1)} = 2\int_0^{1.0} C_p^{(1)}\cdot\frac{x}{L}\cdot d\left(\frac{x}{L}\right). \qquad (9.14)$$

Using (9.14) and (9.13), after integrating and clearing, the expression for the slope is given as

$$\left.\frac{dC_D}{dM_\infty}\right|_{M_\infty = 1.0} = \frac{4 - 2C_D^{(1)}}{\gamma + 1} \quad . \tag{9.15}$$

Equation (9.15) is also given in reference 42, though the development used there is obscure and appears to embody the discrepancy of using (9.10) directly in evaluating this last tangency condition. That is, such a procedure implies that the only difference between C_p and C_D appears in the integral which introduces only body coordinates. Since these coordinates are independent of free-stream Mach number then the supposition is that C_D and C_p have a unique relationship to one another, but this relationship disregards the dependence of C_p on body geometry.

Through equation (9.15) it is seen that the tangency condition is dependent upon the value of C_D obtained for a given body. Thus in the final analysis the slope will depend upon body geometry and on orientation.

It is interesting to note that both (9.10) and (9.15) contain the result of linear theory, but are modified by the terms containing the values of C_p and C_D evaluated at $M_\infty = 1$. That is, according to linear theory

$$\left.\frac{dC_p}{dM_\infty}\right|_{M_\infty = 1} = \frac{4}{\gamma + 1} \tag{9.16}$$

and

$$\left.\frac{dC_D}{dM_\infty}\right|_{M_\infty = 1} = \frac{4}{\gamma + 1} . \tag{9.16}$$

These expressions (9.16) indicate that the tangents are identical, according to linear theory. This may be argued to be approximately true for the limiting case of a very slender body in a uniform transonic stream. It follows then that the expressions (9.10) and (9.15) derived above are more exact and will be more indicative of the true slope values for bodies of moderate thickness. In general, for bodies of practical interest, the differences between linear theory and the values obtained herein will be small, especially for the drag coefficient curve since the value of C_D is usually small for slender bodies. It does not necessarily follow that the same is true for the pressure coefficient curve since this tangency is dependent upon the local value of C_p which may be of sizable magnitude. It is recalled, however, that the local Mach number stationarity concept has been employed herein, and that such a concept is not rigorously applicable over the entire body. Lastly, it has been suggested that the difference between the linear tangency values and those developed here may be considered as a second order correction on the linear theory.

With the knowledge now available from the present analysis, data can be obtained and the values of drag coefficient defined for a range of transonic free stream Mach numbers. Next, a discussion of these results and a comparison with other investigations will be made.

9.3. Presentation of Results.

The values of pressure drag coefficient determined from the analysis presented here are shown in Figure 17. In addition to the present work, some of the available experimental and theoretical results are plotted on this graph. In particular the drag coefficient evaluated from the pressure distribution obtained by Yoshihara[24], for a cone-cylinder body with $\theta_c = 5^\circ$, and the pertenient values from reference (42) are shown for purposes of comparison. Also shown are values of C_D taken from the material presented in reference 66, previously discussed, where these values are for Mach numbers in the supercritical range. These last values are shown only to illustrate the degree of agreement on order of magnitude, and to substantiate the reasoning that there exists but small difficulty in actually fairing the curves for transonic flow to those for the supercritical flow case. In other words, a reasonable fairing of the curves for C_D, obtained under the method presented in this analysis, to the conical flow analysis may be made thereby, giving an approximate (but close) continuous solution for the drag coefficient from the subcritical into the supercritical range of Mach numbers. Unfortunately no work similar to that of references 54 and 55 (for the two-dimensional case) is available for axially symmetric flow over a cone-cylinder. Therefore the fairing through this region, where rotation of the flow field is predominant, must be by "eye".

For the body combination having a semi-apex angle of 5°, the values given in Figure 17 are only for a small range of Mach numbers

close to unity. This range of values is limited since the present analysis will predict only a small variation of free-stream Mach numbers for which the stationarity hypothesis holds. In order to more clearly indicate the graphical picture of this case it should be remarked that the value of C_D from reference (24) and that of the present work agree very closely and thus only a single point is plotted on the graph. The lines designated by "d" are the slope lines predicted by the analysis of the preceeding paragraphs.

The dashed curves, representing the data of reference 66, are marked by vertical bars to indicate the value of Mach number for which: first, the lower limit of conical flow analysis is given; and second, the lower limit value of Mach number for which the body flow is depicted by $M_L > 1.0$. It has been remarked previously that the flow adjacent to the body surface is first subsonic (imbedded in a supersonic flow region behind the head shock) and then supersonic throughout - - the demarkation of these body flow types is indicated by the second vertical bar. Not all body cases studied have been represented for conical flow analysis. The reference data does not give values for all cone angles and no attempt to interpolate has been made. Subsequent reference will be made to an analysis[68] which allows predictions to be made for all cone heads in the supercritical range. Thus results can be joined to yield an approximately complete estimate of drag coefficient extending into the supersonic region.

It is noted that each curve in Figure 17 has a tangent ("d") given for $M_\infty = 1.0$. These tangents were obtained analytically. Accordingly the analysis presented in the previous subsection is plotted on the figure to show the agreement between the actual and predicted slopes. In all cases it is clearly seen that the agreement is excellent.

In the "Introduction" it was mentioned that Heaslet and Spreiter[61] and Miles[62] have treated the cone problem for the sonic free-stream case. So that a clearer understanding of the differences in these methods and the present analysis can be had, a brief outline of these other procedures is given below.

Miles formulated an approximate solution for the drag of a slender body in a sonic free stream by joining the slender body theory (based on the "classical" approach) and the asymptotic solution of Guderley and Yoshihara, "in an appropriate manner". It is recalled that the asymptotic solution is that for an axially symmetric sonic flow at large distances from a body of revolution. In his approximate analysis, Miles argued that these solutions could be joined in an appropriate manner, when it is recognized that at sonic speeds the shock surface for a slender body must be normal to the free stream while that for the asymptotic solution must be inclined downstream. Once these surfaces are brought into agreement at some point in the flow field the drag can then be estimated by defining the momentum change for a region containing the body and the shock surface. This makes the prediction of body pressures forward

of the sonic line possible, and the drag is then defined by integrating the momentum transport across the sonic surface itself.

The drag coefficient obtained by Miles is given in equation form, for $M_\infty = 1.0$, and is

$$C_D = \delta^2 \left[4 \ln 1/\delta - 0.091334 \right] . \qquad (9.17)$$

This expression is based on a total body length of unity, where $\delta = \text{tn } \theta_c$ for the conical head. By studying this equation one may conclude that, for the range of values of θ_c investigated here, the differences in C_D obtained by retaining or deleting the constant in the brackets would not induce an error greater than approximately three percent between results.

The work of reference 61 was carried out in an effort to overcome the inadequacies of the general approach to the transonic problem; namely, the use of the linear theory analysis either extrapolated to the sonic case or used as a first approximation with iterative processes employed for refinements. Heaslet and Spreiter undertook to rederive the governing equations on a momentum basis, taking into account the presence of waves in the flow field. In this manner the difficulty of non-convergence of the series approximation was avoided, with the results specialized for a sonic free-stream. Hence, no extrapolation of analysis is required, and the uncertainity associated with such a procedure is eliminated. Here again results are presented in analytic form, the equation for

the drag coefficient being

$$C_D = - \theta_c^2 \left[1.55 + 2 \ln \theta_c^2 \right] , \qquad (9.18)$$

where θ_c is the semi-apex angle for the conical head. Again, as in the work of Miles[62], the constant quantity is a result of analysis -- though for reference (62), the constant is a consequence of joining the two solutions, while here it is a direct consequence of the analysis itself.

In all fairness it is necessary to point out that the equations are only applicable for small body thickness, and therefore should not be employed for large apex angles.

The table below has been prepared so that these predictions and the results of this investigation can be compared, both from the standpoint of limitation and agreement. All values of C_D presented below are for a sonic free-stream to be consistent with the reference material. The percent error is calculated using the values from this study as a basis. The plus and minus signs are employed to indicate that the reference values are either greater or smaller, respectively, than values obtained in this thesis.

TABLE II. Comparison of $C_D^{(1)}$ by present analysis with similar values from reference materials ($M_\infty = 1.0$ in all cases).

TABLE II

	$C_D^{(1)}$	$C_D^{(1)}$ from the equation and reference indicated			% error based on present analysis		
θ_c(deg)	Present Analysis (Eades)	Equation (9.18) Ref. 61(Heaslet, Spreiter)	Equation (9.17) Ref. 62 (Miles)	Ref. 24 (Yoshi-hara)	Ref. 61	Ref. 62	Ref. 24
5	.0799	.0625	.0738	.0775	- 22	-7.6	- 3
8	.1461	.1217	.1532		-16.4	+4.9	
10	.1698	.1644	.2130		- 3.2	- 25	
14.033	.264	.2446	.3409		- 7.3	- 29	
20	.3705	$C_D < 0$	.5235			- 41	
25	.4512	$C_D < 0$	.6437			- 43	

From the tabulated results it is apparent that the methods described in references (61) and (62) are not applicable to conical heads having large apex angles. This is to be expected since a basic premise in

both formulations was that the bodies were ''slender bodies''. The use of equation (9.18) appears to be limited to only a small range of values of body thickness since the error of prediction is quite large in one sense, and the equation fails to produce positive values of C_D for angles as large and larger than 20^o. It is noted that the error is small in the region of 10 degrees. The reason for this is obvious if a study of the theoretical considerations leading to equation (9.18) is made. It is seen that the equation, in part, depends upon the pressure distribution approximation for a cone described by $\theta_c = 0.1225$ radians. This pressure distribution was obtained by correcting the results of reference 24 according to the similarity law given in reference 30 (by Oswatisch and Berndt).

The degree of approximation imposed on the derivation plus the restriction placed on equation (9.18) are apparently the reasons that the theory cannot predict logical values for a larger range of cone angles.

Though the results obtained from reference 62 (that is, equation (9.17)) do give positive values of C_D for the range of cone sizes indicated in Table II, it is also quite evident that the error becomes increasingly more severe as the apex angle is increased. Primarily the difficulty here can be traced to the restriction on the development. Again the formulation was based on the results of reference 24, but here certain constants were introduced into the equation when the two solutions were ''appropriately joined''. Had the analysis

been based on other than these specific results, a different constant would have appeared in (9.17) and agreement would have been noted for a range of cones different from those now indicated.

Of course, it is to be expected that both results, used in the comparison tabulation, would not agree over the entire range of θ_c due to the very nature of the derivations. However, the present approach to this problem does not suffer from the same limitations since the underlying considerations of the problem are different. It is most apparent that a wider range of θ_c values can be covered by the analysis, and that the degree of approximate agreement is practically the same throughout the entire range of body sizes. The present study has not been made for larger values of θ_c (larger than 25°) since the upper limit of applicability could not be established due to a lack of sufficient comparative data. Also the analysis was not extended to lower values (less than 5°) for the same reason. It does not seem justified to make such extensions as this would be outside the range of practical interest, and the academic interest would lend little to the total analysis.

Now that the versatility of the method has been shown, it would be logical next to illustrate how these results could be joined through similarity relations to provide a most concise and elegant presentation. Unfortunately this cannot be accomplished due to the restrictions placed on the development of the similarity law for axially symmetric compressible flow. However, it will be shown in the

next section that a correlation does exist which allows the data to be collected and presented as a single curve.

10. CORRELATION OF DRAG COEFFICIENT FOR TRANSONIC FLOW

The statement was made earlier that the results of this investigation were found incapable of being correlated under the existing similarity laws. This is in fact pointed out in the literature[63]. In the following analysis, however, a correlation will be shown to exist, and the proof of its existence can be clearly demonstrated by applying it to the results of this thesis.

It will be recalled that the general expression for drag coefficient, as given by equation (9.2b), is

$$C_D = 2 \int_0^{1.0} C_p \cdot \frac{x}{L} \cdot d\left(\frac{x}{L}\right), \qquad (9.2a)$$

where the pressure coefficient is given by (3.28),

$$C_p = \frac{2}{\gamma M_\infty^2}\left(\frac{p_L}{p_\infty} - 1\right). \qquad (3.28)$$

In Section 8 it was shown that the pressure ratio, $\frac{p_L}{p_\infty}$, could be described as a multiple of pressure ratios, with these ratios requiring a different form depending on the range of transonic Mach numbers to which it applied. However, the general expansion form is

$$\frac{p_L}{p_\infty} = \frac{p_L}{p^*} \cdot \frac{p^*}{p_\infty} = G\,\frac{p^*}{p_\infty}$$

from the statements of equations (8.3) and (8.1a). Now, from equations (8.1a) and (8.7) it is seen that the difference in form,

necessitated by the presence of a head shock in the field, is introduced by the definition of the pressure ratio

$$\frac{p^*}{p_\infty} \quad ;$$

where, for $M_\infty \leq 1.0$,

$$\frac{p^*}{p_\infty} = \frac{p^*}{p_\infty} \quad ,$$

and for $M_\infty \geq 1.0$,

$$\frac{p^*}{p_\infty} = \frac{p^*}{p_{stag}} \cdot \frac{p_{stag}}{p_\infty} \quad .$$

It will be recalled that the Rayleigh Equation is used for the last ratio $\frac{p_{stag}}{p_\infty}$, as was pointed out in section 8.

Now, in general, the drag coefficient can be expressed as

$$C_D = \frac{4}{\gamma M_\infty^2} \frac{p^*}{p_\infty} \int_0^{1.0} \frac{p_L}{p^*} \frac{x}{L} \, d\left(\frac{x}{L}\right) - \frac{2}{\gamma M_\infty^2} \qquad (10.1)$$

when the expansion pressure ratios are introduced into (3.28), and that in turn used in equation (9.2a). Again the integral is recognized as the invariant integral for the transonic range of Mach numbers, so that from the definition of K_θ (equation (9.6)), the C_D equation is replaced by

$$C_D = \frac{4}{\gamma M_\infty^2} \frac{p^*}{p_\infty} K_\theta - \frac{2}{\gamma M_\infty^2} \quad . \tag{10.2}$$

This expression indicates that the drag coefficient is functionally dependent upon M_∞, body geometry (δ, for a cone), and the type of gas (described by γ). The influence of these variables is carried in the term K_θ (primarily), which indicates the dependency of C_D on these parameters. The difficulty in explaining a similarity rule for this type of flow and body geometry lies in the inability of expressing the functional dependency of K_θ on these quantities and the proper implicit relationship between them. Rather than resort to the usual similarity treatment, let the expression be reformed, and after manipulation be given as

$$\frac{K_\theta}{C_D + \frac{2}{\gamma M_\infty^2}} = \frac{\gamma M_\infty^2}{4} \frac{p_\infty}{p^*} \quad . \tag{10.3}$$

The right side of this expression is seen to depend only upon the free stream Mach number and the specific heat ratio (which is here considered constant). All the parametrics have now been grouped on the left side of the equation, and furthermore, both sides of this equation are seen to be constants for any given Mach number in the critical range considered.

Since the left hand side of (10.3) depends only upon the free-stream Mach number, (this is apparent regardless of the necessary

relationship demanded for p_∞/p^*), it may be reduced to a single parameter,

$$\widetilde{C_D} = \frac{K_\theta}{C_D + \frac{2}{\gamma M_\infty^2}} \quad . \tag{10.4}$$

Hence from (10.3) it follows that for all cases of body geometry and Mach number, in the transonic range, pertenient to this investigation,

$$\widetilde{C_D} = \text{Constant} \cdot (M_\infty^2 - 1)^n \quad . \tag{10.5}$$

This equation implies that the reduced drag coefficient ($\widetilde{C_D}$) depends only upon ($M_\infty^2 - 1$) for its variation in the range of free stream Mach number for which local Mach number stationarity may be assumed.

In other words, if the stationarity of local Mach number is assumed, then for all similar bodies in the proper range of free stream Mach number, the curve of $\widetilde{C_D}$ versus ($M_\infty^2 - 1$) will correlate into a single representation.

That such a parameter as $\widetilde{C_D}$, for the range of θ_c values here studied, can be given by a single curve is shown in Figure 18. The actual plotting of this curve was done using all the drag data obtained, for all values of θ_c in the entire range of free-stream Mach number in agreement with the assumptions made. As is indicated by this graph the desired correlation has been established without recourse to similarity in the usual sense. In so far as is known, and so far as the literature indicates, the results presented here

describe for the first time the relationship between these quantities in the transonic regime.

To illustrate the value of such a correlation suppose the drag coefficient is needed for a cone in transonic flow. Now, to obtain the coefficient of drag for the conical head, in the critical flow region of Mach number, and for a semi-apex angle not in excess of 25 degrees, the graph is entered at the appropriate free-stream Mach number. From the ordinate the drag coefficient can be obtained. In calculating C_D it is required that the value of K_θ be known - this value is obtained from the equation

$$K_\theta = \left[0.001189\ \theta^\circ \sqrt{1 + \frac{175.94}{\theta^\circ}} + .05977\right]^{0.573} + 0.003\theta^\circ + 0.254 \qquad (10.6)$$

which has been defined from the values determined in this investigation. Of course, the value of K_θ can be gotten from experimental data; the method for defining this constant has been given by the discussion on, and from, equation (8.6).

Should there be a need for estimating the drag in the lower supercritical range of Mach number, a convenient approximation would be a welcome expedient. For the sake of brevity it is mentioned that from the results of reference (68), this approximation may be obtained from the following equation:

$$C_D \approx \left(0.083 + \frac{0.096}{M_\infty^2}\right)\left(\frac{\theta_c}{10^\circ}\right)^{1.69}, \qquad (10.7)$$

where M_∞ is the free stream Mach number for which conical flow theory is applicable, and where θ_c is the semi-apex angle of the conical head given in degrees. This expression is reported to be in close agreement with the Taylor-Maccoll solution; the maximum magnitude of error being approximately ten percent, with the general agreement being much closer.

With this expression available a practical estimate of drag, through the transonic range and into the supersonic range, can now be made. Thus the transonic drag rise and the subsequent asymptotic behavior for the drag coefficient can be predicted with a reasonable degree of accuracy for cone-cylinder bodies of revolution in a zero-lift configuration of flight.

From the complete analysis presented in the foregoing thesis, the salient points will be summarized in the following concluding statements.

11. CONCLUSIONS

The Major results of this investigation are primarily dependent on a relatively few but important facts. As the problem was mainly concerned with transonic phenomenon, related to a cone-cylinder body, the conclusions will be pointed to that flow regime in general.

Without the physical interpretation of theoretical and experimental evidence this analysis could not have been accomplished. For instance, had the Principle of Stationarity of Local Mach Number not been established from experiment, the entire concept of this problem would have been altered, and the simplicity of the study would in all likelyhood have been destroyed. Too, the nature of the changes in the pressure envelope with increasing Mach number can be deduced from the work of Yoshihara[24] and others; this, then, providing a guide by which the physics of the problem is more clearly surmised. Though there are only meager results with which forecasts and conclusions can be made, these, with the pioneering work on the two dimensional flow case, are sufficient to obtain the proper insight into the general problem.

The principal results obtained from this investigation are briefly given in the following statements:

1. Of major importance to this analysis was the defining of the proper affine transformation relations by which the compressible problem could be predicted from a known incompressible solution. In addition to determining the form of this

transformation rule it became evident, after studying experimental results, that the range of Mach numbers for which it was applicable had to be defined. Thus it has been established that Gothert's Rule can be applied to the incompressible problem to predict compressible results, but only as long as the free stream Mach number does not exceed the lower critical value.

2. In order that accurate predictions could be made it was found that the incompressible results were required to have close agreement with experiment. Since classical theory was not capable of providing the desired agreement, a more accurate method - - the method of distributed vortex rings - - has been presented. For the problem investigated here, the correlation between the results of this theory and experiment is excellent. Even though the method requires many hours of computation, adequate compensation is received in the form of accuracy of results obtained. From a practical point of view no elaborate machines are required and most of the calculations can be carried out by slide rule.

The relative simplicity, and the accuracy, of this theory points to its preference over other methods. The inaccuracy of simple linear theory and the complexity of more elaborate formulations are added arguments in favor of the vortex ring analysis.

This method represents a relatively new approach to the problem of three dimensional bodies in axially symmetric fluid flow.

3. One of the most important concepts employed in the problem is the constancy of local Mach number for transonic flow. Although the existence of this has been recognized for some time, the actual using of it has been small. In most cases it appears only in secondary studies (such as the establishment of the curve slopes in Section 9), while if the physical significance of this phenomena is realized it is quite apparent that it is a powerful tool of analysis. In the investigation just completed this one significant fact has allowed the transonic drag to be defined continuously through this entire range of flow speeds. It is this constancy which showed the dependency of drag coefficient on free-stream Mach number rather than on some complex relation involving local flow parameters. This also leads to the simply defined physical interpretation of the happenings in transonic flow.

4. For the first time a solution has been formed, in the axially symmetric flow case, which is a continuous solution from subsonic to supersonic speeds. Also, the solution has been shown to be applicable to a wide range of body sizes, not restrained to fit the usual slender body analysis, or restricted to the subsonic portion of critical flow. Previously theoretical analyses have been restricted by one or more of the above, or have been able to define only sonic phenomena. It is not

intended for these statements to imply that previous investigations are of no value. The basic knowledge of the problem, so necessary to the present analysis, has been gathered from such sources of information. Without the contributions made by these earlier efforts this investigation could not have been accomplished.

5. The smooth transition in transonic flow, from isentropic to non-isentropic flow, is clearly indicated by the continuous nature of the present results. The influence of the free stream and the normal shock on pressure distributions indicates the physical occurances in the entire flow field. The influence of subsonic flow on the supersonic portion of the transonic flow regime is indicated by the retained subsonic character of the pressure envelope. It is only after the bow wave has significant curvature that radical changes in local pressures begin to appear. The continual rise in drag coefficient for speeds above sonic speed is seen to be due to the very presence of the shock formation itself — this formation is the cause for increasing pressure of the stream immediately adjacent to the body, hence the cause of the increase in drag coefficient. Apparently it is after the onset of large flow field rotational components that the drag begins to decrease, and only after the shock wave attaches to the body does the drag coefficient begin to approach a nearly constant value.

6. Though this method does not predict the pressure distribution to a high degree of accuracy it does show the basic causes of drag rise and points to the physics associated with it. The study of Figures 13 indicate the growth of the pressure distribution with increasing free-stream Mach number, and the rearward shifting of the $C_p = 0$ point for each body. It is due to these increasing overpressures that the body forces necessarily increase. It can also be seen that as the free stream Mach number becomes larger (transonically) not only does the pressure diagram shift upward, but it also tends to rotate. This points to a twofold cause in the growth of body-felt pressures. The sum of these effects indicate the nature of changes undergone by a flow field adjacent to a conical body in transonic flow. Physically these effects are produced by the phenomenon associated with the undisturbed stream, for the constancy of the pressure ratio p_L/p^* does not admit these variations. Since the transformed pressure distributions do not indicate the correct values of p_L/p^* at the lower critical Mach number for the body junction plane, it was necessary to adjust these values bringing them into agreement with known physical boundary conditions. Here the adjustment was made in accordance with experimental findings, and in agreement with knowledge gained from such evidence; namely that $p_L/p^* \cong 1.0$ at this body station.

7. This analysis has the facility of leading to a correlation of the drag data, with Mach number, for the conical body in transonic flow. Not only has this been accomplished for the sonic stream, but for the whole of the range of Mach numbers for which the local Mach number remains constant. Of fundamental importance to the definition of the correlation parameter ($\tilde{C}_D$), is the invariant integral of the constant pressure ratio p_l/p^* for each body size. It can be reasoned that such a grouping of the data is correct, for physical evidence again points out that the law of Stationarity of Mach number leads immediately to the constancy of the pressure ratio (p_l/p^*), which in turn leads to the correlation parameter as developed in section 10. For the first time this parametric formulation has been presented, not only for a range of Mach numbers but also for a range of conical head angles as well. There is little reason to expect that this correlation cannot be extended to cover an even wider range of angles, though without the justification of experiment to indicate that the principle assumptions (Stationarity law, etc.) are not violated it would not be advisable to attempt such an extension. In conclusion it is felt that the evidence presented here is valid, and certainly the fundamentals are verified from physical obeervations. A method has been presented which allows the prediction of continuous values of the aerodynamic parameters for transonic speeds - - these speeds being characterized by Mach numbers from

below unity, through unity, to above unity. Not only does the analysis allow individual body values to be described, but it has the facility of reducing all values to a single correlation form. This, in turn, greatly simplifies the predictions in a practical sense, since all solutions are known for all bodies (described by a range of apex angles) in a stream of defined transonic Mach numbers.

12. REFERENCES

1 Goldstein, S., Modern Developments in Fluid Dynamics. Vol. II, Oxford: Clarendon Press, 1938, p. 523.

2 Rankine, W.J.M., On the Mathematical Theory of Streamlines, Especially Those With Four Foci and Upwards, Philosophical Translations, 1871.

3 Laitone, E. V., The Subsonic Axial Flow About a Body of Revolution, Journal of the Aeronautical Sciences, Nov. 1947.

4 Fuhrmann, G., Theoretical and Experimental Investigations on Balloon Models, Dissertations, Gottingen, 1912, published in Zeitsehrift fur Flugtechnik und Motorluftschiffahrt, Vol. II, 1911.

5 Munzer, H. and Reichardt, H., Rotationally Symmetrical Source-Sink Bodies with Predominately Constant Pressure Distribution, British Ministry of Supply, Armament Research Establishment Translation No. 1/50, 1950. (Translation of German Report U.M. 6616, 1944).

6 Riegels, F., and Brandt, M., Stromfunctionen und Geschwindigkeitsfelder Raumlicher Quellstrecken Und Ihr Handlicher Gebrauch Zur Bestimmung Von Deutsch Luftahrtforschung, U. M. Zericht No. 3106.

7 Weinstein, A., On Axially Symmetric Flows, Quarterly of Applied Mathematics, Vol. 4, No. 4, 1948.

8 Vandrey, F., Zur Theoretischen Behandlung des Gegenseitigen Einflusses von Tragflugel und Rumpf. (Luftfahrt-Forschung 14 (1937) S. 347).

9 Sadowsky, M. A. , and Sternberg, E., Elliptic Integral Representation of Axially Symmetric Flows, Quarterly of Applied Mathematics, Vol. 8, No. 2, 1951.

10 von Karman, Th., Calculation of Pressure Distribution on Airship Hulls, NACA TM 574, 1930; from Abhandlungen aus dem Aerodynamischen Institut an der Technischen Hockschule Aachen, No. 6, 1927.

11 Magenau and Murphy, The Mathematics of Physics and Chemistry, Chapters 13 and 14., D. van Nostrand Co., 1943.

12 Weinig, G., Uber schnell konvergierende graphische Lo sungen von Stromungsproblemen durch Integralgleichungen, Zeitschrift fur technische Physik, vol. 9, No. 1, 1928.

13 Kaplan, C., Potential Flow about Elongated Bodies of Revolution, NACA Report No. 516, 1935.

14 Smith, R. H., Longitudinal Potential Flow About Arbitrary Body of Revolution with Application to Airship "Akron", Journal of the Aeronautical Sciences, Vol. 3, No. 1, September 1935.

15 Young, A. D., and Owen, P. R., A Simplified Theory for Streamline Bodies of Revolution, and Its Application to the Development of

High Speed Shapes, British Aeronautical Research Committee R and M 2071, 1943.

16 Kaplan, C., On a New Method for Calculating the Potential Flow Past a Body of Revolution, NACA Report No. 752, 1943.

17 Landweber, L., The Axially Symmetric Potential Flow about Elongated Bodies of Revolution, Navy Department, The David W. Taylor Model Basin, Report 761 (NS 715-084), August 1951.

18 Vandrey, F., A Direct Iteration Method for the Calculation of the Velocity Distribution of Bodies of Revolution and Symmetric Profiles, Admiralty Research Laboratory, A.R.L./R1/G/HY/12/2, October 1951.

19 Vandrey, F., On the Calculation of the Transverse Potential Flow Past a Body of Revolution with the Aid of the Method of Mrs. Flugge-Lotz, Admiralty Research Laboratory, A.R.L./R2/G/HY/12/2, October 1951.

20 Vandrey, F., A Method for Calculating the Pressure Distribution of a Body of Revolution Moving in a Circular Path Through a Perfect Incompressible Fluid, Admiralty Research Laboratory, A.R.L./R3/G/HY/12/2, December 1953.

21 Hildebrand, F. B., Methods of Applied Mathematics, Ch. 4, Prentice-Hall, Inc.,1956.

22 Vandrey, F., Zur theoretischen Behandlung des gegenseitigen Einflusses von Tragflugel und Rumpf, Johrbuck 1938 der deutschen Luftfahrtforschung.

23 Rouse, H. and McNown, J. S., Cavitation and Pressure Distribution, Head Forms at Zero Angle of Yaw, Bulletin No. 32, State University of Iowa, Iowa City, Iowa, 1948.

24 Yoshihara, H., On the Flow over a Cone-Cylinder at Mach Number One, WADC TR 52-295, November 1952.

25 Laitone, E. V., Experimental Measurement of Incompressible Flow Along a Cylinder with a Conical Nose, Journal of Applied Physics, Vol. 22, No. 1, Jan. 1951.

26 Bilharz, H. and Holder, E., Calculation on the Pressure Distribution on Bodies of Revolution in the Subsonic Flow of a Gas. Part I - Axially Symmetric Flow (translation, Zentrole fur wissenschaftliches Berichtsmesen uber Luftfahrtforschung (ZWB), Berlin-Andlershof, Forschungsbericht Nr. 1169/1, Brounsehweig, Jan. 1940.

27 Hess, R. V. and Gardner, C. S., Study by the Prandtl-Glauert Method of Compressible Effects and Critical Mach Number for Ellipsoids of Various Aspect Ratios and Thickness Ratios, NACA TN 1792, 1949.

28 Sauer, R., General Characteristics of the Flow Through Nozzles at Near Critical Speeds (translation). NACA TM 1147, Sept. 1944.

29 Schmiden, C. and Kawalki, K. H., Contribution to the Problem of Flow at High Speed, Part II, Effect of Compressibility in Axially Symmetric Flow Around an Ellipsoid, (Translation). NACA TM 1233.

30 Oswatitsch, K. and Berndt, S. B., Aerodynamic Similarity At Axisymmetric Transonic Flow Around Slender Bodies, Royal Institute of Technology - Division of Aeronautics, KTH - Aero TN 15, Stockholm, 1950.

31 von Karman, Th., The Similarity Law of Transonic Flow, Journal of Mathematics and Physics, Vol. XXVI, No. 3, Oct., 1947.

32 Legendre, R., Ecoulement Subsonique D'un Fluidg Parfait Autour D'un Cone De Revolution, La Recherche Aeronautique No. 50, March-April 1956.

33 Adams, Mac C. and Sears, W. R., Slender Body Theory - Review and Extension, Journal of the Aeronautical Sciences, Vol. 20, No. 2, Feb., 1953.

34 Bennett, A. A., Milne, W. E. and Bateman, H., Numerical Integration of Differential Equations, Dover Press. (Reprint from monograph of National Research Council).

35 Wiley, C. R., Advanced Engineering Mathematics, Section 16, McGraw-Hill, 1951.

36 Jahnke and Emde, Tables of Functions, pp. 73, Dover Publications, Inc. (Reprint), New York, New York.

37 Conner, N. W., Construction and Calibration of the V.P.I. Wind Tunnel, Bulletin No. 29, Engineering Experiment Station, V.P.I. Blacksburg, Va., 1937.

38 Frankl, F. I., and Karpovich, E. A., Gas Dynamics of Thin Bodies, Interscience Publishers, Inc. (translated from Russian by M. D. Friedman), 1953.

39 Gothert B., Ebene und raumliche Stromung bei hohen Unterschallgeschwindigkeiten (Erweiterung der Prandtlschen Regal), Lilienthal-Gesellschaft fur Luftfahrtforschung, Bericht 127, Sept. 1940.

40 Sauer, R., Theoretical Gas-Dynamics, Edwards Press, 1947.

41 Oswatitsch, K., A New Law of Similarity for Profiles, Valid in the Transonic Region, A.R.C. T.R., R and M No. 2714, Ministry of Supply, 1954.

42 Solomon, G. E., Transonic Flow Past Cone Cylinders, NACA TN 3213, September 1954.

43 Reissner, E., On Compressibility Corrections for Subsonic Flow

Over Bodies of Revolution, NACA TN 1815, 1946.

44 Lees, Lester, A Discussion of the Application of the Prandtl-Glauert Method to Subsonic Compressible Flow Over a Slender Body of Revolution, NACA TN 1127, 1946.

45 Sears, W. R., A Second Note on Compressible Flow About Bodies of Revolution, Quarterly Appl. Math., Vol. V, No. 1, April 1947 (pp. 89-91).

46 Matthews, C. W., A Comparison of the Experimental Subsonic Pressure Distribution About Several Bodies of Revolution with Pressure Distributions Computed by Means of Linearized Theory, NACA TN 2519, Feb. 1952.

47 Laitone, E. V., The Extension of the Prandtl-Glauert Rule, Jour. Aero. Sc. (17), Vol. 17, No. 4, pp. 250,251, 1950.

48 Lighthill, M. J., Methods for Predicting Phenomena in the High-Speed Flow of Gases, J.A.S., Vol. 16 No. 2, Feb. 1949 (with Bibliography).

49 Spreiter, J. R., On Alternate Forms for the Basic Equations of Transonic Flow Theory, J.A.S., Vol. 21, No. 1 (pg. 70), 1954.

50 Perl, W. and Klein, M. M., Theoretical Investigation of Transonic Similarity for Bodies of Revolution, NACA TN 2239, 1950.

51 Leipmann, H. W., Ashkenas, H., and Cole, J. D., Experiments in Transonic Flow, AF-TR No. 5667, 1947.

52 Leipmann, H. W. and Bryson, A. E., Jr., Transonic Flow Past Wedge Sections, J.A.S., Vol. 17, No. 12, pp. 745-755, 1950.

53 Bryson, A. E., Jr., An Experimental Investigation of Transonic Flow Past a Two-Dimensional Wedge and Circular Arc Sections, Using a Mach-Zehnder Interferometer, NACA TN 2560, 1951.

54 Vincenti, W. G. and Wagoner, C. B., Transonic Flow Past a Wedge Profile with Detached Bow Wave, NACA TN 2339, 1951.

55 Vincenti, W. G. and Wagoner, C. B., Transonic Flow Past a Wedge Profile with Detached Bow Wave - Details of Analysis, NACA TN 2588, 1951.

56 Guderley, G. and Yoshihara, H., The Flow Over a Wedge Profile at Mach Number One, J.A.S., Vol. 17, No. 11, pp. 723-736, 1950.

57 Guderley, G., Two Dimensional Flow Patterns with a Free-Stream Mach Number Close to One, AF-TR 6343, 1951.

58 Cole, J. D., Solomon, G. W. and Willmarth, W. W., Transonic Flow Past Simple Bodies, J.A.S., Vol. 20, 1953.

59 Heaslet, M. A. and Lomax, H., The Calculation of Pressure on Slender Airplanes in Subsonic and Supersonic Flow, NACA Rept. 1185, 1954.

60 Berndt, S. B., On the Drag of Slender Bodies at Mach Number One. Aeitschrift fur angelwandtl Mathematik und Mechanik, Ad. 35, Heft 9/10, Sept./Oct., 1955.

61 Heaslet, M. A., and Spreiter, J. R., Three-Dimensional Transonic Flow Theory Applied to Slender Wings and Bodies, NACA TN 3717, 1956.

62 Miles, J. W., On the Sonic Drag of a Slender Body, J.A.S., Vol. 23, No. 2, pp. 146-155, 1956.

63 Leipmann, H. W. and Roshko, A., Elements of Gas Dynamics, John Wiley and Sons, 1957.

64 Busemann, A., Drucke auf Kegelformige Spitzen bei Bewengung mit Uberschallgeschwindigkeit., Z.a.M.M., Vol. 9 (1929).

65 Taylor, G. I. and Maccoll, J. W., The Air Pressure on a Cone Moving at High Speed, Proc. Roy. Soc. (A), Vol. 139, (1933).

66 Kopal, Z., Tables of Supersonic Flow Around Cones, M.I.T. Center of Analysis, Tech. Rep. No. 1, M.I.T., 1947.

67 Shapiro, A. H., The Dynamics and Thermodynamics of Compressible Fluid Flow, Vol. 1, Ronald Press, 1953.

68 Tukey, J. W., Linearization of Solutions in Supersonic Flow, Quart. of Applied Math., Vol. V, No. 3, Oct. 1947.

13. ACKNOWLEDGEMENT

This author wishes to express his gratitude to Professor D. H. Pletta, Head of the Applied Mechanics Department, for his patience and encouragement throughout this work. Also to Dr. R. W. Truitt, Head of the Aeronautical Engineering Department, the author expresses his appreciation for the suggestions he made and his time spent in consultation.

The two page vita has been removed from the scanned document. Page 1 of 2

The two page vita has been removed from the scanned document. Page 2 of 2

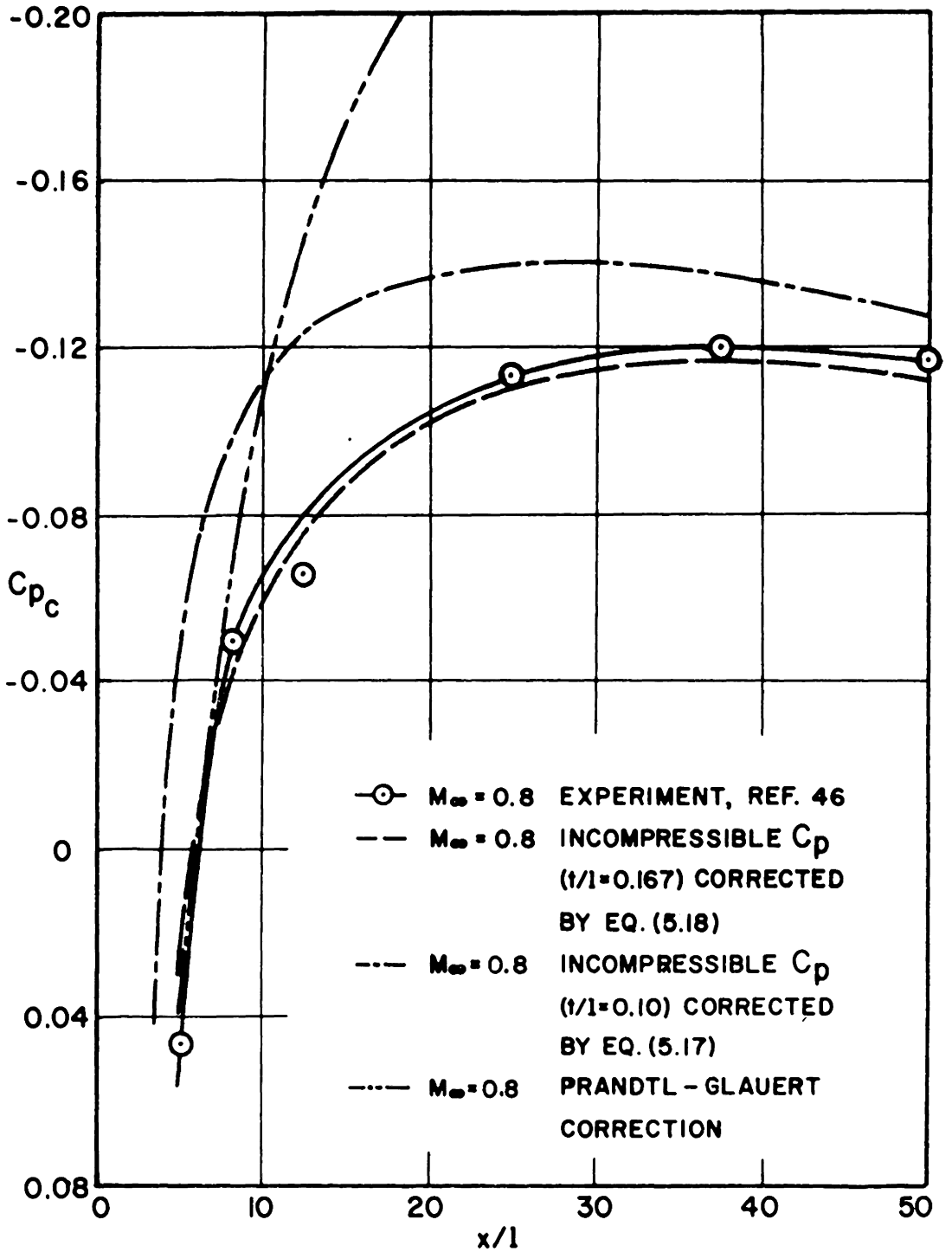

FIG. 1. COMPARISON OF PRESSURE CORRECTIONS FOR AN ELLIPSOID OF REVOLUTION (t/l = 0.167).

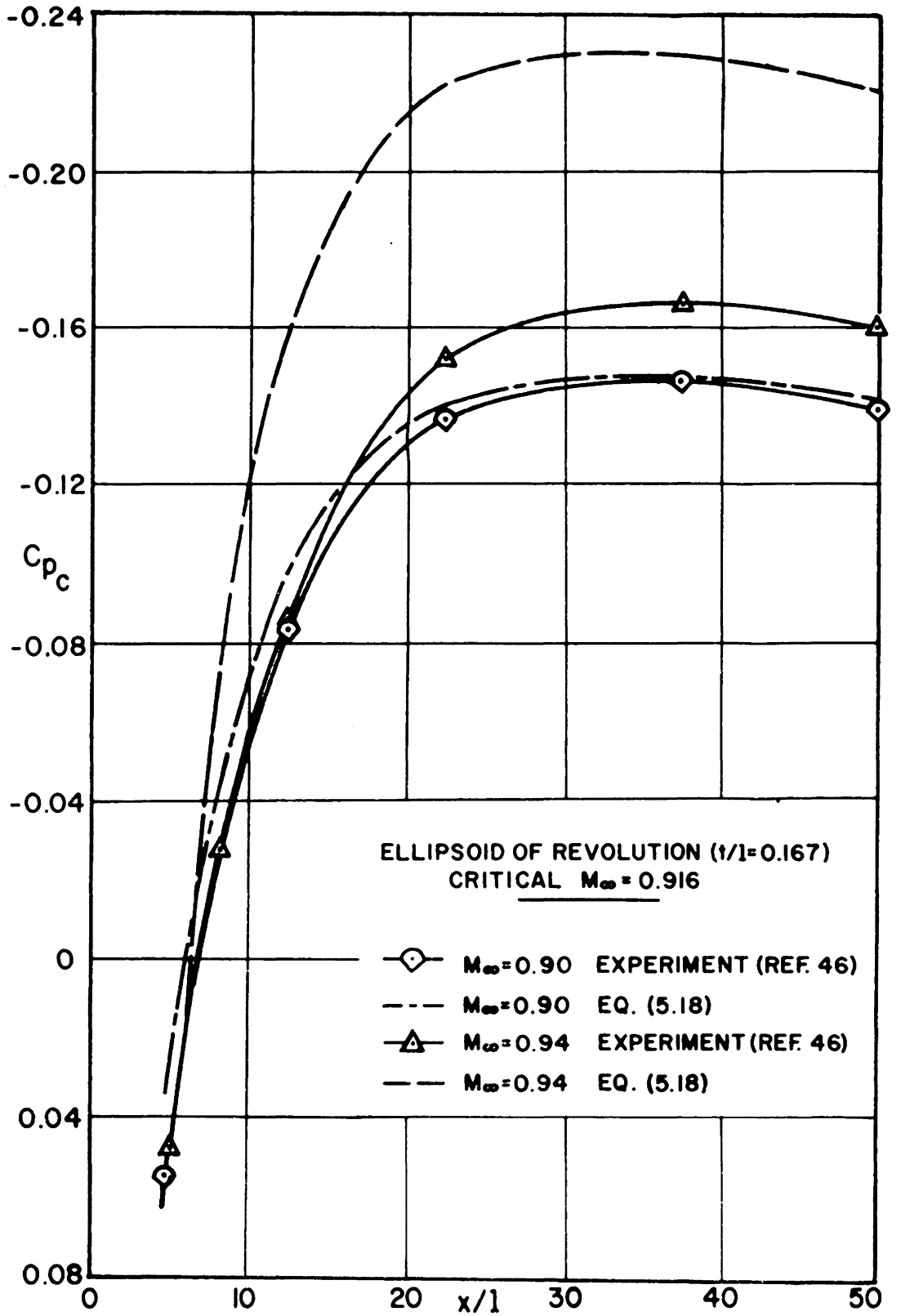

FIG.2. LIMIT FOR LINEAR THEORY PRESSURE CORRECTION.

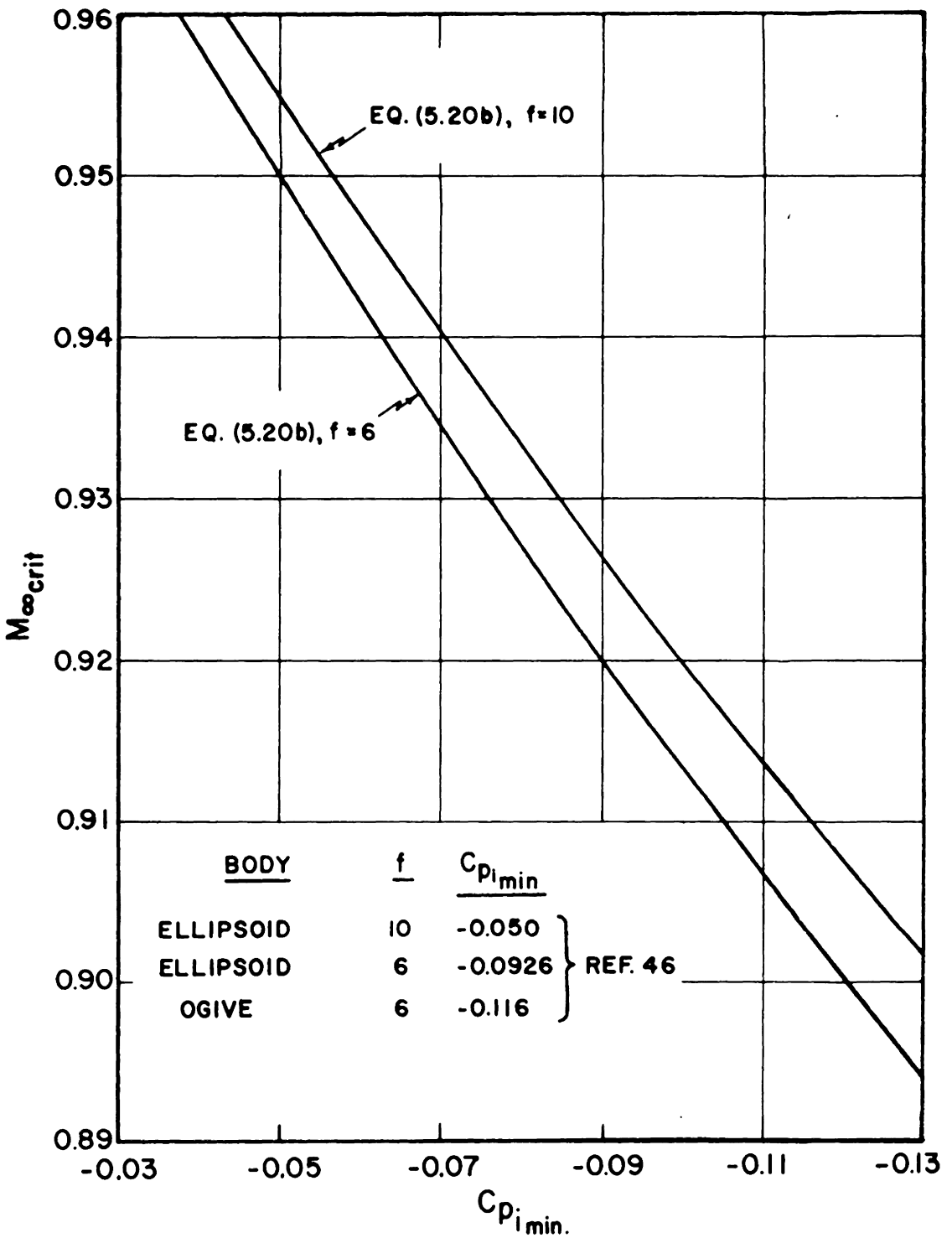

FIG. 3. PREDICTION OF FREE STREAM CRITICAL MACH NUMBER FOR ELLIPSOIDS OF REVOLUTION.

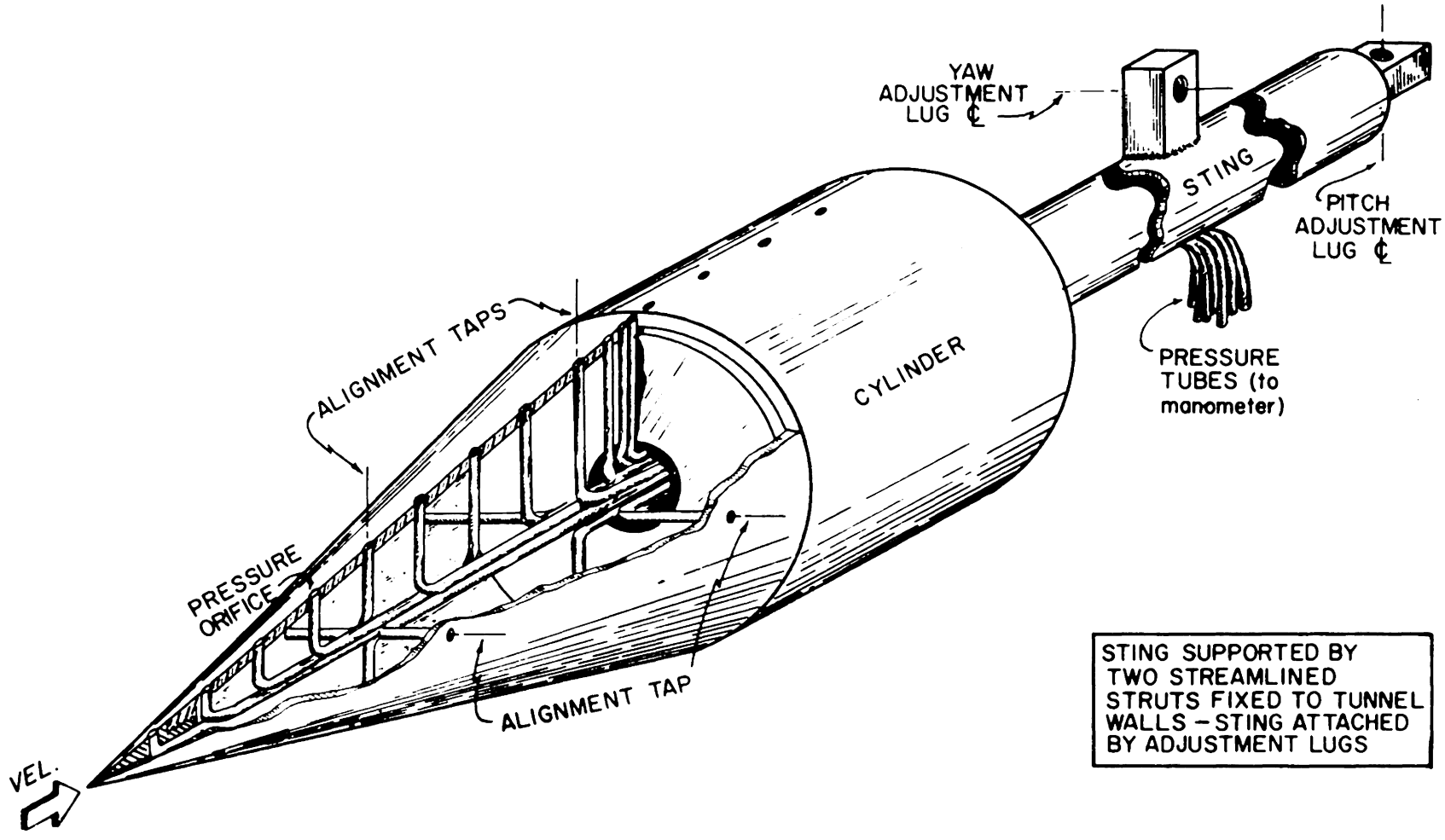

FIG. 4. SCHEMATIC OF A TYPICAL CONE - CYLINDER BODY.

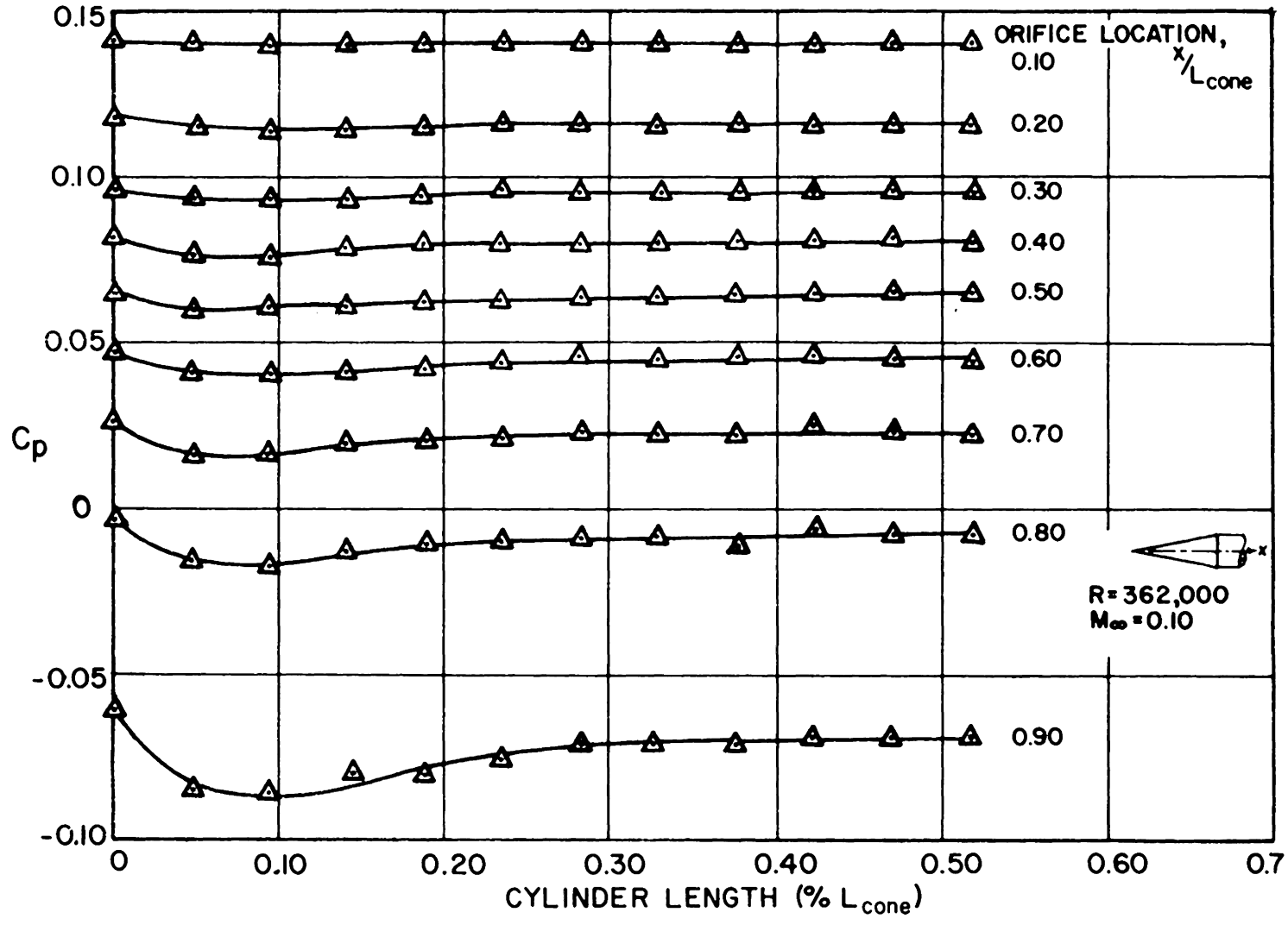

FIG. 5. EFFECT OF AFTERBODY LENGTH ON MEASURED PRESSURE DISTRIBUTION, $\theta_c = 10°$.

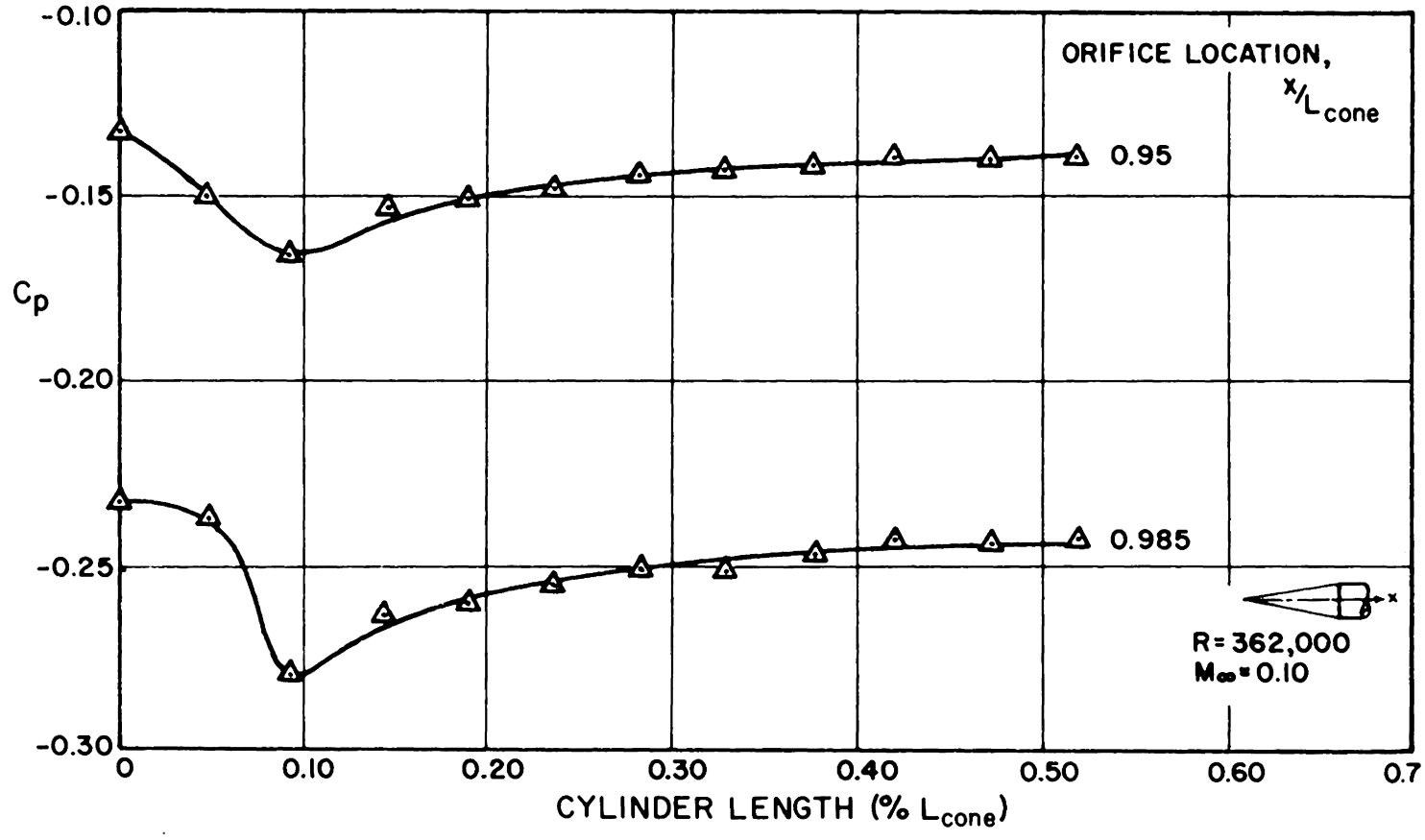

FIG. 5.(con't.) EFFECT OF AFTERBODY LENGTH ON MEASURED PRESSURE DISTRIBUTION, $\theta_c = 10°$.

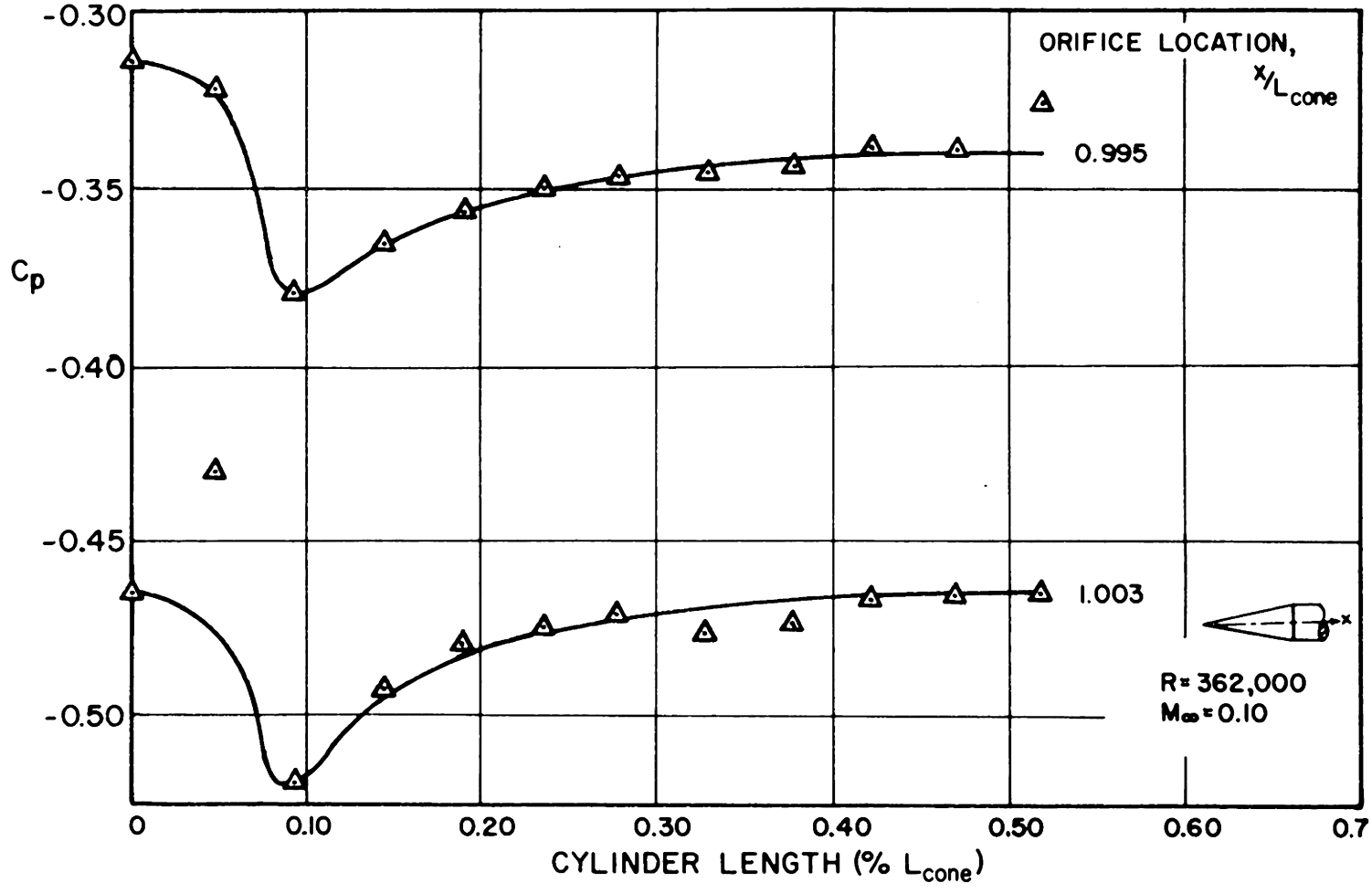

FIG. 5 (con't.). EFFECT OF AFTERBODY LENGTH ON MEASURED PRESSURE DISTRIBUTION, $\theta_c = 10°$.

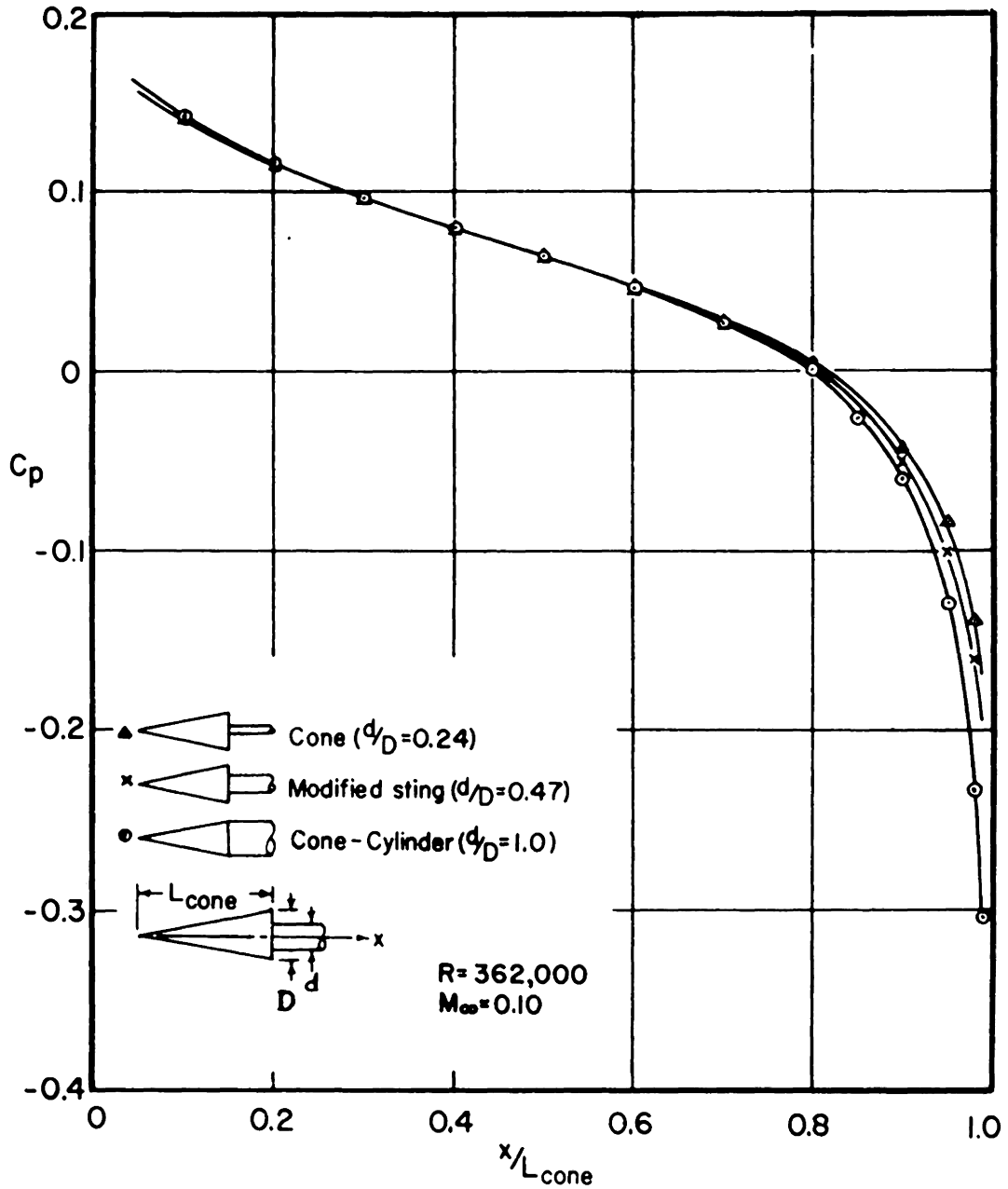

FIG. 6. EFFECT OF RELATIVE STING SIZE ON MEASURED PRESSURE DISTRIBUTION, $\theta_c = 10°$.

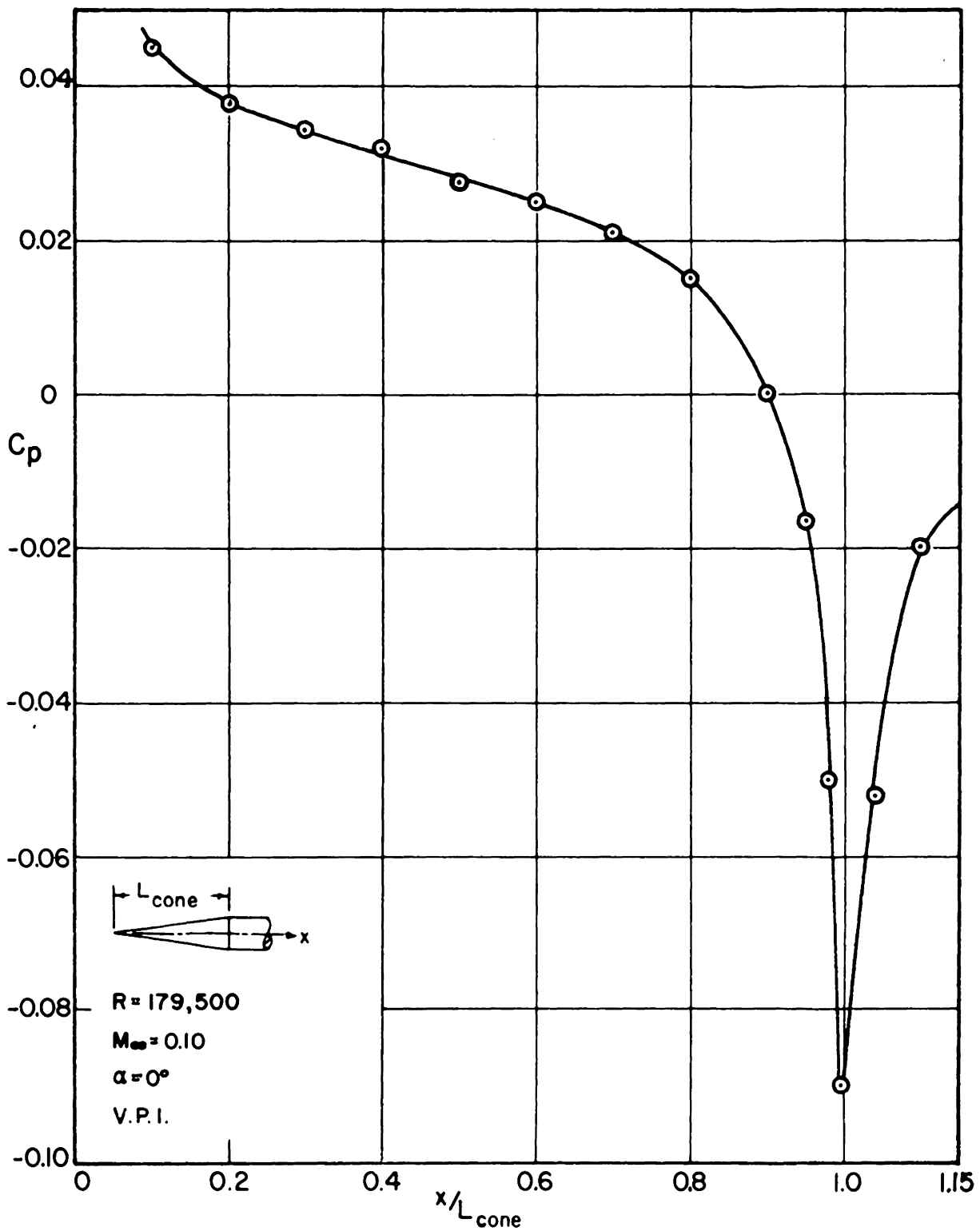

FIG. 7. PRESSURE DISTRIBUTION FOR A CONE - CYLINDER, $\theta_c = 5°$.

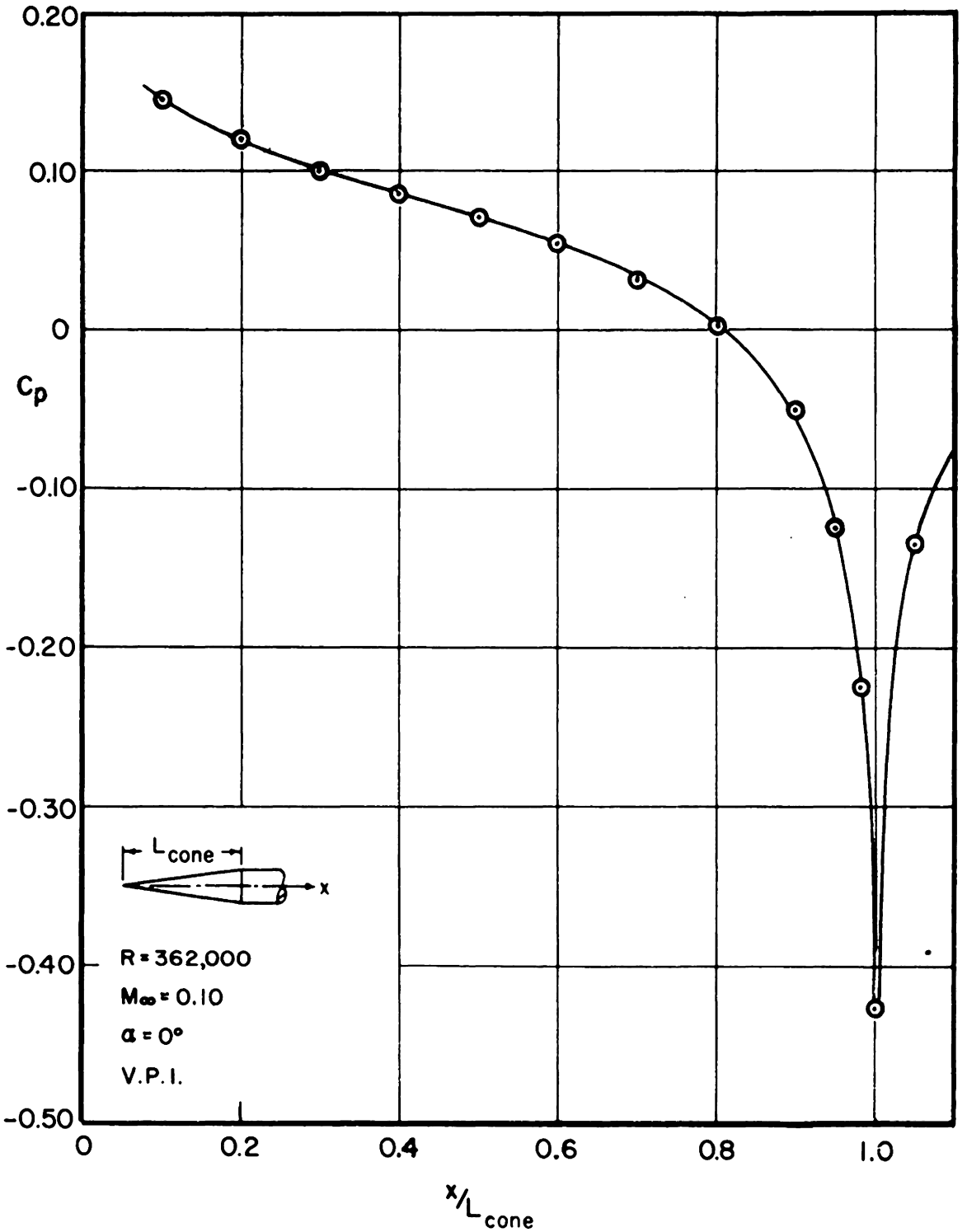

FIG. 7. PRESSURE DISTRIBUTION FOR A CONE - CYLINDER, $\theta_c = 10°$.

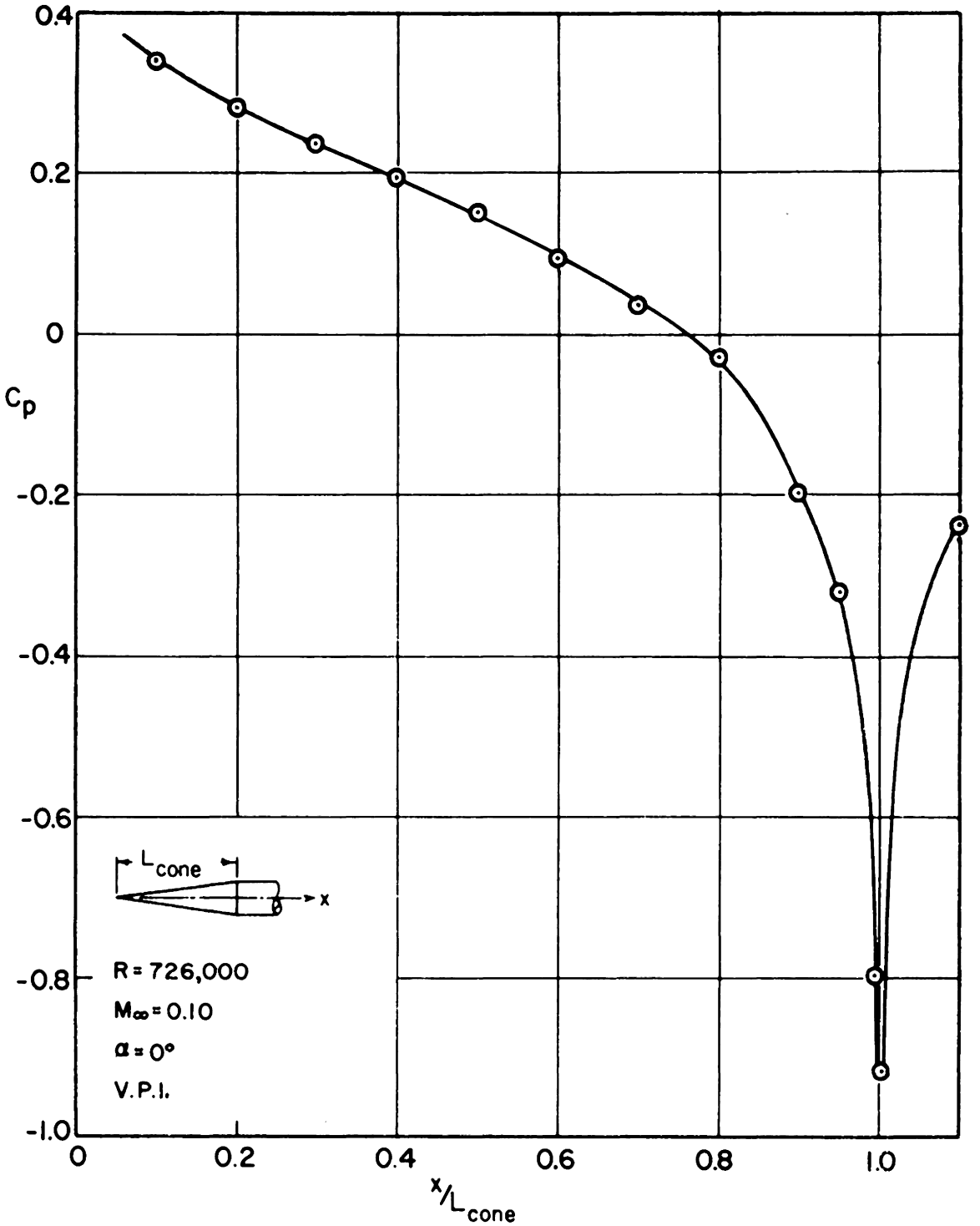

FIG. 7(concluded). PRESSURE DISTRIBUTION FOR A CONE CYLINDER, $\theta_c = 20°$.

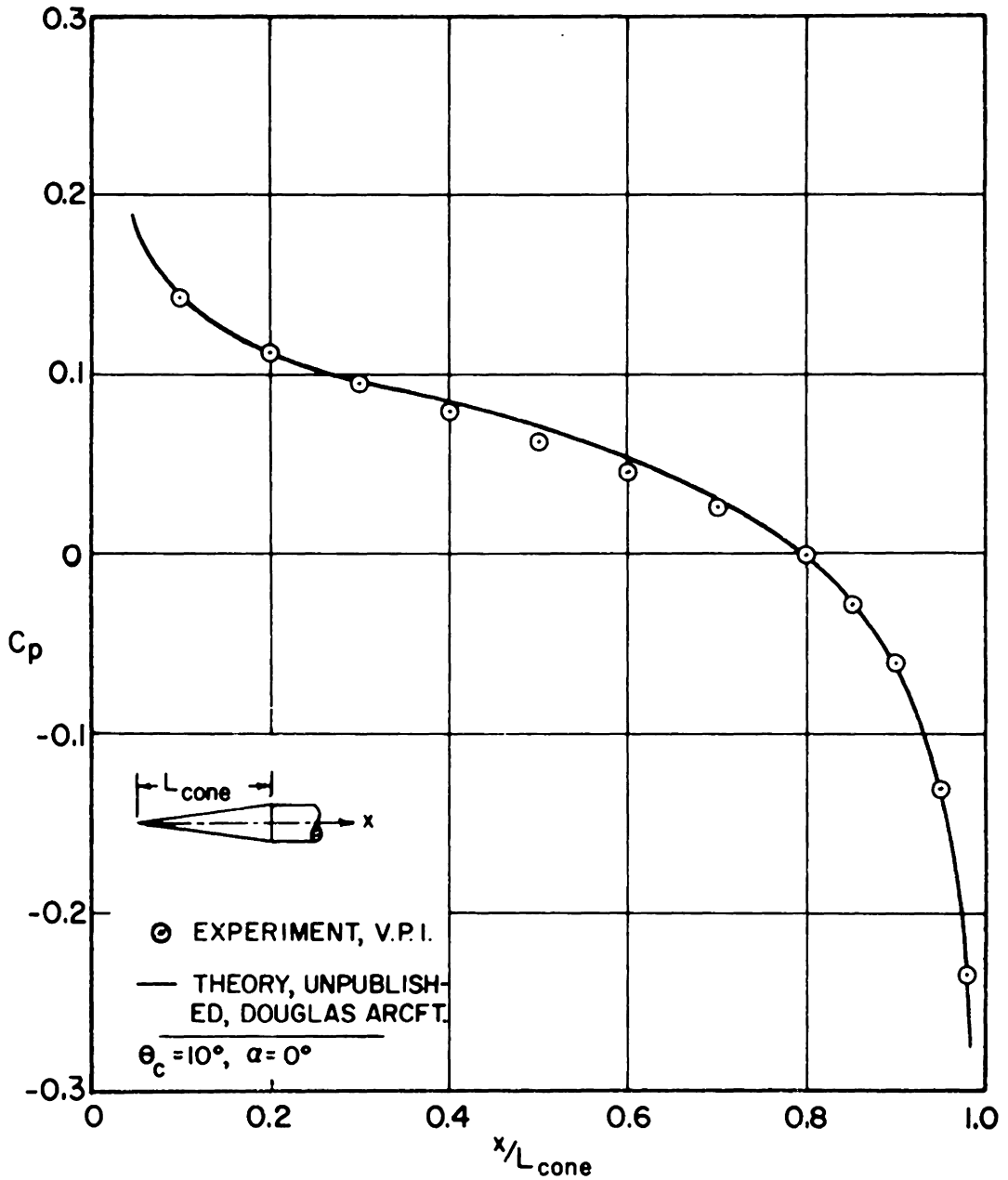

FIG. 8. COMPARISON OF EXPERIMENTAL AND THEORETICAL C_p DISTRIBUTION FOR A CONE, $\theta_c = 10°$

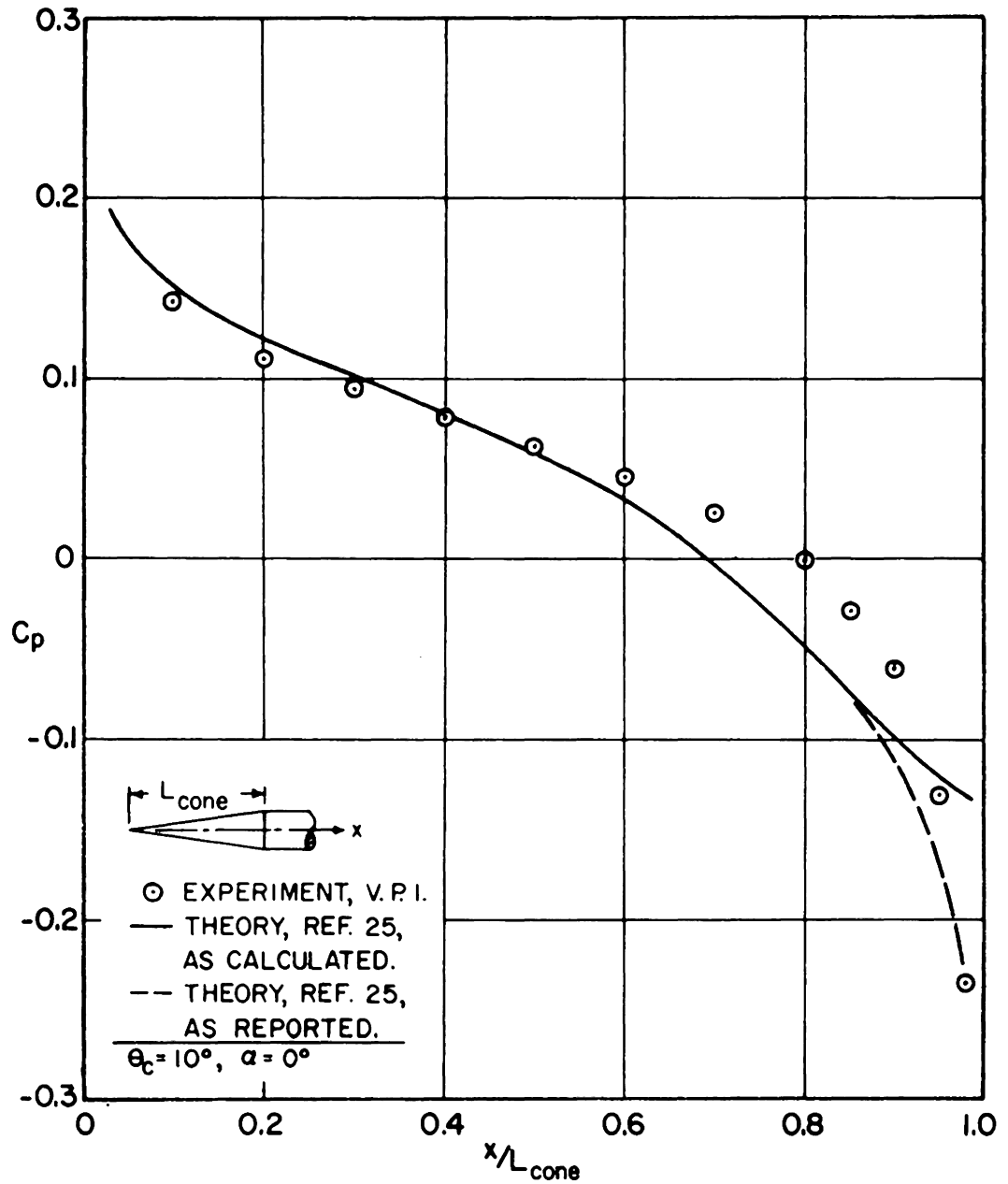

FIG. 9. COMPARISON OF EXPERIMENTAL AND THEOREICAL C_p DISTRIBUTION FOR A CONE, $\theta_c = 10°$

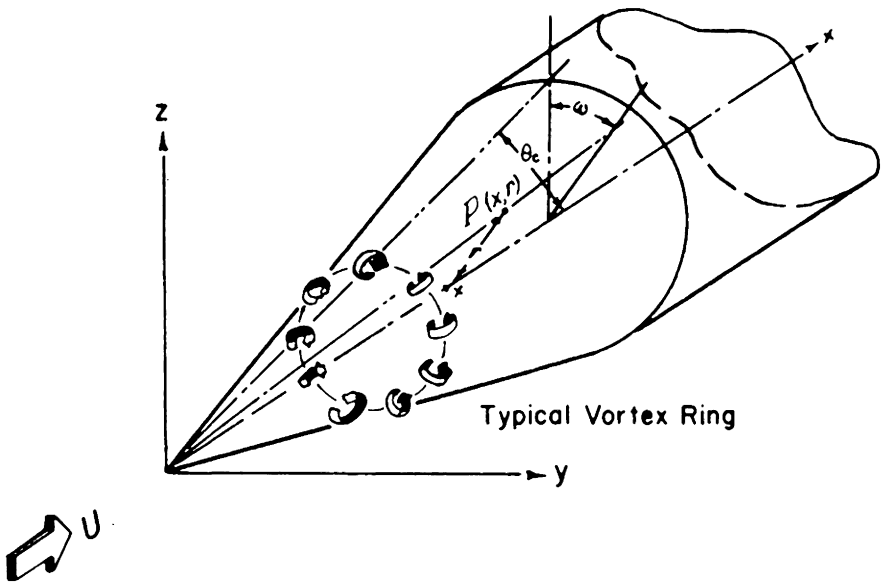

BODY COORDINATES

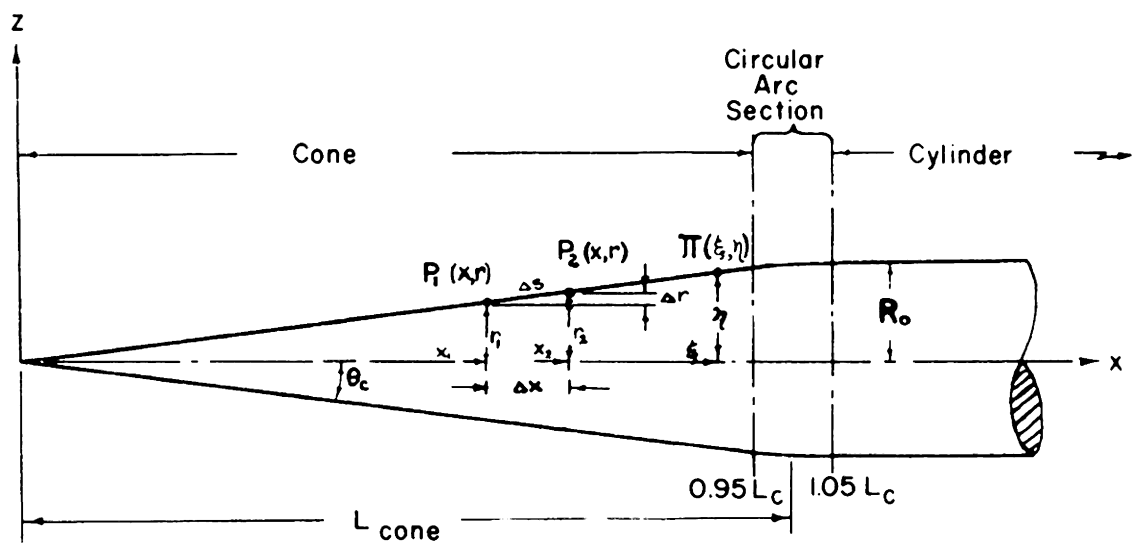

MERIDINAL PLANE OF THE CONE-CYLINDER BODY

FIG. 10a. COORDINATES FOR A TYPICAL BODY ($\theta_c = 10°$).

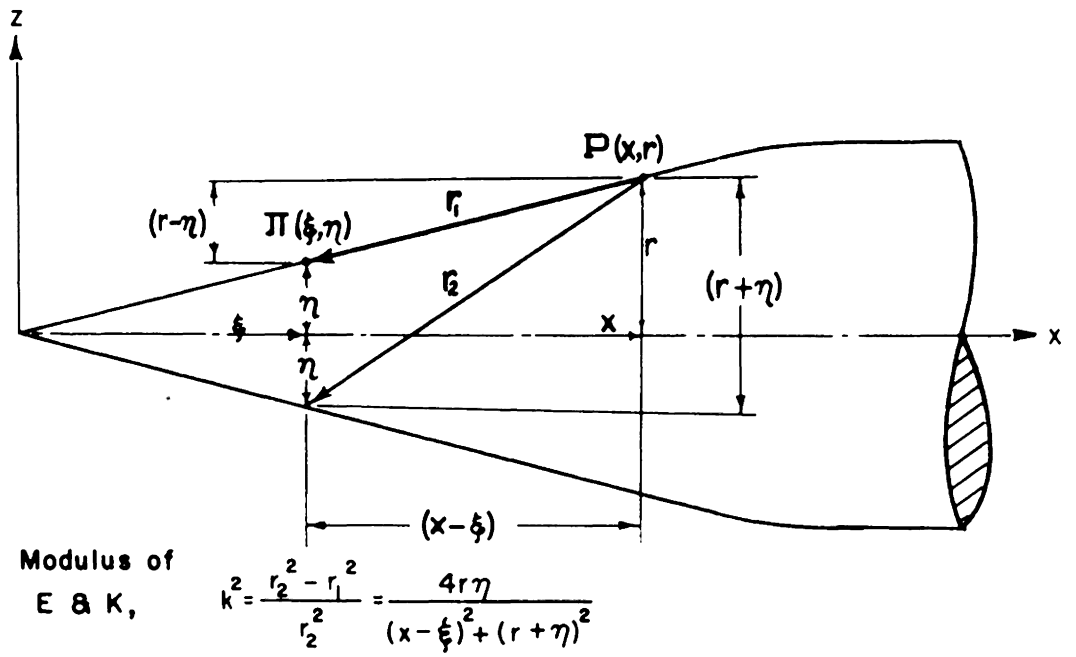

BODY PIVOTAL POINT [P(x,r)] & VARIABLE POINT [Π(ξ,η)].

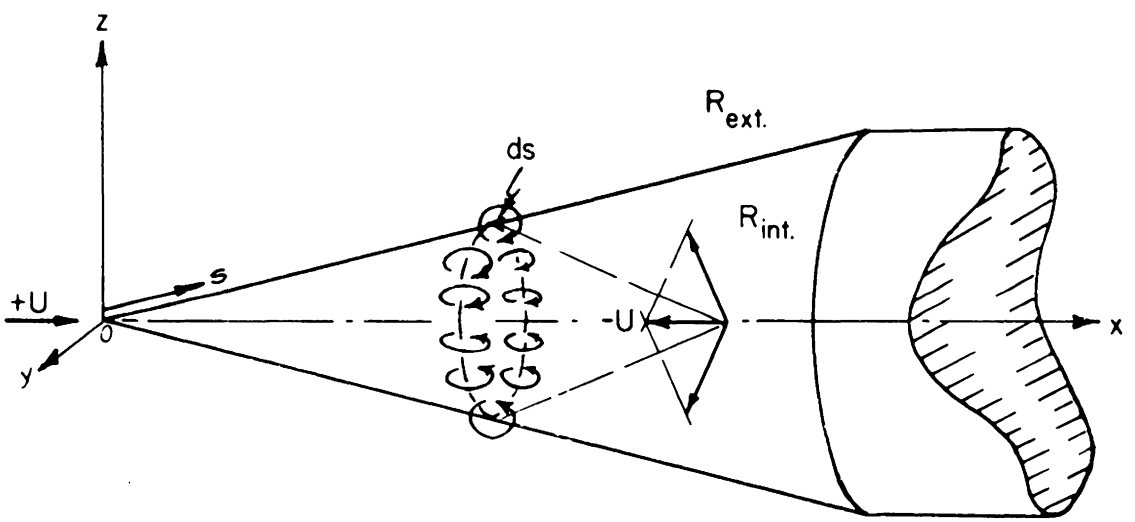

FLOW REGIONS AND DESCRIPTION

FIG. 10b. COORDINATES FOR A TYPICAL BODY.

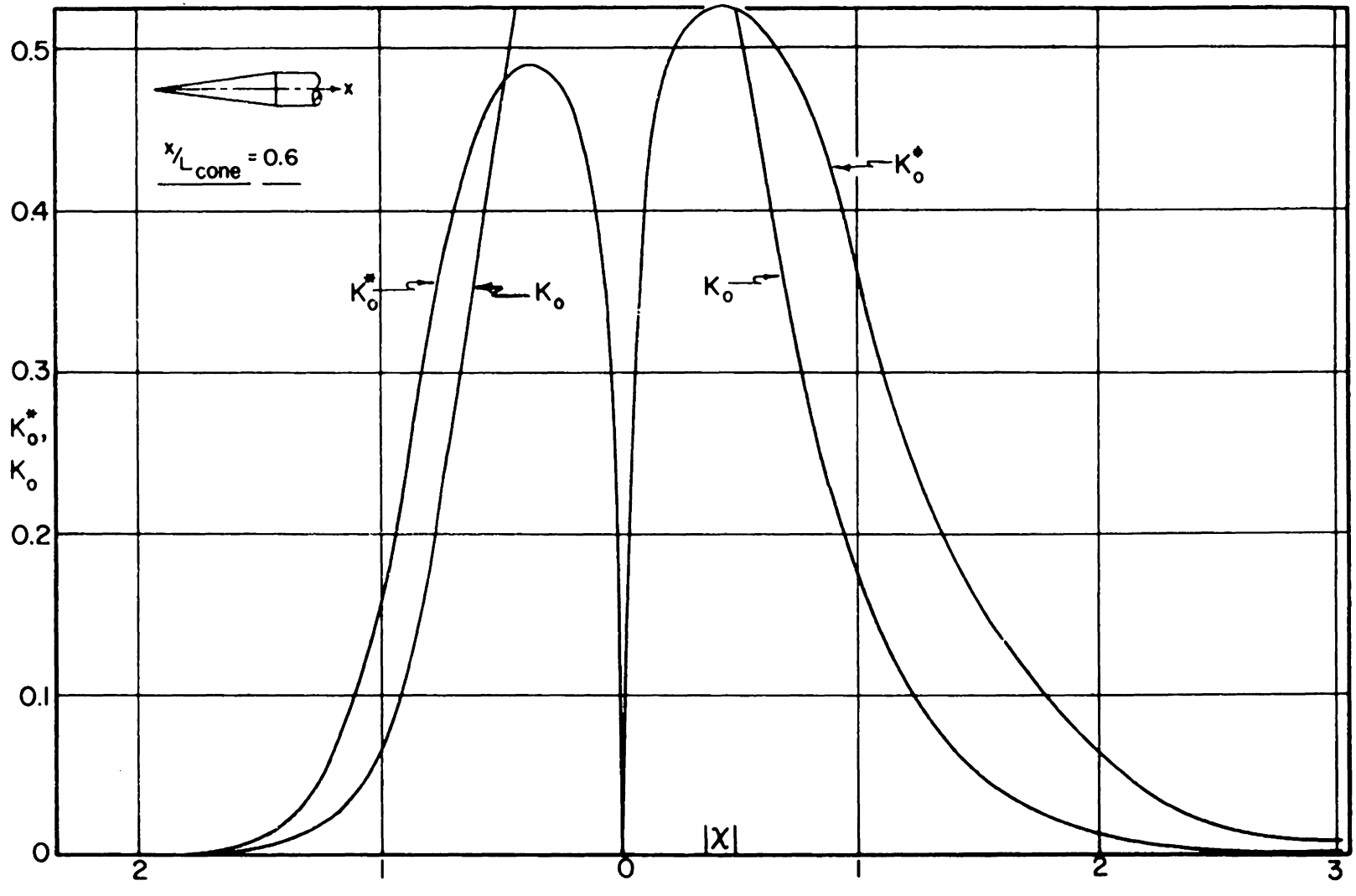

FIG.11. PLOT OF KERNELS FOR A TYPICAL PIVOTAL POINT FOR THE TRANSFORM COORDINATE, χ.

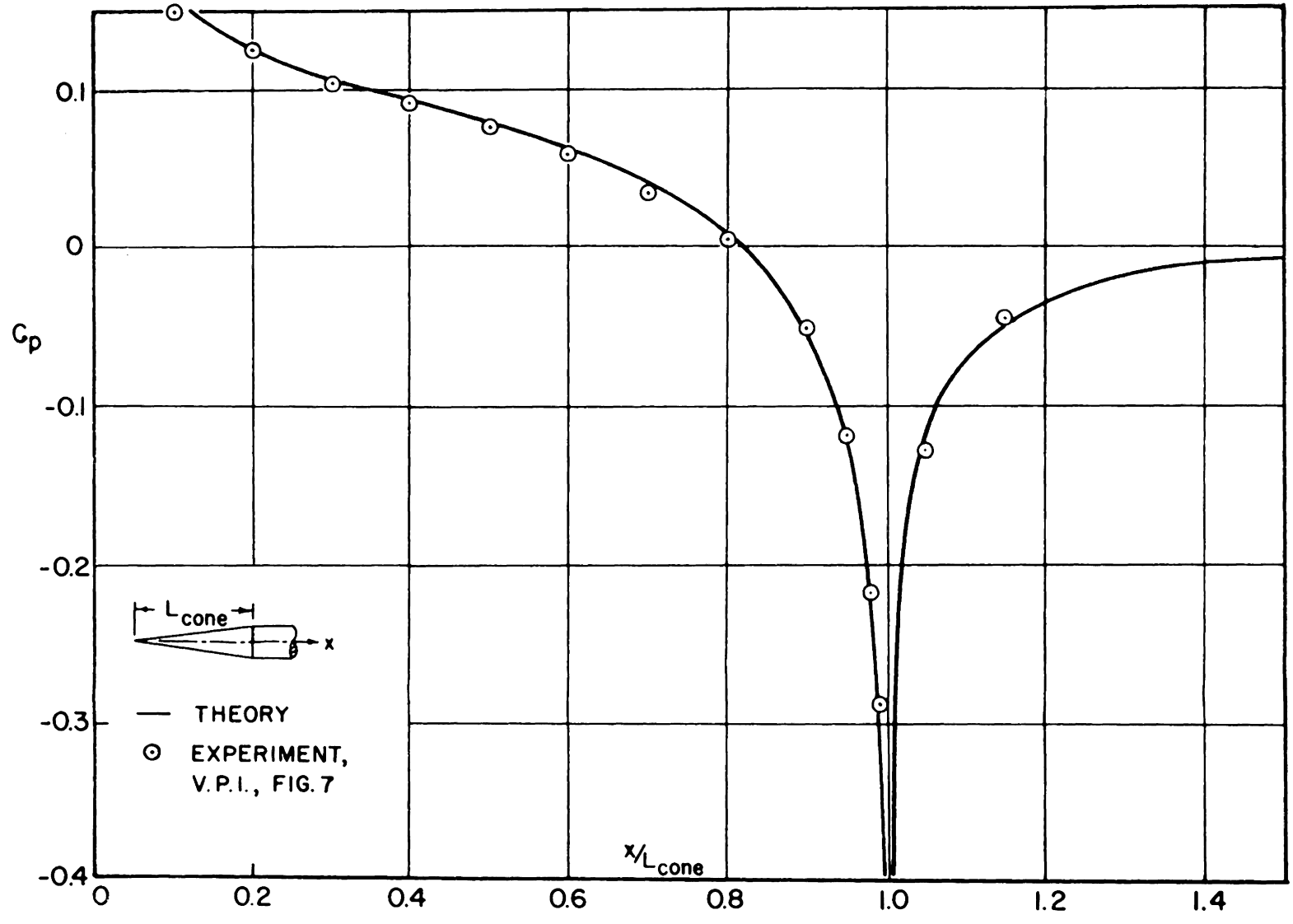

FIG. 12. COMPARISON OF C_p DISTRIBUTION FROM VORTEX RING THEORY & EXPERIMENT, $\theta_c = 10°$.

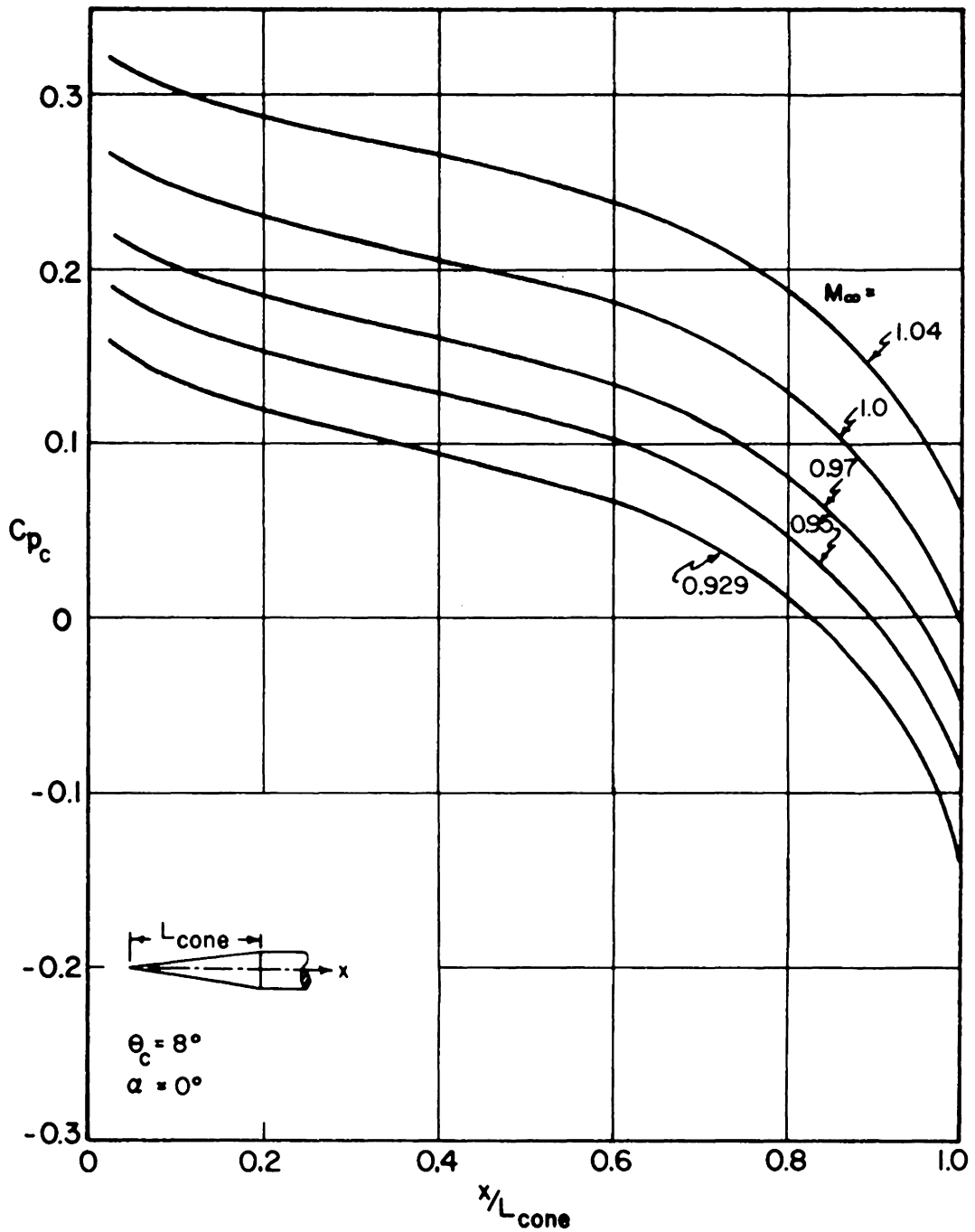

FIG. 13. C_p FOR TRANSONIC RANGE OF M_∞.

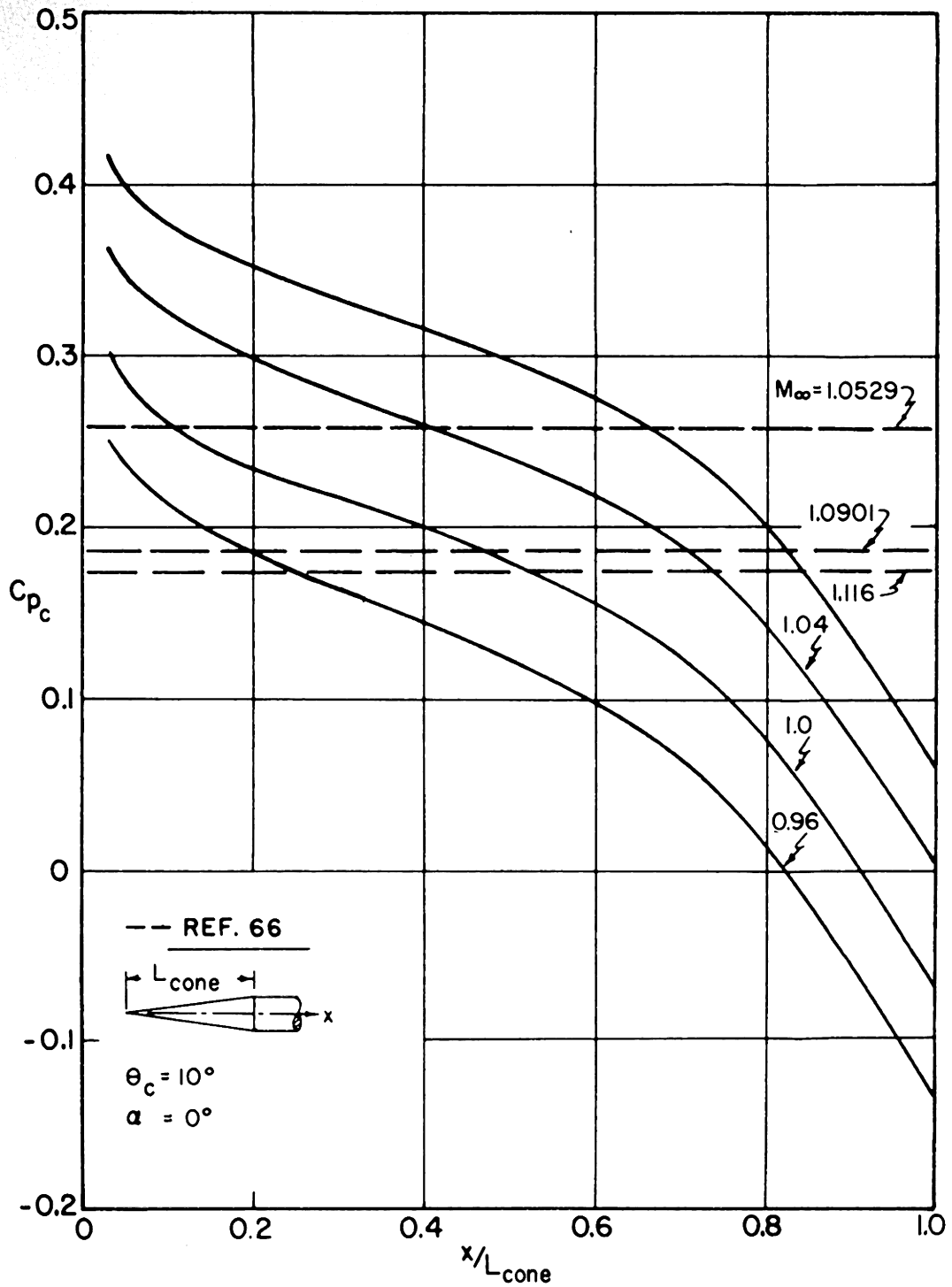

FIG. 13 (con't.). C_p FOR TRANSONIC RANGE OF M_∞.

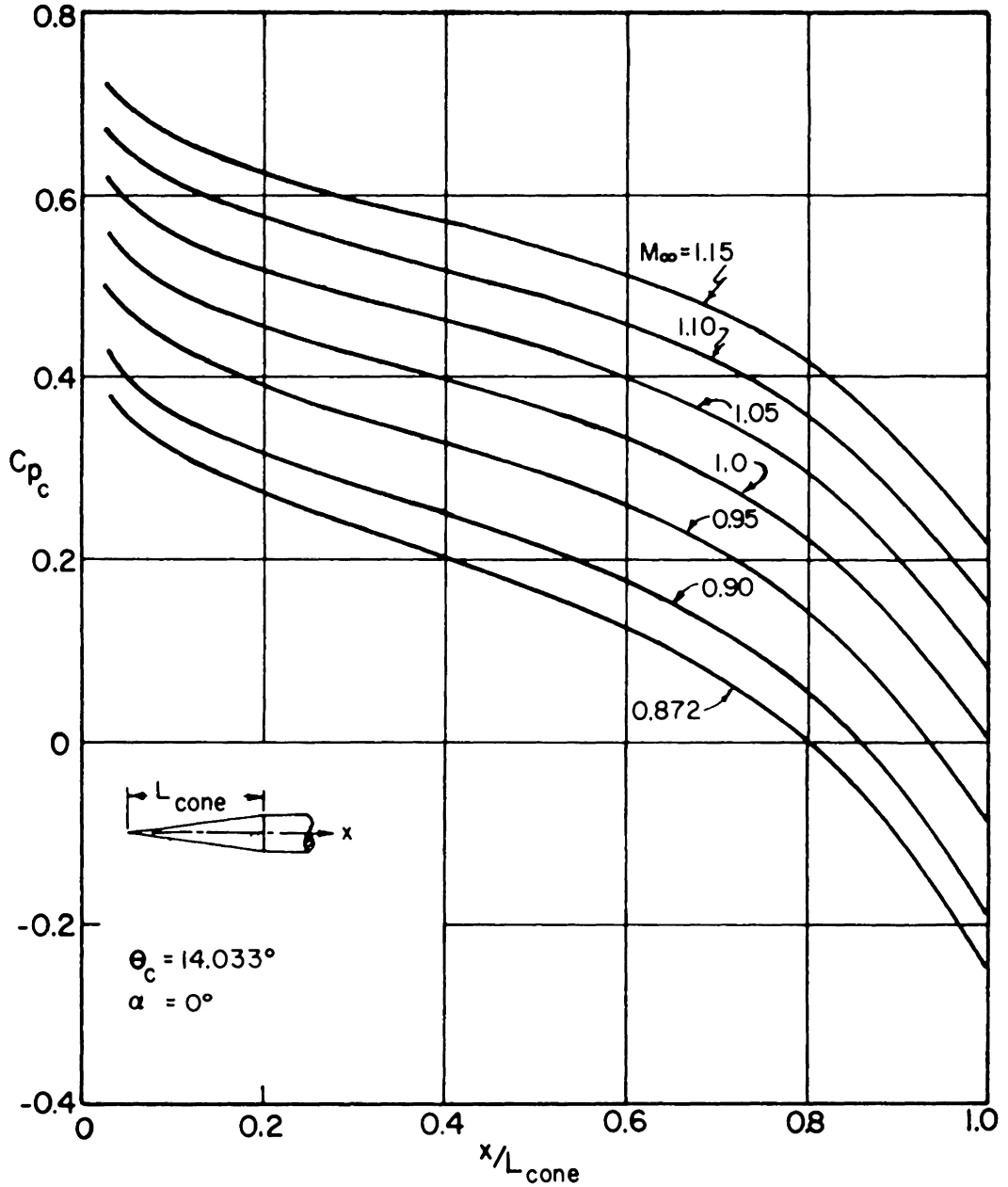

FIG. 13 (con't.). C_p FOR TRANSONIC RANGE OF M_∞.

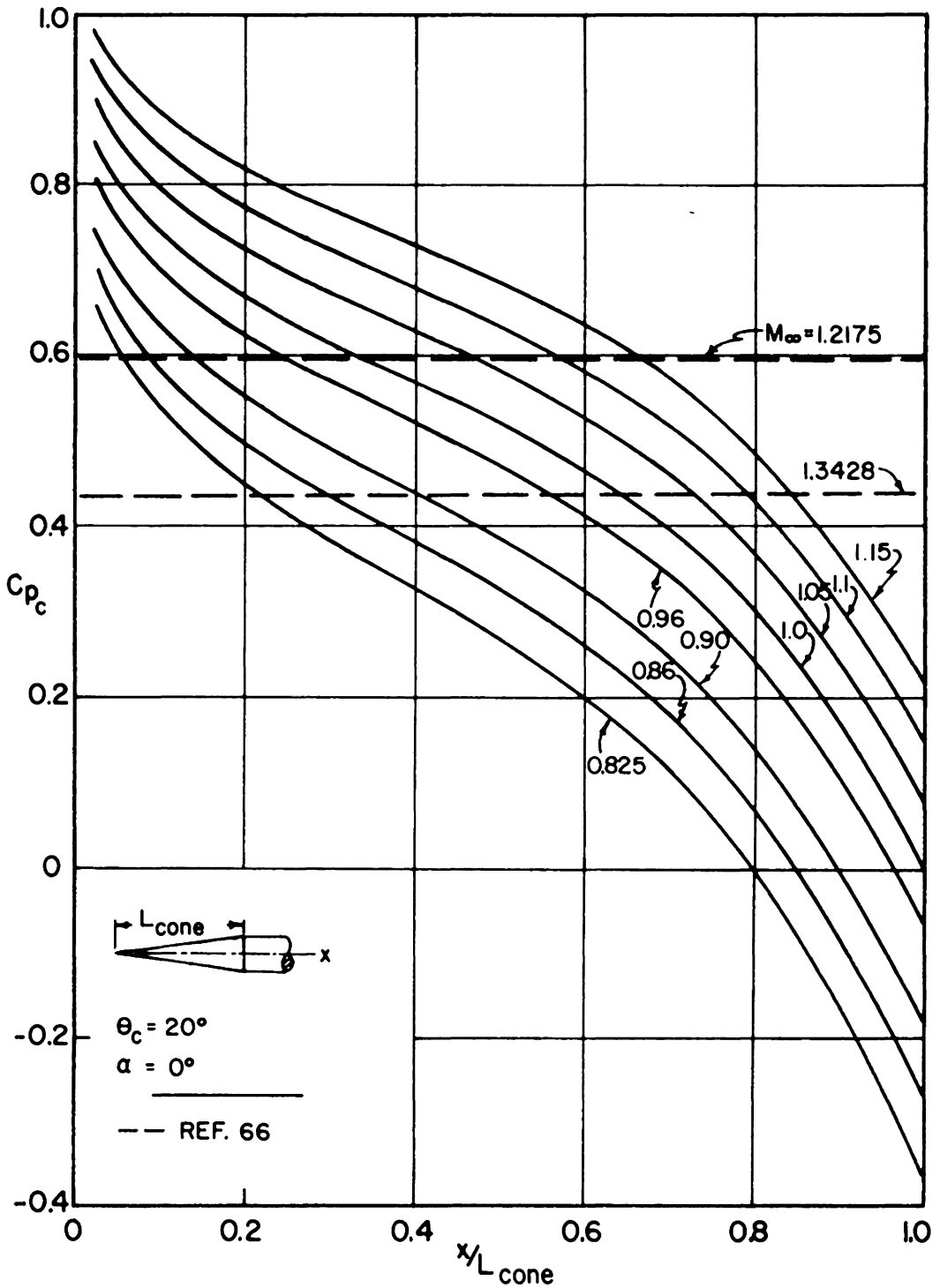

FIG. 13 (con't.). C_p FOR TRANSONIC RANGE OF M_∞.

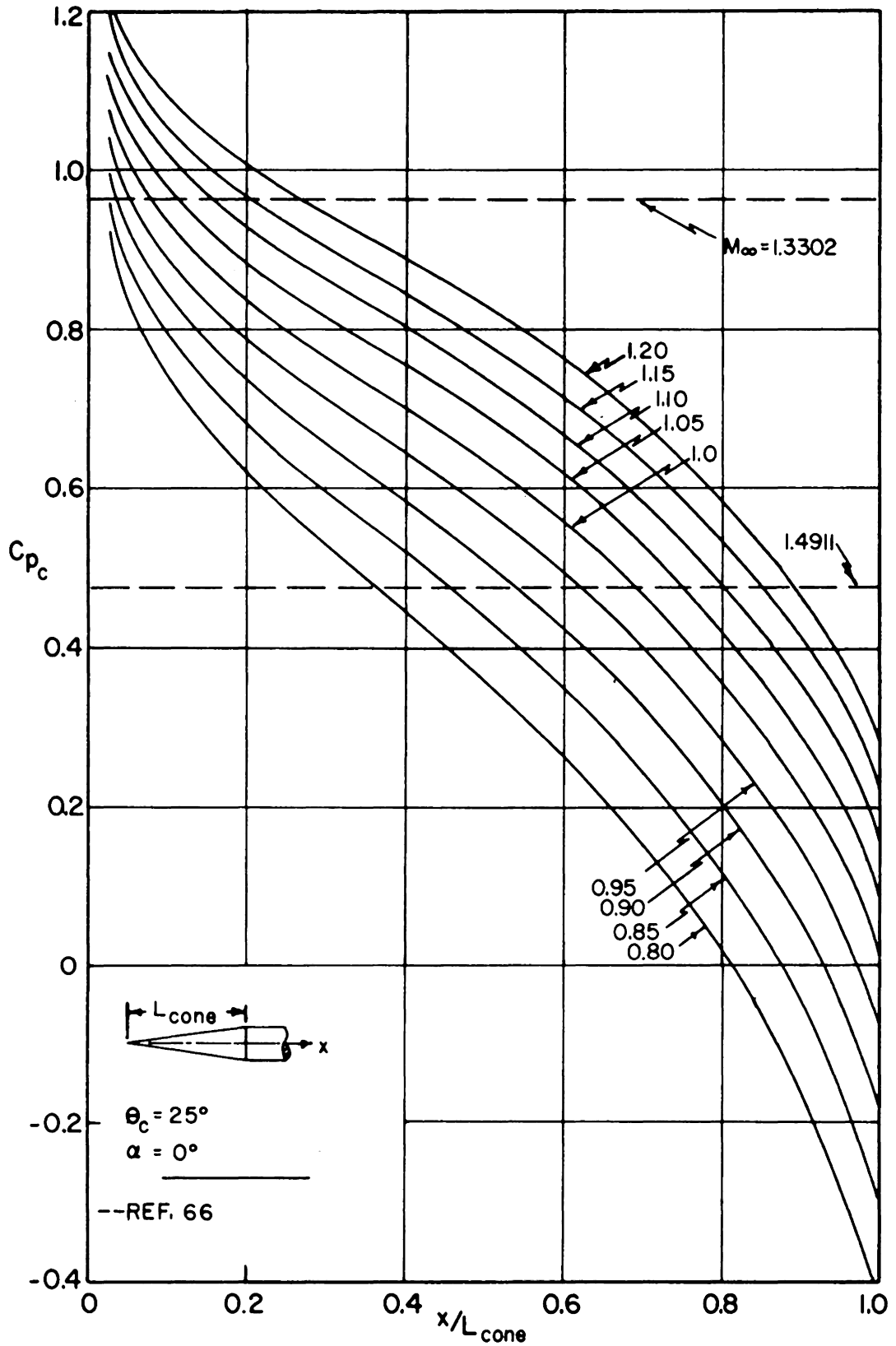

FIG. 13 (concluded). C_p FOR TRANSONIC RANGE OF M_∞.

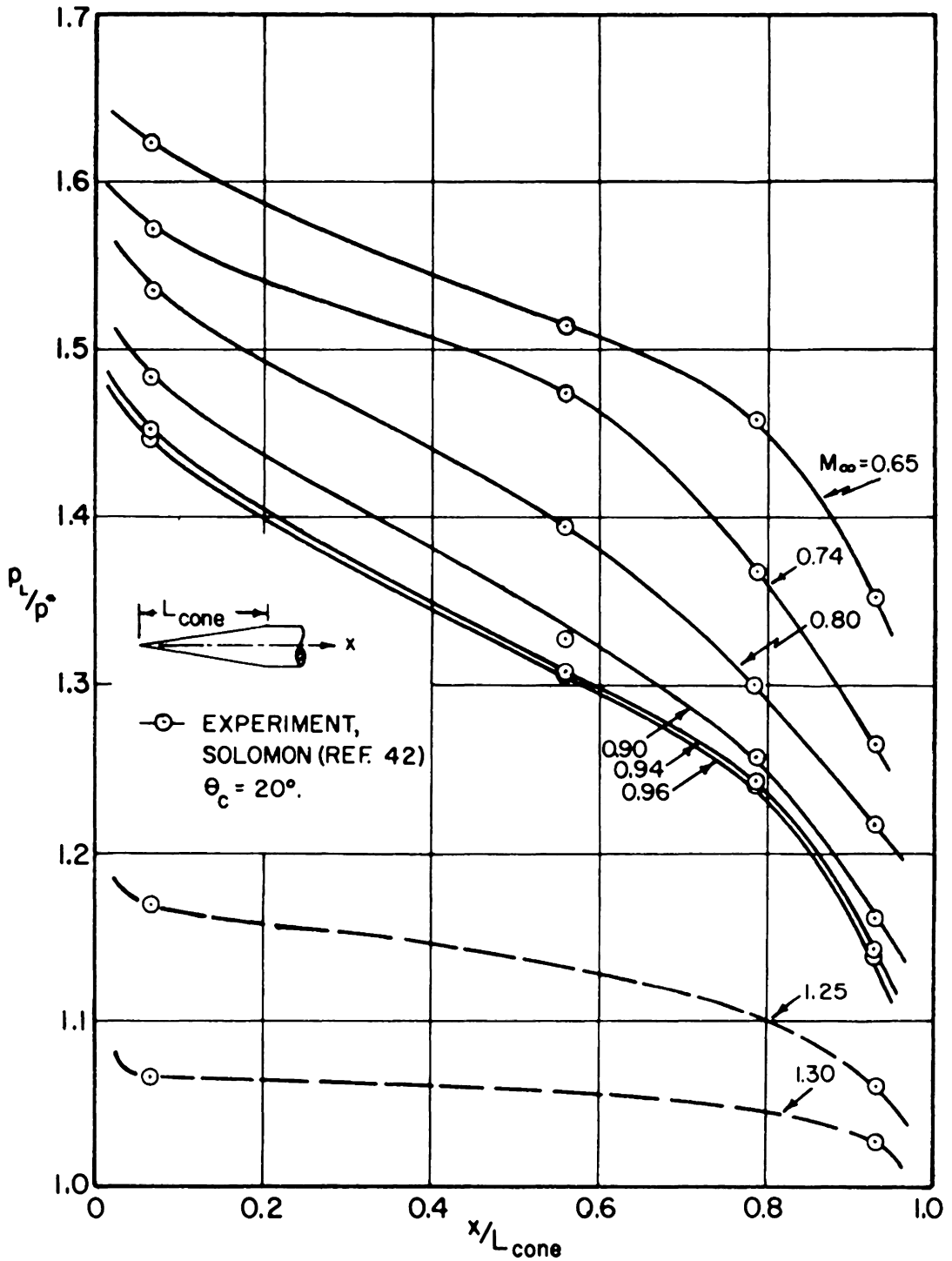

FIG. 14. p_L/p^* DISTRIBUTION FOR A 20° CONE.

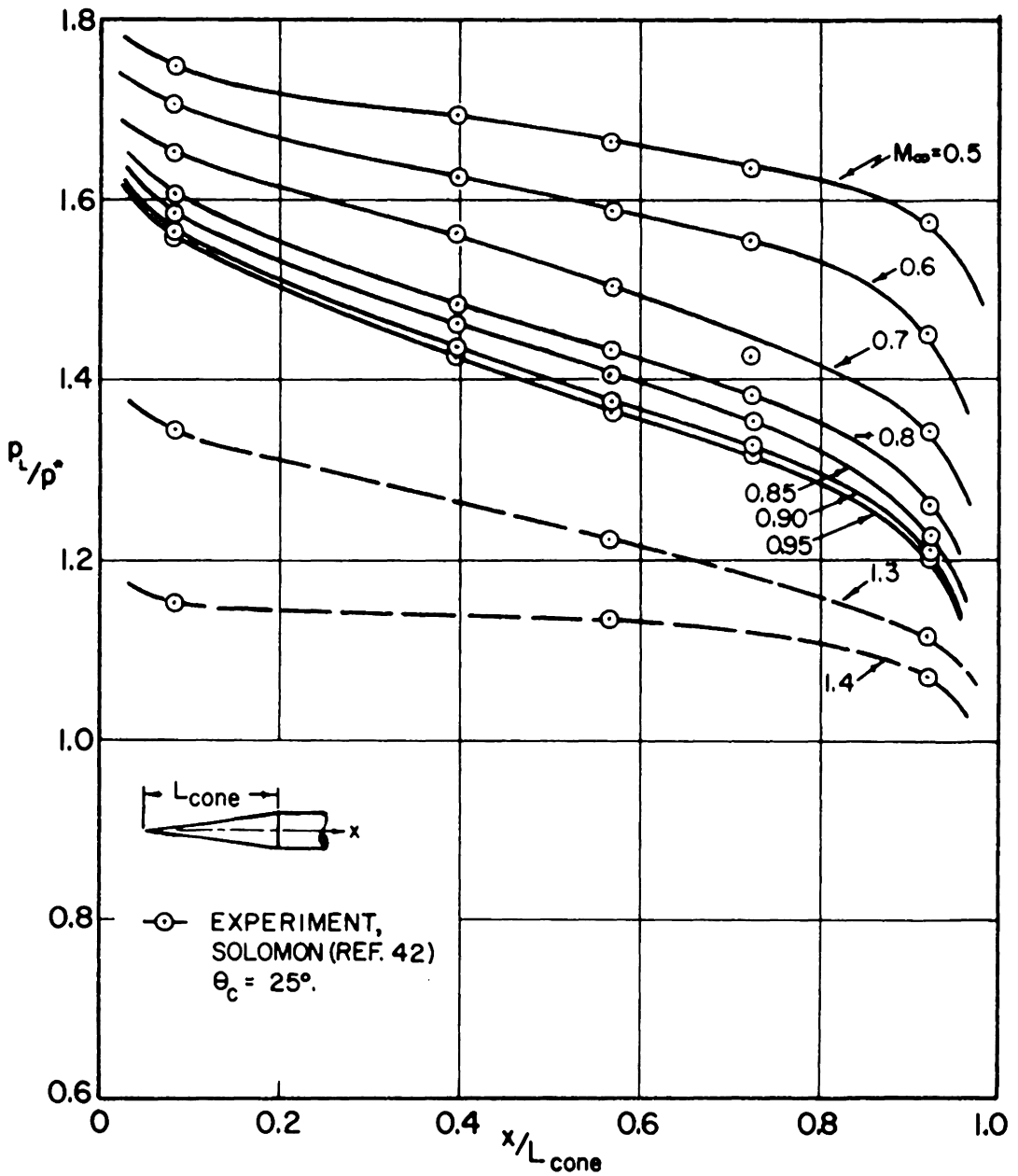

FIG. 14 (concluded). p_L/p^* DISTRIBUTION FOR A 25° CONE.

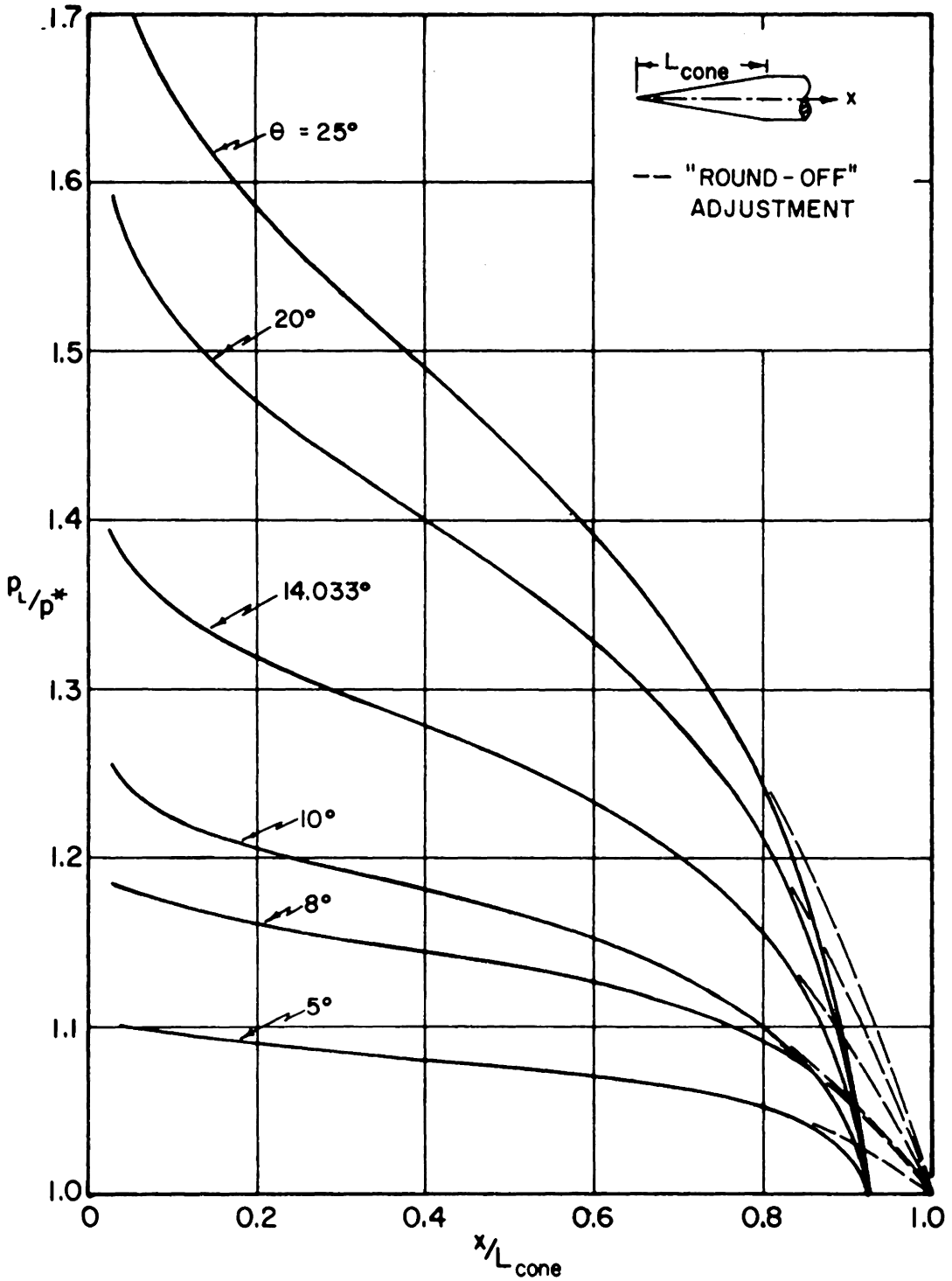

FIG. 15. THEORETICAL p_L/p^* DISTRIBUTION FOR CONES IN TRANSONIC FLOW.

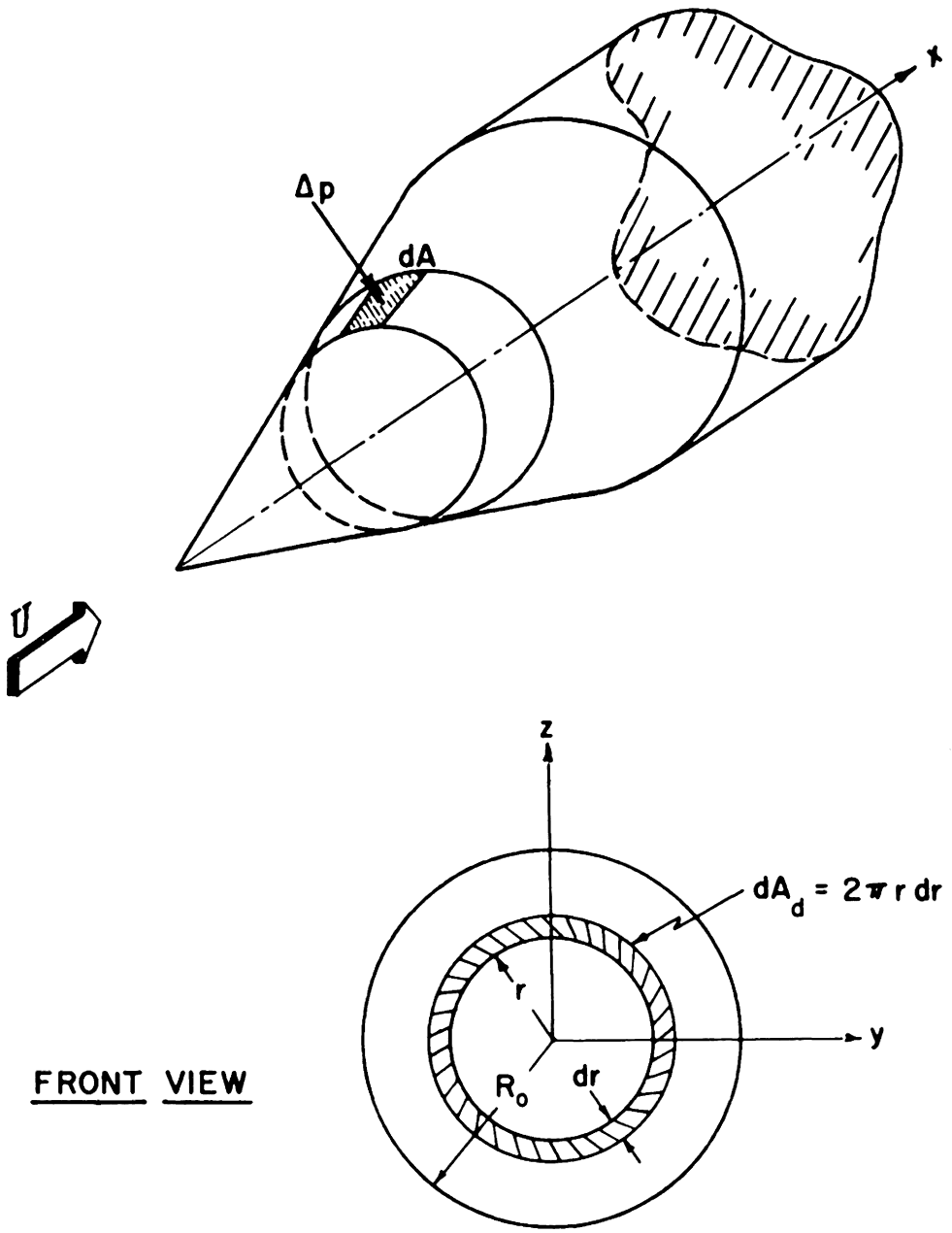

FIG. 16. PRESSURE - AREA RELATION FOR FORCE DEFINITION.

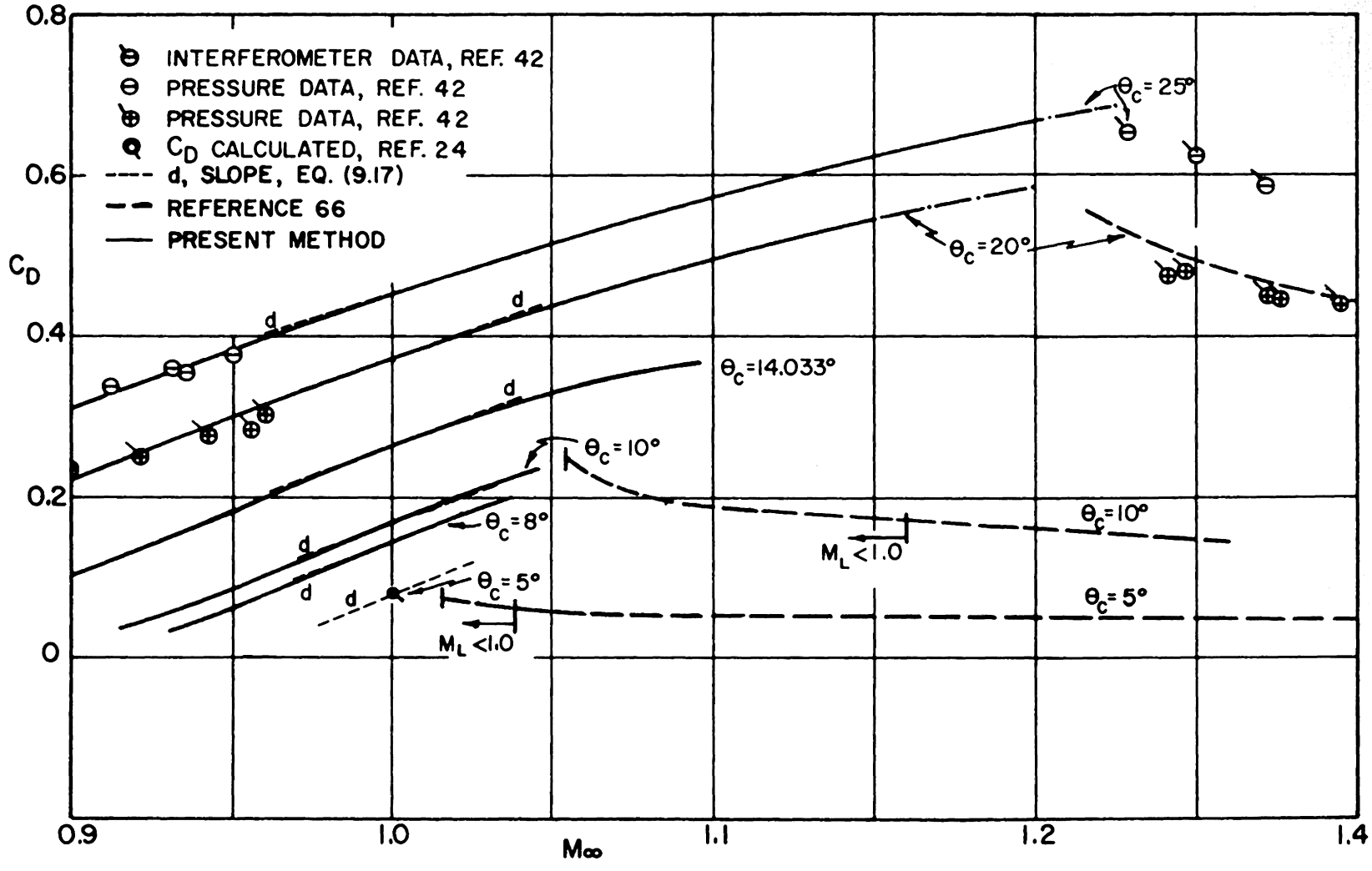

FIG. 17. DRAG COEFFICIENT FOR CONE - CYLINDERS IN TRANSONIC RANGE OF M_∞.

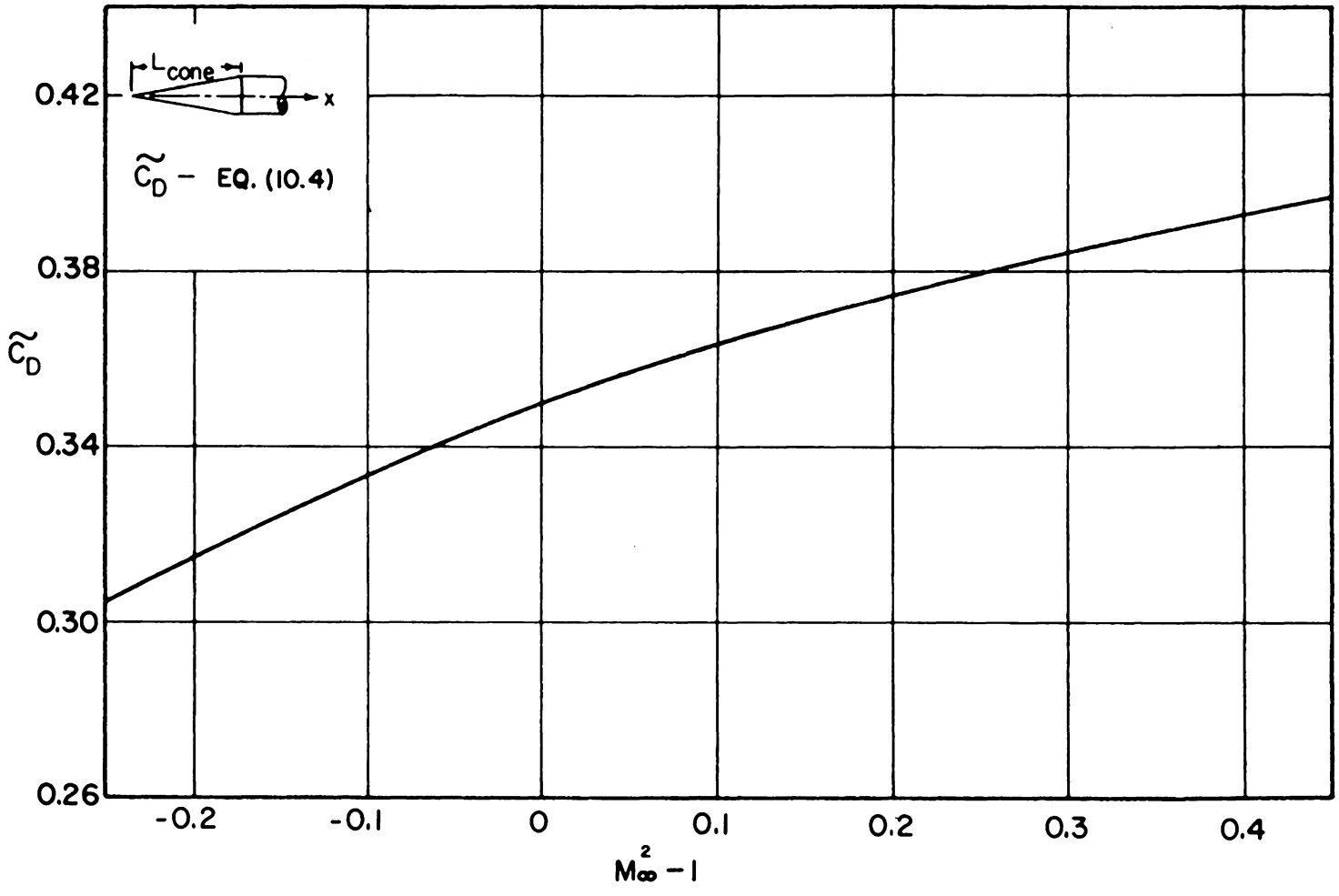

FIG. 18. CORRELATION OF THE NON-DIMENSIONAL PRESSURE DRAG COEFFICIENT FOR CONES IN TRANSONIC FLOW.

AN APPROXIMATE SOLUTION FOR A CONE - CYLINDER IN AXIALLY SYMMETRIC TRANSONIC FLOW

by

James B. Eades, Jr.
Applied Mechanics Department
Virginia Polytechnic Institute

ABSTRACT

In this thesis an approximate method is developed which predicts the aerodynamic force on a cone-cylinder body in axially symmetric transonic flow. The method places more emphasis on the physics of the flow than on the mathematical rigors of solving the typical reduced non-linear transonic equation of motion.

Under the assumptions that the flow is that of a steady, irrotational, inviscid, compressible gas, the body pressures are determined and the associated force defined. Recognizing that the transonic pressures are influenced by the character of the subsonic compressible pressures, which are obtained in this analysis through Gothert's Rule, it is then mandatory that the incompressible case be defined with the best possible accuracy. Comparisons with experiment indicate that the classical method (axially distributed sources and sinks) does not provide this required accuracy. Thus the surface distributed vortex ring theory is used in the present analysis to obtain the incompressible body pressures.

Gothert's Rule, which represents a linear solution for the subsonic case, is known to be applicable up to a limit value of free stream Mach number. An investigation is carried out herein to determine both the correct form of the rule and its limits of applicability. As a result of this investigation it is concluded that the upper limit is the lower free stream critical Mach number. Also, at this Mach number a solution is immediately available for the lower limit of the transonic range of Mach number.

In solving the transonic problem the law of stationarity of local Mach number is of fundamental importance. For an assumed isentropic flow over the body, and for sonic conditions being present at some point on the surface, the body pressures can be described in the ratio p_L/p^*. Here p_L is the local surface pressure and p^* is the sonic (body) pressure. Through the stationarity law this ratio is recognized as an invariant for transonic speeds so long as the flow field remains essentially irrotational. Thus any change in local pressure is only a function of the free stream Mach number for any given body position. By this approach the pressure distribution is defined for a range of Mach number from below to above the sonic stream value. The method is then capable of prediction for almost all of the transonic range of Mach number. It is only when the head shock has significant curvature, causing the flow adjacent to the body to be rotational, that the method fails. Though the procedure developed here is not capable of spanning the entire

transonic range, it does provide a wider range of applicability than other known theories.

Finally, for this problem a correlation of transonic pressure drag data is formulated. This correlation is founded on physical interpretation and is not limited to the usual transonic similarity restrictions. In fact, to the author's knowledge this is the first known such correlation for axially symmetric flow covering the range of body sizes and Mach numbers considered in this investigation.

In so far as is practicable the results obtained in this thesis have been compared to available expreimental results. In particular the drag data from this analysis compare closely with experimental transonic values. Experiment bears out the conclusion that the upper limit for linear theory is the lower critical free stream Mach number. And, the pressures determined by the vortex ring theory agrees well with the low speed experimental results obtained by the author.